MULTIPHASE MODELING OF DNAPL SEEPAGE HISTORY AS POSSIBLE SITE INVESTIGATION TOOL

Influence of geological material, groundwater flow and subsurface morphology on the pathways of DNAPLs

Dissertation
zur Erlangung des Doktorgrades
Dr. rer. nat.
der Mathematischen-Naturwissenschaftlichen Fakultät
der Christian Albrechts-Universität zu Kiel

vorgelegt von
Katharina Erning
Kiel, 19.03.2013

Erster Gutachter:	PD Dr. Dirk Schäfer
Zweiter Gutachter:	Prof. Dr. K. Wallmann

Tag der mündlichen Prüfung:	29.05.2013
Zum Druck genehmigt:	29.05.2013

Der Dekan

---

gez. (Titel, Vor- und Zunahme), Dekan/in

Erklärung

Hiermit erkläre ich, dass die vorliegende Arbeit - abgesehen von der Beratung durch die Betreuer - nach Inhalt und Form meine eigene Arbeit ist.
Die Arbeit hat weder einer anderen Stelle im Rahmen eines Prüfungsverfahrens vorgelegen, noch wurde sie veröffentlicht oder zur Veröffentlichung eingereicht.
Die vorliegende Arbeit ist unter Einhaltung der Regeln guter wissenschaftlicher Praxis der Deutschen Forschungsgemeinschaft entstanden.
Kiel, 19.03.2013

gez. Katharina Erning

Abstract

Modeling of the seepage history of DNAPLs is investigated as a new, non-invasive site investigation tool in order to elucidate the possible position of still unknown DNAPL source zone at many investigated industrial sites.
Therefore, the spatio-temporal spreading behavior of the DNAPL TCE is studied with the multiphase modeling software TMVOC in small and large scale 2D multiphase scenarios with varying parameter sets concerning groundwater flow, composition of aquifers and aquitards and subsurface morphologies, as depressions and trenches.
The small scale models were calibrated by laboratory experiments conducted at La Sapienza University, Rome. They exhibited that even groundwater pore velocities of $v_w = 0.05$ m/d have a strong impact on the spreading behavior and the position of a DNAPL body. Downstream inclined percolation path ways, enhanced dissolution rates and lateral transportation in downstream direction are the most dominant impacts. Small scale layering of the subsoil with horizontal lenses of impermeable materials affects the distribution pattern only slightly at $v_w > 5$ m/d, which are common flow velocities in many gravelly aquifers in Europe.
Upscaling of the models to field scale problems exhibited potential transportation length in downstream direction of several hundreds of meters, assuming a moderate spill rate of ca. 3 kg/day over an area of several square meters.
Investigating real subsurface morphology including real material parameters provided by the ModelPROBE reference site Chimica di Bianchi in Rho, Italy, revealed that the DNAPL TCE will be transported out of moderate depressions (slope of 2.5°) even at groundwater flow velocities of $v_w \leq 1$ m/d, which is in the range of documented groundwater flow velocities at the reference site. Moreover, the documented material classes, which comprise the aquitard at the site, are not in general impermeable for percolating DNAPLs. Only pure clays with a hydraulic conductivity of $k_f \leq 10^{-9}$ m/s are long-term barriers for vertical DNAPL percolation.
The conducted investigations deliver a reasonable explanation for the often unknown position of DNAPL source zones at former industrial sites and are, as far as it is known, the first large scale scenarios of DNAPL spreading behavior in real subsurface morphology.
Based on the conducted research it can be concluded that at the reference site Chimica di Bianchi the main mass of DNAPLs was not at the assumed hot spot, which was encapsulated in the 1980s, but probably migrated considerable distances in downstream direction, passing through or following partly the topography of the aquitard.
But the applicability of multiphase modeling as additional non-invasive site investigation tool is still challenging due to software restriction concerning size and resolution of the models and handling of heterogeneous permeability fields.

Kurzfassung

Die Simulation der Ausbreitung von fluiden Phasen in der gesättigten Zone wird als neue, nicht-invasive Untersuchungsmethode erforscht, um die mögliche Position der noch unbekannten DNAPL Quellbereiche an zahlreichen industriellen Standorten aufzuklären.
Hierfür wird beispielhaft das räumlich-zeitliche Ausbreitungsverhalten des DNAPLs TCE in klein- und großskaligen 2D Modellen mit dem numerischen Mehrphasensimulator TMVOC untersucht. Qualifiziert und quantifiziert wird hierbei das Ausbreitungsverhalten, die Geometrie und die finale Position des DNAPL-Körpers in Abhängigkeit von Grundwasserfließgeschwindigkeiten, Materialkomposition der hydraulischen Einheiten sowie von der morphologischen Ausprägung der Grundwassergeringleitern.
Die anhand von Laborversuchen kalibrierten kleinskaligen Untersuchungen haben gezeigt, dass bereits Grundwasserfließgeschwindigkeiten von $v_w = 0.05$ m/d einen starken Einfluss auf das Versickerungsverhalten und die Position des Phasenkörpers haben. Der DNAPL weist einen in abstromiger Richtung abgelenkten Versickerungspfad auf, wird als pool in seiner oberstromigen Ausbreitung gehemmt und in seiner abstromigen Ausbreitung verstärkt und ist erhöhten Lösungsraten ausgesetzt. Ein inhomogener Aufbau des Untergrundes, z.B. durch eingebettete undurchlässige Linsen, ergab nur bei geringen Fließgeschwindigkeiten eine Beeinflussung des DNAPL Ausbreitungsverhaltens. Grundwasserfließgeschwindigkeiten von $v_w > 5$ m/d, wie sie für viele kiesige Grundwasserleiter in Europa typisch sind, dominieren über Effekte eines inhomogenen Untergrundes.
Um Fragestellungen auf Feldskala beantworten zu können, wurde ein Upscaling der kleinskaligen 2D Modelle durchgeführt (500 m Länge, 11 m Tiefe, ein Aquifer und ein Aquitard). Es ergaben sich bei Fließgeschwindigkeiten von 0.05 m/d $< v_w <$ 1 m/d und einer Versickerungsrate von 3 kg/d m^2 mögliche abstromige Transportweiten von mehreren hundert Metern innerhalb von 75 Jahren.
Modellierungen des realen Referenzstandortes Chimica di Bianchi in Rho, Italien ergaben, dass der DNAPL TCE bei $v_w \leq 1$ m/d bereits moderate Steigungen von 2.5° innerhalb eines Grundwasserstauers überwinden kann und somit Depressionen und Senken innerhalb eines Aquitard nicht zwangsläufig einen DNAPL in seinem Ausbreitungsverhalten hemmen müssen. Zusätzlich durchgeführte Untersuchen bezüglich der Barriereeigenschaften des vor Ort dokumentierten Aquitards führten zu der Feststellung, dass das als Aquitard angesprochene Material in seiner Zusammensetzung sehr heterogen und nicht flächenhaft verbreitet ist. Durch die unvollständige Verbreitung des Aquitardmaterial bestehen mögliche hydraulische Verbindungen zwischen den beiden Aquiferen an dem Referenzstandort und es ist möglich, dass der DNAPL durch ein hydraulisches Fenster in den tieferen Aquifer migrierte. Darüber hinaus ergaben die Untersuchungen, dass die Materialklassen, aus denen sich der Aquitard zusammensetzt, nur teilweise Stauer für vertikal versickernden DANPL darstellen. Von den fünf vorkommenden Materialklassen, stellten einzig reine Tone ($k_f < 10^{-9}$ m/s) langfristige DNAPL-Stauer dar.
Die durchgeführten Untersuchungen liefern plausible Erklärungen für die oft unbekannte Position von DNAPL Quellzonen an vielen bereits erkundeten Industriestandorten.
Basierend auf den Ergebnissen der Mehrphasensimulation kann der Schluss gezogen werden, dass sich am Standort Chimica di Bianchi die Hauptmasse der DNAPL Kontamination nicht an der Position befindet bzw. befand, die in den 1980ern eingekapselt und gesichert wurde. Aller Wahrscheinlichkeit nach migrierte der DNAPL stromabwärts. Ob er dabei von dem

Aquitard in seiner vertikalen Ausbreitung gehemmt wurde und /oder dessen Morphologie folgte, ist aufgrund der Datenlage des Feldstandortes momentan nicht feststellbar.
Die Anwendung der Mehrphasensimulation als zusätzliche Untersuchungsmethode an kontaminierten Feldstandorten stellt immer noch eine Herausforderung dar, da erhebliche Restriktionen bezüglich Modellgröße, Diskretisierung sowie der Implementierung von heterogen Durchlässigkeitswerten (k_f) bestehen.

Table of Contents

Abstract ..... **I**

Leere Seite ..... **II**

Kurzfassung ..... **III**

List of Figures ..... **VIII**

List of Tables ..... **XI**

List of Abbreviations ..... **XII**

1 Introduction **1**

1.1 Reason and incentive 1
1.2 Structure and scope of the thesis 4
1.3 Historical overview 6
1.4 Recent research focus on site investigation and site remediation 6
1.5 Physico-chemical properties of DNAPLs 8
1.6 Ecotoxicological potential of selected chlorinated solvents 9
1.6.1 Tetrachloroethylene (PCE) 10
1.6.2 Trichloroethylene (TCE) 10
1.6.3 Cis-Dichloroethylene (cis-DCE) 10
1.6.4 Vinyl chloride (VC) 12
1.7 Movement of DNAPLs in the subsoil 12
1.7.1 General Principles 12
1.7.2 Mathematical-physical principles of multiphase flow 14
1.7.3 Influence of heterogeneities of the subsoil 20
1.7.4 Influence of groundwater flow 21

2 Methods **22**

2.1 Applied software 22
2.1.1 Multiphase modeling software TMVOC 22
2.1.2 Geological modeling software GMS 23
2.2 Primary Data 23
2.2.1 Laboratory experiments for calibration of the multiphase model 24
2.2.2 Literature study / historical site investigation 26
2.2.3 Borehole data set of former site investigation campaigns 28
2.3 Structural 3D models of Rho, Italy 31
2.3.1 Model 1 – Structural hydraulic 3D model based on layers of the Modflow –model 31
2.3.2 Model 2 – Structural hydraulic 3D model based on boreholes 33
2.3.3 Model 3 – Structural geological 3D model based on boreholes 36

3 Simulation of DNAPL distribution depending on groundwater flow velocities using TMVOC 39
Abstract 39
3.1 Introduction 39
3.2 Influence of Groundwater flow velocities on DNAPL movement 40
3.2.1 Methodology 40
3.2.2 Results 41
3.3 Discussion 42
3.4 Conclusion 42
3.5 Further prospects 42
Acknowledgements 43
References 43
4 Simulation of DNAPL infiltration and spreading behaviour in the saturated zone at varying flow velocities and alternating subsurface geometries 44
Abstract 44
4.1 Introduction 44
4.2 Methodology 47
4.2.1 Calibration model 47
4.2.2 Scenario Modeling 50
4.3 Results and discussion 52
4.3.1 Calibration model 52
4.3.2 Homogeneous scenario 53
4.3.3 Layered Scenarios 55
4.4 Conclusions 59
4.4.1 Homogenous scenario 59
4.4.2 Layered scenarios 59
4.4.3 Summary conclusions 61
4.5 Further prospects 61
Acknowledgments 61
References 61
5 Multiphase model driven site assessment of the area of the former industrial facility Chimica di Bianchi in Rho / Italy 65
5.1 Introduction 65
5.2 Methodology of multiphase model driven site assessment 66
5.2.1 Historical site investigation and literature studies 67
5.2.2 Geological site modeling based on pre-existing data 68

5.2.3 Multiphase modeling of potential DNAPL pathways 71
5.2.4 Results and Discussion 73
5.3 Conclusion 76
Literature 77
6 Multiphase modeling of the impact of groundwater pore velocities on DNAPL migration in the multi-aquifer formation of Rho, Italy 78
Abstract 78
6.1 Introduction 78
6.2 Methods 80
6.2.1 Field site 80
6.2.2 Primary data 82
6.2.3 Geometry of multiphase model 83
6.2.4 Hydraulic conditions and material parameters 84
6.2.5 Scenario combinations 85
6.2.6 DNAPL infiltration 86
6.2.7 Data interpretation 86
6.3 Results 87
6.3.1 Spatial distribution of the DNAPL 87
6.3.2 Position of DNAPL and Center of mass 90
6.3.3 Mass of the DNAPL 92
6.3.4 Volume of the DNAPL 93
6.4 Discussion 94
6.4.1 Spatial distribution and position of centre of mass 94
6.4.2 Mass of DNAPL 95
6.4.3 Volume of DNAPL 96
6.4.4 Implication for former industrial site Chimica di Bianchi, Rho 96
6.5 Conclusion 97
Acknowledgments 99
References 99
7 Conclusion 103
8 Acknowledgements 108
9 References 109
Curriculum vitae 118

List of Figures

Figure 1.1 Principles of DNAPL distribution in the subsoil (after Domenico & Schwartz, 1990) 1
Figure 1.2 Techniques and methods covered by ModelPROBE and their application within an idealized cyclical approach (P. Dietrich, MOSAIC; http://www.ufz.de/index.php?de=16349) 8
Figure 1.3 Sketch of principle methodology of model driven site assessment 8
Figure 1.4 Wettability of the system water – DNAPL – air (after Helmig, 1997) 13
Figure 1.5 Principle of the representative elementary volume (Helmig, 1997) 15
Figure 1.6 Continuum-theorem (Helmig, 1997) 15
Figure 1.7 Capillary pressure – saturation relation by Brooks & Corey and by Van Genuchten (Helmig, 1997) 17
Figure 1.8 Curves of relative permeability – saturation for varying grain sizes (after Helmig, 1999) 21

Figure 2.1 Typical runtime of simulations of the two-phase system NAPL-water in TMVOC in dependancy of discretization of model domain 23
Figure 2.2 Schematic set-up of the experimental tank (Luciano et al., 2010), all length in cm 24
Figure 2.3 Minimum and maximum thicknesses of hydraulic units at Rho, based on values provided in literature (Beretta et al., 2005; Bozzano et al., 2007; Cardarelli and Di Filippo, 2009; Leccese et al., 2007; Pedretti et al., 2012; Werban et al., 2007) 26
Figure 2.4 Position of boreholes (dots) with geological descriptions used for 3D modeling 30
Figure 2.5 Position of boreholes (dots) with hydraulic descriptions used for 3D modeling.....30
Figure 2.6 Area of interest, overlaid by aerial picture (adapted from Google Earth, 2010), coordinates in Gauss-Boaga, extension of all conducted structural, geological and hydraulic models 31
Figure 2.7 Perspective view of Modflow model, all hydraulic units, z magnification 1 : 25.....32
Figure 2.8 Perspective view of top of aquitard, modflow model, z magnification 1 : 25 32
Figure 2.9 Topographic surface map in perspective view of top of aquitard of model 1 – Modlfow layer based, z-magnification 1 : 25 33
Figure 2.10 Topographic surface map of top of aquitard of model 2 version 1.....34
Figure 2.11 Topographic surface map in perspective view of top of aquitard of model 2 version 1, z magnification 1 : 25 34
Figure 2.12 Topographic surface map of top of aquitard of model 2 version 2.....35
Figure 2.13 Topographic surface map in perspective view of top of aquitard of model 2 version 2, z magnification 1 : 25 35
Figure 2.14 Topographic surface map of top of aquitard of model 3, on top of surface map of Rho.... 36
Figure 2.15 Topographic surface map in perspective view of top of aquitard of model 3, z magnification 1 : 25 37
Figure 2.16 Surface of aquitard in model 3 (dark brown dots) in comparison to aquitard of model 1 (light brown dots) in perspective view, z magnification 1 : 25.....37

Figure 2.17 Perspective view of Aquitard and Prima Falda (Superficiale not shown), z magnification 1 : 25 38
Figure 2.18 2D cross section converted for multiphase modeling, z magnification 1 : 25 38

Figure 3.1 Simulated TCE saturation at v_w = 0.00 m/day (base case scenario) and v_w = 40.00 m/day. Small differences in the lateral distribution of the base case scenario are due to the resolution of the model and the interpolation method (kriging) 41

Figure 4.1 Schematic set up of the experimental tank (Luciano et al., 2010), all length in cm 47
Figure 4.2 Model domain in TMVOC, low permeable lenses in black, overlaid by discretization grid, groundwater flow from left to right (AOI = area of interest of the laboratory experiments) 49
Figure 4.3 Geometrical set ups of the different scenarios (detail of model domain from 1.5 m < X < 4.0 m), the cross marks infiltration point, black horizontal bars mark impermeable layers, overlaid by discretisation grid 52
Figure 4.4 Area of interest (AOI) of laboratory experiment with v_w = 21.25 m/d overlaid by results of model calibration (isolines showing modelled DNAPL saturation of the model domain) at t = 3 690 s 53
Figure 4.5 Simulated TCE saturation at v_w = 0.00 m/d (base case scenario) and v_w = 40.00 m/d. The uneven spreading front of the percolation path is caused by the discretization of the model domain (Erning et al., 2010) 54
Figure 4.6 Spatial position of TCE at t = 6 000 s (end of infiltration period) for alternating groundwater flow velocities and subsurface geometries, cross marks infiltration point, detail of model domain (1.5 m < X < 4.0 m), applied geometries in columns, applied flow velocities in rows. 56
Figure 4.7 Spatial position and length of the DNAPL pool at t = 24 000 s 57
Figure 4.8 Box whisker plots of a) start position of DNAPL pool, b) pool length, showing minimum & maximum (whiskers), 25th quartile & 75th quartile (length of box), and median 58

Figure 5.1 Potential pathways for DNAPLs at the Rho site: a) potential transport of DNAPL by streaming groundwater prior to / after installation of encapsulation including potential passage to deeper aquifer through a hydraulic connection b) migration through aquitard prior to / after installation of encapsulation, passage as free phase into deeper aquifer c) migration into aquitard, storage as free phase in aquitard, dissolution into deeper aquifer 66
Figure 5.2 Sketch of principle methodology of model driven site assessment 67
Figure 5.3 Position of industrial site and Pump & Treat facility (Coordinates in GAUSS-BOAGA; source: GOGGLE EARTH, 2010, edited) 68
Figure 5.4 Example of varying models based on different classification of primary dataset: a) distribution of hydraulic defined Aquitard. b) Distribution of geological defined aquitard, consisting of silt and clay layers. Detail of model domain. 70

Figure 5.5 Topography and thickness of assumed ubiquitous Aquitard on top of the Prima Falda (cut off at depth = 125 m), Superficiale not shown, height super-elevated by factor 15 70
Figure 5.6 Spatial position of TCE at t = 6 000 s (end of infiltration period) for increasing groundwater flow velocities and subsurface geometries, cross marks infiltration point, detail of model domain (1.5 m < X < 4 m), groundwater flow from left to right 72
Figure 5.7 Lateral distribution of TCE in scenarios aquitard A - D at the time steps 25 yrs, 50 yrs and 75 yrs, at v_w = 0 m/d and v_w = 1 m/d and with seepage periods (spill times) of 25 years and 50 years. 75

Figure 6.1 Area of interest, overlaid by aerial picture (adapted from Google Earth, 2010), coordinates in Gauss-Boaga.....80
Figure 6.2 Perspective view of Modflow model, all hydraulic units, z magnification 1 : 25.....82
Figure 6.3 Perspective view of Aquitard and Prima Falda (Superficiale not shown), z-magnification 1 : 25 83
Figure 6.4 2D cross section converted for multiphase modeling 84
Figure 6.5 Spatial distribution and saturation of DNAPL at varying material compositions and groundwater flow velocities for eight varying scenarios (2a_0, 2e_0, 2a_1, 2e_1, 4a_0, 4e_0, 4a_1and 4e_1) after 50 years and 75 years
a) at t = 50 a & v_w = 0 m/d, b) at t = 50 a & v_w = 1 m/d, c) at t = 75 a & v_w = 1 m/d and d) at t = 75 a & v_w = 1 m/d 88
Figure 6.6 Spatial distribution of mobile TCE_{NAPL} (S_{TCE} > 0.05) as isolines and Center of Mass as dots of all conducted scenarios (z-magnification 1 : 25) 91
Figure 6.7 Variance in position of centre of mass at t = 75 a for v_w < 0m/d (Vel1), 0 m/d < v_w < 1 m/d (Vel2) and $v_w \geq$ 1 m/d (Vel3) 92
Figure 6.8 Boxplots of effects of groundwater flow velocity on mass of TCE at time steps 25 a, 50 a and 75 a for v_w < 0m/d (Vel1), 0 m/d < v_w < 1 m/d (Vel2) and $v_w \geq$ 1 m/d (Vel3).....92
Figure 6.9 Boxplots of effects of groundwater flow velocity on volume of TCE at time steps 25 a, 50 a and 75 a for v_w < 0m/d (Vel1), 0 m/d < v_w < 1 m/d (Vel2) and $v_w \geq$ 1 m/d (Vel3) 93

List of Tables

Table 1.1 Statistic of contaminations in Germany per federal state (after Umweltbundesamt, 2011) 2
Table 1.2 Physico-chemical properties of selected chlorinated solvents at t = 25 °C (* = 20 °C) 11

Table 2.1 Material parameters of the artificial porous media (provided by Luciano et al., 2010) 25
Table 2.2 Physico-chemical properties of HFE-7100 and TCE 25
Table 2.3 Boundary conditions of the laboratory experiments (Luciano et al. 2010) 25
Table 2.4 Hydrogeological parameters at the Rho Site based on literature studies (Beretta et al., 2005; Bozzano et al., 2007; Leccese et al., 2007) 27

Table 3.1 Impacts of groundwater flow velocities on DNAPL distribution in the saturated zone at t = 24 000 s 41

Table 4.1 Material parameters of the artificial porous media (provided by Luciano et al. 2010) 47
Table 4.2 Physico-chemical properties of HFE-7100 and TCE 48
Table 4.4 Determined parameters for capillary pressure and relative permeability 50
Table 4.5 Material parameters of the model domain 50

Table 5.1 Hydrogeological parameters at the Rho Site supplied by different literature studies of previous investigations 69
Table 5.2 Material parameters of the different applied aquitards 73

Table 6.1 Range of hydrogeological parameters at the Rho Site from, provided by literature studies (Beretta et al., 2005; Bozzano et al., 2007; Leccese et al., 2007) 81
Table 6.2 Material parameters of scenario modeling 85
Table 6.3 Combination of parameters for scenario modeling 86

List of Abbreviations

α_P	Parker scaling parameter [-]
α_{VG}	Van Genuchten scaling parameter [-]
cis-DCE	Cis-1,2-Dichloroethylene
d	Effective pore diameter [m]
DNAPL	Dense non-aqueous phase liquid
DCM	Dichloromethane
dh/dl	Gradient of hydraulic head
ϵ	Mualem parameter for pore connectivity, in general $\epsilon = \frac{1}{2}$ (Kueper and Frind, 1991)
F_β	Darcy flux of phase β [m/s]
g	Annotation for gaseous phase
G	Magnitude of gravitational acceleration [m/s²]
γ_{VGM}	Mualem parameter for pore connectivity, in general $\gamma = \frac{1}{3}$ (Kueper and Frind, 1991)
k	Intrinsic permeability [m²]
k_f	Hydraulic conductivity [m/s]
KORA	Research project *Kontrollierter natürlicher Rückhalt und Abbau von Schadstoffen bei der Sanierung kontaminierter Grundwässer und Böden*, financed by Bundesministerium für Bildung und Forschung, BMBF, Duration 2002-2007
k_r – S	Relative permeability – saturation function
$k_{r\beta}$	Relative permeability for phase β
$k_{r\beta}k$	Effective permeability for the given phase β in the respective medium [-]
λ_{BC}	Brooks & Corey scaling parameter [-], generally $0.2 < \lambda_{BC} < 3$ (Helmig, 1997)
LNAPL	Light non-aqueous phase liquid
m amsl	Meter above mean sea level
m bgl	Meter below ground level
MCL	Maximum concentration level [mg/l]
ModelPROBE	*Model driven soil probing, site assessment and evaluation*, financed by European Union under the 7th European Framework, Duration: 2008-2012
m_{VG}	Van Genuchten scaling parameter [-]
m_P	Parker scaling parameter $m_P = 1 - \frac{1}{n_P}$ [-]
μ_β	Dynamic viscosity of phase β [Pa s]
n	Annotation for non-wetting phase, generally gas
NAPASAN	Research project *Einsatz von Nano-Partikeln zur Sanierung von Grundwasserschadensfällen*, financed by Bundesministerium für Bildung und Forschung, BMBF, Duration 2010-2013
n_P	Parker scaling parameter [-]
n_S	Stone scaling parameter [-]
n_{VG}	Van Genuchten scaling parameter [-]

NAPL	Non-aqueous phase liquid
q	Darcy flux [m/s]
Q	Volumetric discharge [m^3/s]
PCE	Perchloroethylene
P	Pressure [Pa]
P_β	Fluid pressure of phase β [Pa]
$P_{c\beta}$	Capillary pressure [Pa]
P_c – S	Capillary pressure – saturation function
$P_{c\,nw}$	Capillary pressure between NAPL – water [Pa]
$P_{c\,gw}$	Capillary pressure between gas – water [Pa]
$P_{c\,gn}$	Capillary pressure between gas – NAPL [Pa]
P_d	Entry pressure [Pa]
REV	Representative Elementary Volume
RUBIN	Research project *Reinigungswände und –barrieren im Netzwerkverbund. Anwendung von Reinigungswänden für die Sanierung von Altlasten* financed by Bundesministerium für Bildung und Forschung, BMBF, Duration RUBIN I 2000 – 2006, RUBIN II 2006-2009
ρ_β	Density of phase β [kg/m^3]
ρ_w	Density of water [kg/m^3]
S_β	Saturation of phase β
S_e	Effective saturation [-]
$\overline{S_l}$	Effective liquid saturation [-]
S_m	Minimum / irreducible wetting saturation [-]
S_n	Saturation of non-wetting phase, generally gas [-]
SOILCAM	Research Project *Soil Contamination: Advanced intergrated characterisation and time-lapse monitoring*, financed by European Union under the 7th European Framework, Duration: 2008-2012
S_w	Water saturation [-]
$\overline{S_w}$	Effective water saturation [-]
S_{wr}	Residual water saturation [-]
TCE	Trichloroethylene
t-DCE	Trans-1,2-Dichloroethylene
US EPA	US Environmental Protection Agency
VC	Vinyl chloride
v_w	Pore velocity of water [m/d]
w	Annotation for wetting phase

1 Introduction

1.1 Reason and incentive

Many industrial sites worldwide are contaminated with toxic chemicals due to accidents or improper handling over long time periods. The major group of contaminants is composed of volatile chlorinated hydrocarbons as e.g. chlorinated solvents. Due to their widespread application in various industrial areas since the 1920s, they are the most common groundwater contaminations worldwide (Pankow and Cherry, 1996; Teutsch et al., 1997; Grandel and Dahmke, 2008). Most chlorinated solvents are so-called Non-Aqueous Phase Liquids (NAPL), defined as a liquid immiscible with water at standard conditions. Based on the density of NAPLs, they are either categorized as Dense Non-Aqueous Phase Liquids (DNAPL) or Light Non-Aqueous Phase liquids (LNAPL), depending on their density relative to the density of water.

Especially DNAPLs pose a significant threat to the environment and human health due to their physico-chemical behavior and their toxicity (cp. *Chapter 2*). When released into the environment, they seep away into the subsurface, forming long-term source zones of contamination as distinct NAPL phase and causing long plumes of dissolved contaminants in the groundwater. Plumes emanating from DNAPL source zones can reach lengths of several hundreds of meters (Teutsch et al., 1997).

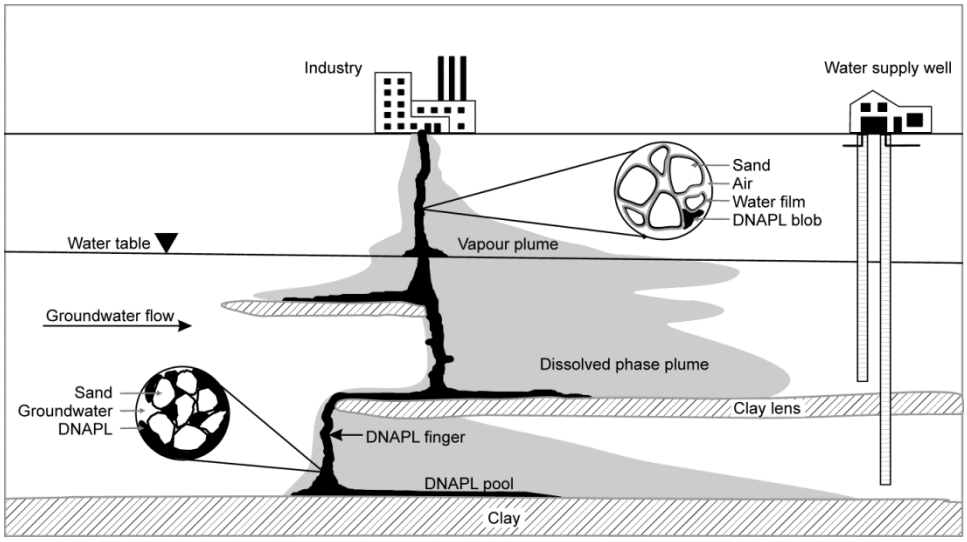

Figure 1.1 Principles of DNAPL distribution in the subsoil (after Domenico & Schwartz, 1990)

In the USA, chlorinated solvents are among the most common DNAPLs causing groundwater contamination (Moran et al., 2006), being present in 17 % of all wells investigated by the US Geological Survey´s National Water-Quality Assessment Program (Gilliom et al., 1995). More than 30 % of the groundwater samples taken contained mixtures of several chlorinated solvents. In its Toxic Release Inventory, the US Environmental Protection Agency (US EPA) listed a total release of ca. 1 800 t of perchloroethylene (PCE) and of ca. 5 000 t trichloroethylene (TCE) onshore and offshore for the years 1998 – 2001 (Hassanizadeh et al., 2004).

In Germany, more than 14 200 contaminated sites (legal term “Altlast”, table 1.1) are registered at the Umweltbundesamt (Umweltbundesamt, 2011), of which 64 % are contaminated with chlorinated solvents (Teutsch et al., 2001; Grandel and Dahmke, 2008). Therefore the following chapters are restricted to the group of chlorinated solvents as typical DNAPL – compounds, although some chlorinated solvents are gases at standard conditions, as e. g. vinyl chloride (VC), chloroethane and chloromethane (CM).

Table 1.1 Statistic of contaminations in Germany per federal state (after Umweltbundesamt, 2011)

Federal state / Germany	Finished remediation of contaminations in 2011	Current contaminations	Contaminations currently in remediation	Contaminations currently monitored
Baden-Württemberg	2624	2219	620	435
Bayern	1658	1051	966	85
Berlin	191	937	71	72
Brandenburg	4073	1476	131	234
Bremen	621	408	42	167
Hamburg	426	533	147	140
Hessen	880	436	236	51
Mecklenburg-Vorpommern	1155	999	359	396
Niedersachsen	1597	3482	381	535
Nordrhein-Westfalen	6158	-	-	-
Rheinland-Pfalz	128	296	168	58
Saarland	156	456	35	64
Sachsen	2927	627	434	1474
Sachsen-Anhalt	1680	186	71	50
Schleswig-Holstein	974	320	66	54
Thüringen	837	783	191	71

contamination = legal term "Altlast" in German

Remediation of contaminations due to chlorinated solvents prove to be extraordinary difficult. They are hard to detect, hard to remove and neither biologically nor chemically easy to degrade, resulting in long-term risk potential.

A typical example for complex contamination, challenging site investigation and difficult site remediation is the former industrial area Chimica di Bianchi in Rho, Italy. Nearly eighty years of industrial use and over twenty years of containment and remediation actions did not significantly improve the water quality at the site. The long-term industrial production of dyes led to a heavy contamination of the aquifers at the site mainly with the DNAPLs trichloroethylene (TCE) and perchloroethylene (PCE). Although the former hot spot of the contamination, an open disposal basin, was encapsulated in the 1980s and a well gallery is capturing the plume, concentrations of dissolved TCE are still unchanged high in the deeper one of the two aquifers at the site. It is postulated, that a DNAPL pool with unknown position acts as long time source zone for the plume.

Aim of this thesis is to model DNAPL pathways over the whole time time frame of activities of industrial production as well as of remediation activities above ground at the site in order to deliver supplementary information for the site investigation and site remediation teams. Information delivered by scenario modeling can answer most prominent open questions at a

site, helping to plan next steps of site investigation and site remediation in a more time and cost efficient way.
Based on the already existing information about the site, e.g. geological and hydrogeological information of former site investigation campaigns, the possible current position and amount of remaining DNAPLs shall be assessed by multiphase modeling.
But, as it is a real field site and not a simplified laboratory experiment, basic principles of DNAPL migration in the subsoil have to be investigated first, before being able to conduct models of a realistic field scale. The main challenges can be categorized as four issues and resulting questions:

Issue 1 – Documented natural groundwater flow velocities at many industrial sites are much higher than typical groundwater flow velocities investigated in already conducted laboratory experiments and scenario models. Groundwater flow can furthermore be increased, when Pump & Treat facilites operate at the sites. At the former industrial site Chimica di Bianchi natural groundwater flow velocities are approximately 1 – 2 m/d and several wells are capturing the plume of dissolved contaminants.

Could increased groundwater flow velocities have affected the position of the DNAPL source zone?

Issue 2 – Geological descriptions of hydraulic units as aquifers and aquitards vary generally by several orders of magnitude in reality. At the site Chimica di Bianchi, the geological description of the present aquitard includes mixtures of silty sand, sandy silt, silty clay and pure clay, and acting as overall impermeable layer for groundwater. In general groundwater aquitards are assumed to be effective barriers for vertical DNAPL movement.

Are the assumed aquitard materials also impermeable for DNAPLs?

Issue 3 – Spatial information about the distribution of hydraulic units is generally sparse, because traditional site investigation is mostly drilling and only in single cases supported by geophysical areal investigations. The distribution of geological units has to be interpolated in most cases from point data (bore-logs, borehole informations). At Chimica di Bianchi in Rho it is assumed that the impermeable material of the aquitard is omnipresent at the site, but geological modeling conducted in this study indicate that the aquitard may have several missing areas.

Is it possible that the DNAPL migrated through a gap in the aquitard to the deeper aquifer?

Issue 4 – Aquitards and low permeable units are in reality charcterized by complex morphological features, as depressions, trenches, ridges and eroded areas. Assuming an omnipresent, impermeable aquitard at the site Chimica di Bianchi, the surface of this aquitard shows typical subsurface morphology with trenches, depressions and ridges.

What are the influences of subsurface morphologies on the DNAPL movement and its final position?

Addressing these issues in a combined four step investigation process, the current position of the DNAPL at the Rho site can possibly be approximated. Moreover, the basic principles and questions, which are addressed at the Rho site, appear at many brownfield sites worldwide. They cover the typical problems every site investigation team encounters. Results gained in this thesis can easily be applied to similar sites, improving the knowledge about long-term source zones in the subsoil.
The investigations performed at the former industrial site Chimica di Bianchi are integrated in the EU - project ModelPROBE - *Model driven soil probing, site assessment and evaluation* (7^{th} European framework), which develops and improves innovative low-invasive site investigation techniques for an iterative site investigation progress as new cost and time efficient tools.

1.2 Structure and scope of the thesis

The current knowledge about DNAPLs, especially chlorinated solvents, is summarized in the following introductionary chapters. They provide a short overview of the history of production and usage (*Chapter 1.3*), current research focus and the project ModelPROBE (*Chapter 1.4*), physico-chemical properties and toxicology of chlorinated solvents as typical DNAPLs in *Chapter 1.5* and *1.6*. The general principles of DNAPL movement as well as the mathematical formulation for calculation applied in this thesis are presented in *Chapter 1.7*, which also includes the summary of the already internationally conducted research about the influence of heterogeneities and groundwater flow velocities on DNAPLs.
Chapter 2.1 shortly lists the features and restrictions of the applied software bundles TMVOC, PetraSim and GMS. *Chapter 2.2* presents the primary data that is the base for the modeling. It contains a brief description of the laboratory experiments conducted and published by Luciano et al (2010), which are the basis for the calibration of the multiphase model. A short overview of the results of the literature study concerning the site Chimica di Bianchi is included. The following *Chapter 2.2.3* presents the already existing geological and hydrogeological information of the former industrial area Chimica di Bianchi. The data-set contains more than 250 boreholes in the area and data of monitoring campaigns of nearly 20 years. Based on the borehole data-set, structural geological models of the geological material classes as well as of the hydraulic units were conducted in order to identify subsurface morphology and potential gaps in the aquitard. The structural 3D models of the site are presented and discussed in detail in *Chapter 2.3*.
The results of the investigations performed are presented in the following chapters.
Chapter 3 addresses *Issue 1 – "Could increased groundwater flow velocities have affected the position of the DNAPL source zone?"* and governs the calibration of the multiphase model by means of the conducted laboratory experiments and the influence of high groundwater flow velocities on the position of the DNAPL in a homogeneous and planar scenario. The work is published as:

Erning, K., Schäfer, D., Dahmke, A., Luciano, A., Viotti, P. and Petrangeli Papini, M. (2009): Simulation of DNAPL infiltration into groundwater with differing flow velocities using TMVOC combined with PetraSim. TOUGH Symposium 2009. Proceedings TOUGH Symposium. LBNL. Berkeley, CA, USA.

Erning, K., Schäfer, D., Dahmke, A., Luciano, A., Viotti, P. and Petrangeli Papini, M. (2010a): Simulation of DNAPL distribution depending on groundwater flow velocities using TMVOC. In: M. Schirmer, E. Hoehn and T. Vogt (Editors). IAHS Publication: Groundwater Quality Management in a Rapidly Changing World. Proceedings of the 7th International Groundwater Quality Conference held in Zurich, Switzerland, 13-18 June 2010. Red Books. IAHS. Oxfordshire. pp. 128-131.

Erning, K., Schäfer, D., Dahmke, A., Luciano, A., Viotti, P. and Petrangeli Papini, M. (2010b): Simulation of DNAPL distribution depending on groundwater flow velocities using TMVOC. International Groundwater Quality Conference 2010. Zurich, Switzerland.

The next step includes the influence of groundwater flow velocities and subsurface geometries, which were represented by a layering of different material sets in the model. The results are presented in *Chapter 4* and are published as:

Erning, K., Schäfer, D., Grandel, S., Dahmke, A., Luciano, A., Viotti, P. and Petrangeli Papini, M. (2010c): Model investigation of DNAPL distribution in the saturated zone for varying groundwater flow velocities and subsurface geometry. ConSoil 2010. Salzburg, Austria.

Erning, K., Grandel, S., Dahmke, A. and Schäfer, D. (2012): Simulation of DNAPL infiltration and spreading behaviour in the saturated zone at varying flow velocities and alternating subsurface geometries. Environmental Earth Sciences 65(4): 1119-1131.

Issue 2 – "Are the assumed aquitard materials also impermeable for DNAPLs?" is addressed in *Chapter 5*. It includes the project report performed for the research project ModelPROBE and investigates the possible implications of the formerly conducted research for the field site on a simplified model. It is published as:

Erning, K. and Schäfer, D. (2011): Multiphase model driven site assessement of the former industrial facility Chimica di Bianchi in Rho / Italy. In: M. Kästner (Editor). ModelPROBE report second period (12/2009-05/2011): Workpackage 9.2: Field Demonstration and Cross Validation. pp. 187-197.

Issue 3 – "Is it possible that the DNAPL migrated through a gap in the aquitard to the deeper aquifer?" and *Issue 4 – "What are the influences of subsurface morphologies on the DNAPL movement and its final position?"* are addressed in *Chapter 6*.
The influence of varying groundwater pore velocities, the hydraulic gradient, material composition of aquifers and aquitard and of the subsurface morphology of the aquitard are investigated with respect to their impact on the position and mass of the DNAPL. Statistical analyses were performed in order to identify sensitive parameters. Implications for similar field sites are drawn. The work is going to be submitted to the journal **Italian Journal of Engineering Geology and Environment** as:

Erning, K., Dahmke, A. and Schäfer, D. (2013 (submitted)): Multiphase modeling of the impact of groundwater flow velocities on DNAPL migration in the multi-aquifer formation of Rho, Italy. Italian Journal of Engineering Geology and Environment.

Chapter 7 summarizes and discusses the results of the conducted research, highlights main advantages as well as main points of criticism and concludes with a perspective for the application of multiphase modeling as a future field site investigation tool.

1.3 Historical overview

Production and distribution of chlorinated solvents in Germany is documented for the first time in the 1930s (Grandel & Dahmke, 2008). The main products tetrachloroethylene (PCE) and trichloroethylene (TCE) were used in chemical dry cleaning and in broad applications in metallurgy, with increasing consumption since the 1960s. In the 1970s, groundwater contaminations with chlorinated solvents were detected for the first time. Increasing knowledge about the occurrence of chlorinated solvents in groundwater was gained in the beginning of the 1980s, as technical advances in analytical chemistry enabled detection of concentrations in the range of µg/l, causing growing risk awareness.
In 1986 volatile organic hydrocarbons were categorized as substances hazardous to water ("wassergefährdende Stoffe") in Germany. From then on, their use and distribution has been restricted by the federal law (Grandel and Dahmke, 2008) and drinking water levels have been defined as 0.01 mg/l. The US EPA published 1987 the drinking water value for TCE as 0.005 mg/l (Pankow and Cherry, 1996). In the same period Schwille (1988) conducted fundamental research about the occurrence, distribution, and behavior of chlorinated solvents in the saturated zone, exploring their long-term risk potential.
Since the end of 1980s, the general knowledge grew that volatile organic hydrocarbons exist as a distinct free phase (NAPL) in the saturated zone (e.g. Mackay et al., 1985; Mercer & Cohen, 1990; Schwille, 1988, Feenstra et al., 1996, Mackay et al., 1991). Before that time it was assumed that chlorinated solvents enter the subsoil as dissolved components in seepage water.
Currently it is known, that chlorinated solvents are mainly present as DNAPLs in the saturated zone, forming long-term source zones in aquifers and aquitards (Kavanaugh et al., 2003; Grathwohl, 2006), which is the main reason for the difficult remediation, e.g. the ineffectiveness of conventional remediation actions by Pump & Treat (Mackay and Cherry, 1989; National Research Council (NRC), 1994; Stroo et al., 2003).

1.4 Recent research focus on site investigation and site remediation

Over the last 30 years intensive research was conducted on potential DNAPL remediation. Several national and international research projects investigated and tested new methods of site clean-up, as for example natural attenuation (KORA), reactive permeable barriers (RUBIN), air sparging, thermal treatment combined with soil vapor extraction, nano-iron (NAPASAN), chemical oxidation and phytoremediaton. But most of these techniques are designed to remediate the plume of dissolved chlorinated solvents, because either the position of the source zone is unknown in detail or the concentrations in the source zone are too high for

possible remediation. In its 2003 published report on DNAPL remediation, the U.S. EPA stated that:
"[...] because of the risk of failure in achieving certain regulatory targets after implementing a source-depletion technology [...], combined with ***uncertainties in site characterization (i.e., the location and amount of DNAPL in groundwater at a site),*** *[...], in prediction of life cycle costs, and uncertainties regarding the acceptability of alternative clean-up levels, many site owners have been reluctant to undertake aggressive source-depletion technologies.Thus, at the majority of DNAPL sites,* ***containment of the source zone*** *and/or* ***management of the dissolved plume for cost-effective risk/liability reduction*** *and regulatory compliance have been the dominant strategies of choice."*

Therefore, recent and current research and development projects such as ModelPROBE or Soilcam specifically aim for a more effective and efficient localization and characterization of contaminations in the subsurface, because the unknown position and unknown mass of contaminants create huge uncertainties for site remediation action plans.

The ModelProbe project aims for the development and improvement of innovative site investigation methods at a wide variety of contaminated sites. The methods rely on a cyclical approach, with the intent of short feedback-loops in order to create a time and cost efficient approach for modern site assessment. In most cases, the conventional approach of site characterization consists of a one-way investigation line of drilling, sampling, analysis of samples and decision making. This approach is well known and its data and results are considered reliable. But the numbers of drillings and samples are often limited by time and finances at disposal, even if the site would require much more detailed information for a thorough risk assessment. Therefore smart feedback-loops in a new integrated cycle of site assessment are investigated within ModelPROBE in order to improve site assessment (figure 1.2).
The ModelPROBE approach consists of (Kästner et al., 2012):

- a toolbox of innovative investigation techniques allowing for short-term (on-site) feedback-loops in order to adapt investigation concepts frequently based on the most recent data
- a series of methods to interpret and assimilate data gained by multiple techniques and
- an overall cyclical approach to design field investigation campaigns in a sophisticated and structured way.

The multiphase modeling may prove itself as a supplementary data processing technique, with the possibility to give supporting information about data gaps, uncertainties regarding geological parameters or distribution of contaminants. It can theoretically be implemented after the first step of site investigation improving the decision making process for planning of the next investigation cycle. Based on the available primary data of the site, it may even be possible to improve the approximation of the position and amount of contaminants and their behavior during site remediation as e.g. pump and treat (figure 1.3):

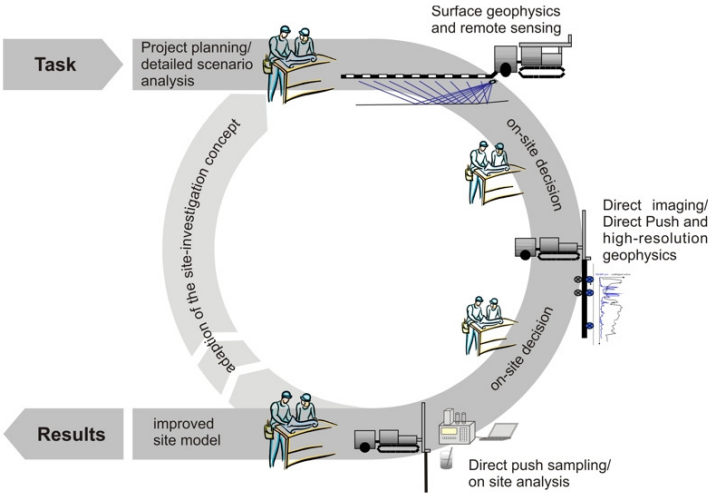

Figure 1.2 Techniques and methods covered by ModelPROBE and their application within an idealized cyclical approach (P. Dietrich, MOSAIC; http://www.ufz.de/index.php?de=16349)

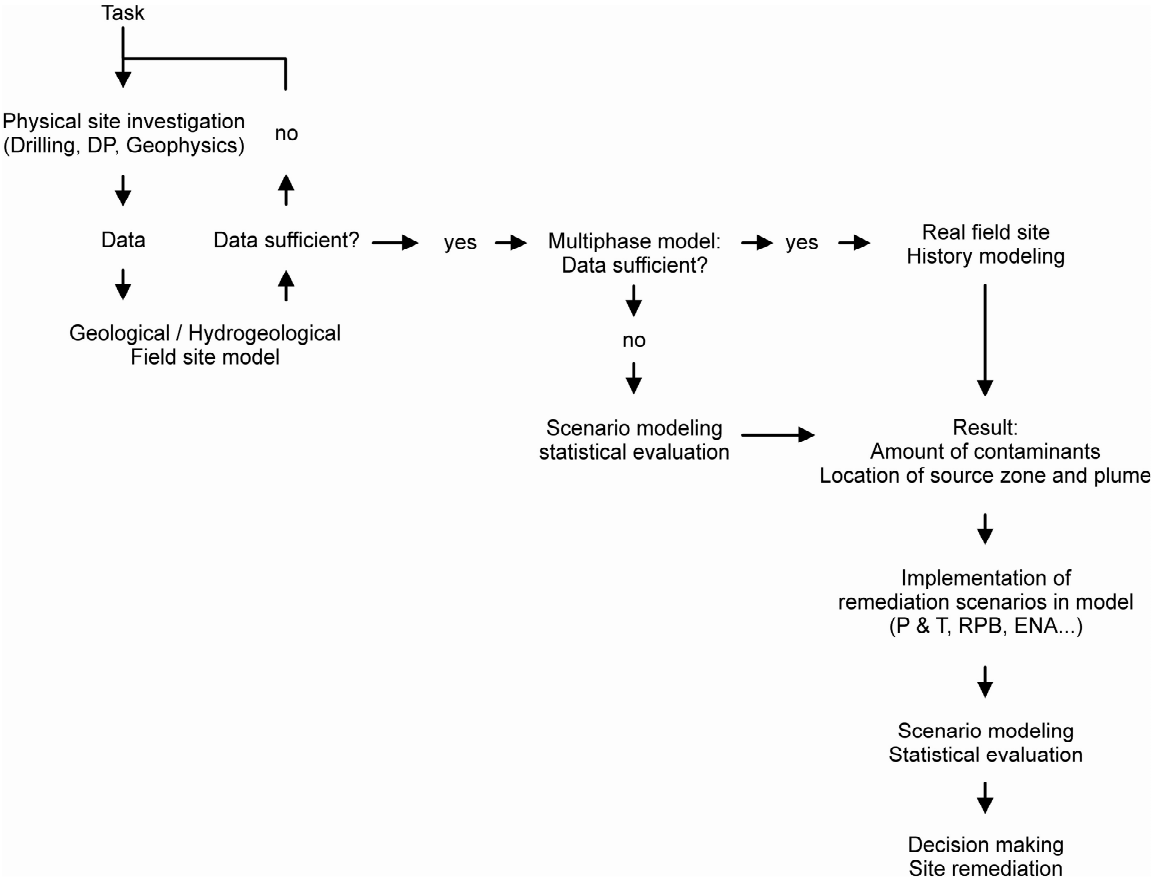

Figure 1.3 Sketch of principle methodology of model driven site assessment

1.5 Physico-chemical properties of DNAPLs

Dense Non-Aqueous Phase Liquids (DNAPLs) comprise a group of fluids that have a density higher than water. Typical DNAPLs are chlorinated solvents, polychlorinated biphenyles,

coal tar, creasote and extra heavy crude oil. Typical compounds of chlorinated solvents are Tetrachloroethylene (PCE), Trichloroethylene (TCE), 1,1,1-Trichloroethane, Dichloromethane (DCM), Trichloromethane (Chloroform), Carbon tetrachloride (CT), 1,2-Dichloroethane, 1,2-Dichlorobenzene, 1,3-Dichlorobenzene, 1,1,2-Trichloroethane and 1,1,4-Trichlorobenzene.

In general, chlorinated solvents have a high volatility. Historically this led to the misbelief that openly disposed chlorinated solvents would evaporate to the atmosphere. But it is known since the 1980s (Pankow and Cherry, 1996) that major amounts infiltrated the subsurface and were transported across the capillary fringe to the saturated zone. The transport across the capillary fringe can be extremely slow, which complicates remediation (McCarthy and Johnson, 1992). High volatility increases the risk of inhaling and can cause serious damage to the health (cf. *Chapter 1.6*).

Densities of chlorinated solvents range from 1.2 g/cm^3 to 1.7 g/cm. If enough liquid is spilled, DNAPLs can penetrate the capillary barrier of the capillary fringe and infiltrate into groundwater. Once within the saturated zone, vertical movement of the DNAPL is predominant and complicates site remediation actions (Pankow and Cherry, 1996).

The low viscosity of most DNAPLs in combination with the high density enhances rapid downward movement within the subsoil (Cohen and Mercer, 1993). Moreover, the viscosity of DNAPLs decreases further with increasing temperatures.

The movement in the subsoil is furthermore enhanced by their low interfacial tension. It promotes the entrance into small pore spaces and fractures and complicates the removal (Pankow and Cherry, 1996). The absolute solubilities of most chlorinated solvents ranges at 1 mg/l, which causes longevity of fingers, blobs and pools of DNAPLs (cf. figure 1.1 and *Chapter 1.6.1*) in the range of decades to centuries in the subsoil (Johnson and Pankow, 1992). But comparing the absolute solubilities of chlorinated solvents to the levels of drinking water standards, their maximum solubility is still far above acceptable levels (table 1.2).

Chlorinated solvents bind only weakly to soil particles due to their low partitioning to the soil-matrix. Retardation capacities of soils are therefore not significant.

Chlorinated solvents are not easily degradable, neither by biological nor by abiotic-chemical processes. Degradation process is generally in terms of decades or longer, but can chemically or biologically be enhanced.

1.6 Ecotoxicological potential of selected chlorinated solvents

Due to the historical usage, only PCE, TCE and their degradation products cis-DCE and vinyl chloride are presented in detail. For ecotoxicological potential of the other chlorinated solvent, please consult the GESTIS Stoffdatenbank (Institut für Arbeitsschutz der Deutschen Gesetzlichen Unfallversicherung (IFA), 2012). Generally, chlorinated solvents can cause irritation of the respiratory tract, the eyes and the epidermis. They can harm the liver, the kidney and the central nervous system. Some chlorinated solvents are suspected and / or known to be cancerogenic and mutagenic.

1.6.1 Tetrachloroethylene (PCE)

PCE is a colorless, ethereal non-combustible, volatile liquid at standard conditions. It causes acute or chronic health hazards and is hazardous to the aquatic system (Pozzani et al., 1959). The main intake pathways for PCE are via the respiratory tract or through the skin. Inhaled PCE reaches the blood via the lung and it is easily absorbed via the intact skin. Acute toxic effects are irritation of the mucous membranes and skin, disturbance of the central-nervous system and damage to the liver and the kidneys at high exposure rates. Chronic toxic effects comprise disturbances of the central-nervous system as well as functional disturbances of the liver and the kidneys. In poisoning cases, drunkenness, unconsciousness, motoric, sensory and tropic disturbances to the extremities, symptoms in the airways (cough, dyspnoea), collapse and signs of damage to the liver and kidneys were also registered. PCE is suspected to cause a risk of impairment of the reproductive capability and the development of the embryo or fetus. Moreover, it is potentially cancerogenic, based on studies on rats and mice (Institut für Arbeitsschutz der Deutschen Gesetzlichen Unfallversicherung (IFA), 2012)

1.6.2 Trichloroethylene (TCE)

TCE is a colorless, sweetish-ethereal non combustible liquid at standard conditions. Main route of exposure is via inhalation. It can also penetrate the skin, but is not under suspicion to contribute via this intake route to inner exposures at normal conditions. The rate of absorption via the gastrointestinal tract is high because TCE easily penetrates the mucous membranes. Acute toxic effects are irritation of the skin and the mucous membrane, neurotoxic effects and disturbances of the heart / circulatory system. Chronic toxic effects comprise irritation of the respiratory tract, inflammation of the skin and disturbances of the heart functions (Institut für Arbeitsschutz der Deutschen Gesetzlichen Unfallversicherung (IFA), 2012). Acute inhalative toxicity includes dizziness, headache, and blurred vision, disturbances to the coordination, confusion, tremor, nausea, vomiting and sleepiness. Additional, cardiac arrhythmia and metabolic changes are possible. In extreme cases, paralysis of the respiratory system and the circulatory centre as well as damage to kidneys and liver can happen. Oral poisoning can cause coma and death. Principal symptoms of serious oral poisoning are: abruptly occurring unconsciousness, cerebral coma, centrally conditioned respiratory paralysis, disturbances to functions of the heart (arrhythmia) and liver (Moeschlin, 1986). Long-term exposure to TCE causes irritation of the airways, headaches, double vision, disturbances to the coordination, anxiety, dizziness, weakness and tremor. It can also lead to chronic damage to the livers. TCE is cancerogenic.

1.6.3 Cis-Dichloroethylene (cis-DCE)

Cis-DCE is a colorless, ethereal, highly inflammable liquid with acute or chronic hazards to health and environment. Main route of exposure is the respiratory tract. Acute toxicity is caused by irritation of the skin and the mucous membranes, cloudiness of the cornea, sleepiness, dizziness, nausea, ataxia and tremor (Institut für Arbeitsschutz der Deutschen Gesetzlichen Unfallversicherung (IFA), 2012). Chronic toxicity covers loss of appetite and weight, fattening of liver and kidney and irritation of the gastrointestinal system. Additionally, Cis-DCE is potentially genotoxic.

Table 1.2 Physico-chemical properties of selected chlorinated solvents at t = 25 °C (* = 20 °C)

	Molar mass [g/mol]	Density [g/cm³]	Absolute / Dynamic viscosity [cP]	Kinematic viscosity [cS]	Vapor pressure [kPa]	Boling point [°C]	Solubility [g/L water]	Interfacial tension phase- water [dyn/cm]	Interfacial tension phase- air [dyn/cm]	Partition coefficient octanol - water [log K ow]	Sorption coefficient log K_{oc} (l/kg) at 20 - 25° C	Drinking water limits (Prüfwert) Germany [mg/L water] (1)	Drinking water limits USA MCL [mg/L] (2)
Tetrachloroethylene (PCE)	165.80	1.63	0.90	0.54	2.50	121.10	0.14*	44.40	32.86	2.88	2.43	-	0.005
Trichloroethyle ne (TCE)	131.40	1.46	0.57	0.39	10.00	0.87	1.10*	34.50	29.50	2.42	1.26	-	0.005
cis-1,2-Dichloroethylene (cis -DCE)	96.90	1.28	0.48	0.38	28.20	0.60	0.80*	30.00	24.00	1.86	1.38	0.05	0.07
trans-1,2- Dichloroethylene (t -DCE)	96.90	1.26	0.40	0.32	40.70	0.48	0.60*	30.00	24.00	2.09	1.46	-	0.1
Vinyl chloride (VC)	62.50	0.91*	-	-	354.80	-13.70	1.60*			1.27	0.39	0.0005	0.002
1,1,1-Trichloroethane	133.40	1.35	0.84	0.62	16.60	73.90	0.87*	45.00*	28.28	2.49	2.45	-	0.2
1,1,2-Trichloroethane	133.40	1.44	1.19	0.83	4.00	113.60	3.97		37.40	2.34	1.75	-	0.005
1,1-Dichloroethane	99.00	1.17	0.50	0.43	30.90	57.30	5.10*		27.03	1.79	1.76	-	-
1.2-Dichloroethane	99.00	1.25	0.84	0.67	11.20	83.60	8.60*	30.00	35.43	1.46	1.76	0.003	0.005
Chloroethane	62.40	0.92*	-	-	1.34	12.30	5.70*			1.40	1.25	-	-
Carbontetrachloride (CT)	153.80	1.59	0.97	0.61	14.40	76.70	0.81*			2.77	2.67	-	0.005
Trichloromethane (Chloroform, CF)	119.40	1.48	0.56	0.38	25.10	61.40	8.30*	32.80*	29.91	1.95	1.93	0.05	0.08
Dichloromethane (DCM)	84.90	1.33	0.44	0.32	57.50	40.10	17.00*	28.30*	30.41	1.31	1.23	-	0.005
Chloromethane (CM)	50.50	0.92*	-	-	575.40	-24.20	7.20*			0.91	1.40	-	-
Sum of chlorinated solvents												0.01 (1) / 0.01 (3)	-

(1) Bundesrep ublik Deutschland (1999)
(2) US EPA (2012)
(3) Instituto Superiore per la Protenzione e la Ricerca Ambientale (2006)

1.6.4 Vinyl chloride (VC)

VC is a colorless, sweetish, extremely flammable gas under normal conditions with acute and chronic health risk. Main route of exposure is inhalation. Acute toxic effects by contact with the under cooled liquefied VC are injuries to the skin and the mucous membranes. Possible hazards at high exposure levels to gaseous VC are narcotic effects, depression of the central nervous system and functional disturbances of the heart. Chronic exposure causes tissue changes of the liver, damage to the skin and disturbance of the blood supply in the hands. VC is highly mutagenic and possibly also cancerogenic (Grandel & Dahmke, 2008, Institut für Arbeitsschutz der Deutschen Gesetzlichen Unfallversicherung (IFA), 2012)

1.7 Movement of DNAPLs in the subsoil

1.7.1 General Principles

Up to the 1980s it was assumed that the main input of chlorinated solvents into the saturated zone happened as components dissolved in percolating water, as for example by industrial discharge of aqueous waste or by leaching of contaminated soil in the vadose zone (Feenstra et al., 1996). During the 1980s, first laboratory experiments exhibited that the main amount of chlorinated solvents occurred as distinct phase in the subsoil. Enhancing the investigations by additional laboratory studies (Schwille, 1988), field experiments (Poulsen and Kueper, 1992; Kueper et al., 1993b; Broholm et al., 1999) and model results (Feenstra et al., 1996; TeKrony and Ahlert, 1998; Unger et al., 1998; Abriola and Lemke, 2002; Illangasekare et al., 2002; Abriola, 2003; Gerhard and Kueper, 2003a; b; c; Imhoff et al., 2003; Grant and Gerhard, 2004; Kamon et al., 2004; Christ et al., 2005; Enfield et al., 2005; Falta et al., 2005a; Falta et al., 2005b; Rivett and Feenstra, 2005; Fure et al., 2006; Putzlocher et al., 2006; Gerhard et al., 2007; Grant et al., 2007; Page et al., 2007; Basu et al., 2008b; a; Christ et al., 2009; Yoon et al., 2009; Christ et al., 2010), it is now common knowledge, that chlorinated solvents form blobs, fingers and pools in the saturated zone. Fingers and ganglia are vertical percolation path of DNAPLs, whereas pools are long term stored DNAPLs on top of impermeable layers, e.g. in depressions. Blobs are singular droplets of phaseous NAPLs, retained in the subsoil by capillary forces. They can also come into existence at the end of DNAPL fingers or ganglia, when supply of DNAPL ceases (cf. figure 1.1). DNAPL migration in porous media can be subdivided into three different aspects (Feenstra et al., 1996): a) conditions of DNAPL entering the subsoil, b) conditions for DNAPL flow and c) static distribution in residual saturation after the flow has ceased.

The entry of DNAPLs into porous media is controlled by capillary phenomena, which are caused by the interfacial tensions between two immiscible fluids, the small pore openings and the wettability of the system. The *wettability* of a liquid is caused by its physico-chemical properties as viscosity, and depends on the force balance between adhesive and cohesive forces. When the adhesive forces between fluid and medium are much stronger than the cohesive forces within the fluid, then the fluid will spread completely on the surface, i.e. it is wetting.

In the two-phase system water – DNAPL, water will be the wetting fluid and the DNAPL will be the non-wetting fluid. Although there are some NAPLs, which are wetting, in general

DNAPLs can be considered as non-wetting fluids. In a three-phase system consisting of water, DNAPL and air, water is wetting, DNAPL is intermediate wetting and air is non-wetting phase (figure 1.4).

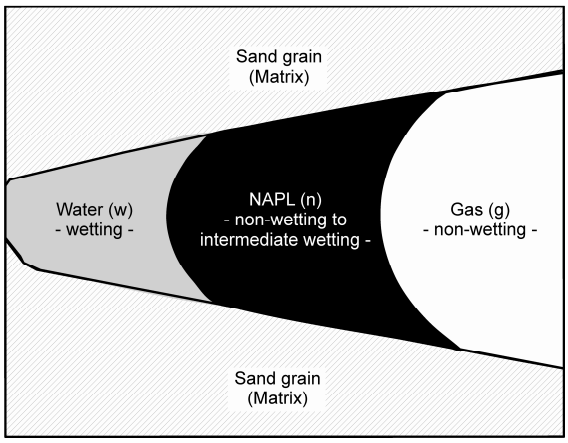

Figure 1.4 Wettability of the system water – DNAPL – air (after Helmig, 1997)

The pressure difference at the interface of wetting and non-wetting phase is defined as capillary pressure. The *capillary pressure* depends on the properties of the fluid, the porous medium and the respective saturation of the involved phases (for details see *Chapter 1.6.2*). High capillary pressure promotes the mobility of non-wetting fluids (as DNAPLs), while low capillary pressure inhibits the penetration of the soil by the non-wetting fluid. In the subsoil, the wetting fluid water coats the surface of the grains and fills the smaller pore spaces. When the non-wetting DNAPL enters the system, it is restricted to larger openings, because the capillary forces acting between the two fluids suppress the displacement of the wetting fluid by the non-wetting fluid.

The spatial movement of DNAPLs in the saturated zone is governed by the function of density and viscosity of the DNAPL and its forcing pressure due to its release. In order to move in the saturated zone, the DNAPL must overcome the capillary resistance, i.e. the entry pressure of the pore throats. The entry pressure is directly proportional to the interfacial tension between the wetting and the non-wetting fluid and inversly proportional to the size of the pore throat. This means, that the smaller the pore throats are, the more pressure the DNAPL needs to enter the medium. Therefore, low permeable material can act as a barrier for DNAPLs, if its pressure is not sufficient. The amount of pressure a DNAPL can act on a pore throat is a result of its density and mass. In general terms, DNAPL move preferentially in permeable medium with larger pore throats and cannot easily enter fine-grained material.

Highly permeable material, large amounts of DNAPL and high DNAPL saturation will allow increased flow rates. DNAPLs will move in the subsoil as long as the driving forces exist, but only if the DNAPL is continuously distributed in the interconnected pore space. There it forms a separate, interconnected phase immiscible with water. When the DNAPL supply ends, because the source of the spill is removed, the driving forces decrease and the DNAPL becomes disconnected in the pore space. As long as the remaining DNAPL can overcome the entry pressure of the pore throats, it will continue its movement. Summarized, the rate of DNAPL flow depends on density and viscosity of the DNAPL, the pressure driving the

DNAPL, the intrinsic permeability of the porous medium and the degree of DNAPL saturation of the pore space.
When the distributed DNAPL cannot exceed the entry pressure of the pore throats anymore, it will remain as not connected, single blobs in the bigger pore spaces, unable to move, forming a static distribution. The amount of remaining DNAPL is called residual saturation and depends on the physico-chemical properties of the DNAPL and the permeability of the geological medium. In soil column experiments, entrapped residual NAPL saturations typically range from 5 % to 35 % of the pore space (Wilson et al., 1990; Powers et al., 1992; Powers et al., 1994a; Powers et al., 1994b; Bradford et al., 1999).
Detailed, small scale DNAPL pathways on the scale of centimeters and decimeters are generally unpredictable (Pankow and Cherry, 1996), even when considerable information on the subsurface is available. But the general direction of the DNAPL movement can be calculated and predicted, accepting necessary simplification and restrictions in the accuracy of the scenarios.

1.7.2 Mathematical-physical principles of multiphase flow

1.7.2.1 Representive Elementary Volume and Continuum – Theorem

The physical and mathematical processes, which govern the movement of immiscible fluids in the subsoil, happen on different scales. On the one hand, molecular forces determine the physical properties of the fluid, as density, viscosity, diffusion, surface of grains etc. Most of the parameters needed for calculations on micro scale are hard to obtain, because of the complexity and heterogeneity of the subsoil system. On the other hand, the general distribution and movement of phases happens on a macro scale, which takes into account the distribution of pore spaces and the slope of impermeable layers. Macroscopic acting forces are for example hydraulic head and constant of gravitational acceleration. Parameters of interest can be derived as an average over a specific volume (Helmig, 1997), which represents all aspects of the subsoil. This specific volume is called *Representative Elementary Volume (REV).* When the chosen volume is too small, specific features of the subsoil will be missed, because either only phase or only grains or a not representative mixture of both will be present in the volume. When the REV is chosen too large, it is possible to unwillingly include heterogeneities of the subsoil, e.g. fractures and stratigraphic boundaries, which are not aim of the investigation.
For example: A volume of sandy aquifer should be modeled. If the chosen REV is too small, only one single sand grain in contact with its wetting phase is represented (figure 1.5). If the chosen REV is too big, heterogeneities as the underlying fractured limestone or stratigraphic boundaries are included and flow behavior may change. If the REV is chosen correctly, all investigated phases will be present in a typical distribution pattern and flow behavior can be investigated. It is only possible within the REV to describe the distribution as well as the absolute and relative amount of phases present. Within the REV, the subvolume S_β (saturation of phase β) is the ratio of the pore volume filled with phase β and the total available pore volume in the REV. Additionally, the investigated space has to be considered as a continuum (Helmig, 1997). The Continuum-Theorem calls for a hypothetic continuous distribution of all the phases in the porous medium (figure 1.6). The separate phases can then be described by continuously differentiable functions of time and place. By applying the REV

and Continuum-Theorem it is possible to mimic the system on the macro scale with neglection of the micro scale, to calculate the investigated parameters mathematically and to measure the parameters macroscopically, e.g. in the laboratory.

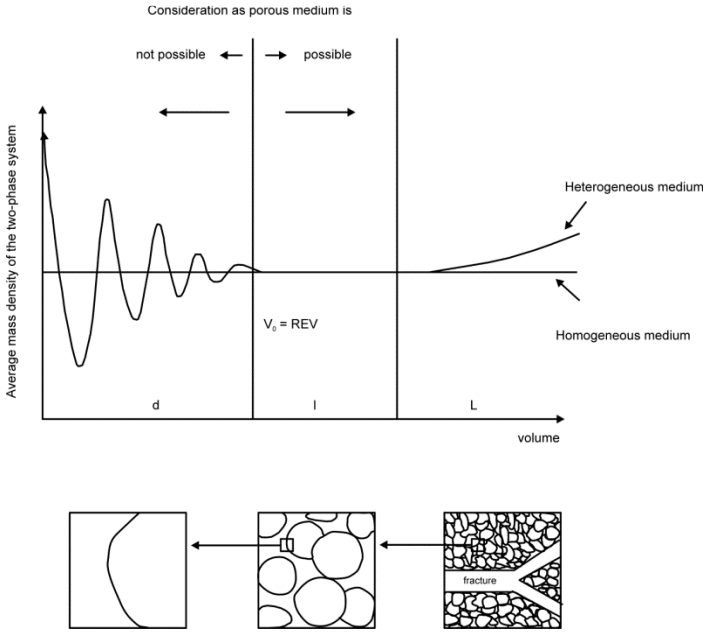

Figure 1.5 Principle of the representative elementary volume (Helmig, 1997)

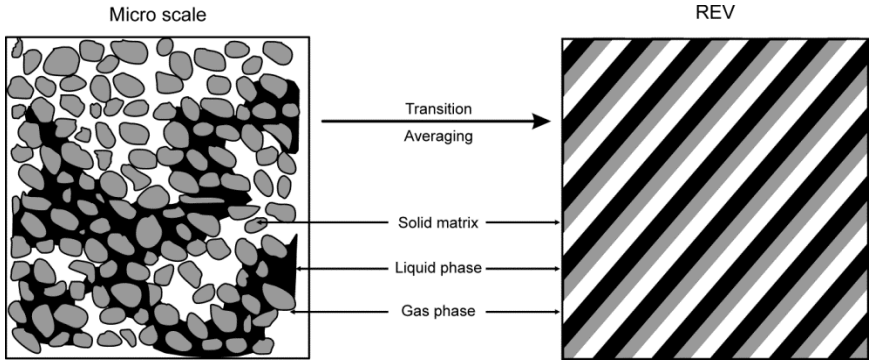

Figure 1.6 Continuum-theorem (Helmig, 1997)

1.7.2.2 Multiphase extension of Darcy´s Law

Darcy´s Law governs the single fluid flow of water through porous medium. It is a one-fluid flow equation for water, based on laboratory experiments and on observations of the water supply of the city Dijon, France (Darcy, 1856):

$$Q = -k_f A \frac{dh}{dl} \tag{1.1}$$

Where

Q	Volumetric discharge
k_f	Hydraulic conductivity
A	Cross-sectional area
dh/dl	Gradient of hydraulic head

It can also be expressed in terms of specific discharge or Darcy flux q, which is the volumetric discharge Q, divided through the cross-sectional area A:

$$q = \frac{Q}{A} = -k_f \frac{dh}{dl} \tag{1.2}$$

When several immiscible fluids are present, they influence each other in their flow behavior. Therefore Darcy´s law needs extension for multiphase flow in order to calculate flow of each fluid correctly. By introducing the term of relative permeability and considering the physical properties of the respective fluid β, the Darcy Flux for each fluid can be calculated (Pruess et al., 2002):

$$F_\beta = \rho_\beta\, q = -k\, \frac{k_{r\beta}\rho_\beta}{\mu_\beta} (\nabla P_\beta - \rho_\beta G) \tag{1.3}$$

Where

F_β	Darcy flux of phase β [m/s]	
ρ_β	Density of phase β [kg/m³]	
k	Intrinsic permeability of the material	[m²]
$k_{r\beta}$	Relative permeability to phase β [-]	
μ_β	Dynamic viscosity of phase β [Pa s]	
P_β	Fluid pressure in phase β [Pa]	
G	Gravitational acceleration [m/s²]	

The intrinsic or absolute permeability of the material is an intensive property that is a function of the material structure only and is not dependent on the pore space filling phase. It can be calculated from hydraulic conductivity (k_f) with respect to water *(w)* by

$$k = k_f \frac{\rho_w\, G}{\mu_w} \tag{1.4}$$

The fluid pressure P_β consists of the pressure P in the reference phase and the capillary pressure $P_{c\beta}$ between the involved fluids. Therefore

$$P_\beta = P + P_{c\beta} \tag{1.5}$$

1.7.2.3 Capillary pressure – saturation function ($P_c - S$)

Capillarity on the macro scale depends directly on the saturation of the wetting and the non-wetting fluid. For each set of fluids and solid phase, there is a critical capillary pressure value, at which infiltration of the non-wetting fluid can start. This so-called entry pressure has to be overcome by the DNAPL in order to infiltrate the subsoil and displace the wetting phase water. The capillary pressure takes into account the surface tension of the phase, which depends on the temperature and the chemical properties of the fluids, the diameters of the pores and the distribution of the pore space. Therefore, the capillary-pressure function is a unique set for each combination of phases and materials. Because of this complexity, it cannot be determined analytically, but is established by several derived functional correla-

tions based on laboratory experiments, which were verified over the last decades. The most commonly applied correlations for capillary pressure and saturation are the formulation of Brooks and Corey (1964) and Van Genuchten (1980) for the two phase system gas (air) – water and of Parker et al. (1987) for the three-phase-system water-NAPL-gas:
Brooks & Corey (1964) based their formulation on the pore space geometry and assume that the capillary pressure has to be larger than the entry pressure in the respective system for infiltration of the non-wetting fluid. For $P_{c\beta} \geq P_d$:

$$S_e\left(P_{c\beta}\right) = \frac{S_w - S_{wr}}{1 - S_{wr}} = \left(\frac{P_d}{P_{c\beta}}\right)^{\lambda_{BC}} \tag{1.6}$$

where

S_e	Effective saturation [-]
S_w	Water saturation [-]
S_{wr}	Residual water saturation [-]
P_d	Entry pressure [Pa]
λ_{BC}	Brooks & Corey scaling parameter [-], generally $0.2 < \lambda_{BC} < 3$ (Helmig, 1997)

The lambda λ_{BC} introduces the sorting of the grains. Small λ_{BC} are applied for well-sorted or single grain size material, whereas big λ_{BC} take into account non-uniform grain sizes and poor sorted material. Whereas Van Genuchten (1980) stated that infiltration can take place as soon as $P_{c\beta} > 0$ (figure 1.7).

$$S_e\left(P_{c\beta}\right) = \frac{S_w - S_n}{1 - S_w} = \left[1 + (\alpha_{VG} P_{c\beta})^{n_{VG}}\right]^{m_{VG}} \tag{1.7}$$

where

S_n	Saturation of non-wetting phase [-]
$\alpha_{VG}, n_{VG}, m_{VG}$	Van Genuchten scaling parameters [-]

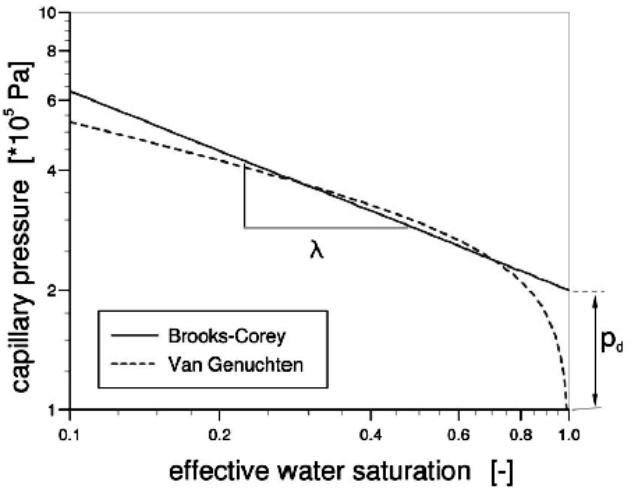

Figure 1.7 Capillary pressure – saturation relation by Brooks & Corey and by Van Genuchten (Helmig, 1997)

Parker et al. (1987) extended the formulation of Van Genuchten to the three phase system water – NAPL – gas. They considered the minimum or irreducible saturation S_m of a porous medium as stable and immobile and not as part of the effective pore space. The minimum saturation is the amount of wetting phase, which cannot be removed from the soil. Therefore it has to be regarded as solid phase and not as part of the open pore space or the available fluid phases. Thus, the effective water saturation $\overline{S_w}$ in a fully water saturated system is:

$$\overline{S_w} = \frac{(S_w - S_m)}{(1 - S_m)} \tag{1.8}$$

The total effective liquid saturation $\overline{S_l}$ is accordingly:

$$\overline{S_l} = \frac{(S_w + S_n - S_m)}{(1 - S_m)} \tag{1.9}$$

Based on the concept of minimum saturation S_m, the capillary pressure in the NAPL – water system can be calculated by:

$$P_{c\,nw} = P_{c\,gw} - P_{c\,gn} \tag{1.10}$$

$$P_{c\,gn} = -\frac{\rho_w G}{\alpha_{P\,gn}}\left[\left(\overline{S_l}\right)^{\frac{-1}{m_P}} - 1\right]^{\frac{1}{n_P}} \tag{1.11}$$

$$P_{c\,gw} = -\frac{\rho_w G}{\alpha_{P\,nw}}\left[\left(\overline{S_w}\right)^{\frac{-1}{m_P}} - 1\right]^{\frac{1}{n_P}} - \frac{\rho_w G}{\alpha_{P\,gn}}\left[\left(\overline{S_l}\right)^{\frac{-1}{m_P}} - 1\right]^{\frac{1}{n_P}} \tag{1.12}$$

where

$\overline{S_w}$	Effective water saturation [-]
S_m	Minimum / irreducible wetting saturation [-]
$\overline{S_l}$	Effective liquid saturation [-]
$P_{c\,nw}$	Capillary pressure between NAPL – water [Pa]
$P_{c\,gw}$	Capillary pressure between gas – water [Pa]
$P_{c\,gn}$	Capillary pressure between gas – NAPL [Pa]
ρ_w	Density water [kg/m^3]
α_P, n_P, m_P	Parker scaling parameters with $m_P = 1 - \frac{1}{n_P}$ [-]
G	Magnitude of gravitational acceleration [m/s^2]
w, n, g	Annotations for wetting (w), non-wetting (n) and gas (g)

1.7.2.4 Relative permeability – saturation function (k_r – S)

The permeability for varying phases differs in a medium. On the one hand due to viscosity and density of the fluids – and thus the capillary pressure – , on the other hand due to changes in the effective pore space the respective phase can enter.
Assume a porous medium with water and NAPL present: Part of the pore space will be filled with water and part of it will be filled with NAPL. The presence of water hinders the mobility of NAPL and vice versa. Therefore, the permeability for a given phase depends on the saturation of the phase. The dependency between permeability and saturation can be de-

scribed by introducing the term of relative permeability. The hydraulic conductivity k_f accounts for the viscosity and density of the respective fluids and the adhesive forces at the soil surfaces. For a given multiphase system, the hydraulic conductivity is defined as

$$k_f = k_{r\beta} k \frac{\rho_\beta G}{\mu_\beta} \tag{1.13}$$

for all water saturations with:

$$0 \leq \sum_{\beta=1}^{n} k_{r\beta}(S_\beta) \leq 1 \tag{1.14}$$

where

$k_{r\beta}$	Relative permeability for phase β, depending on saturation of the respective fluid [-]
k	Intrinsic permeability, solely dependent on soil material [m²]
$k_{r\beta}k$	Effective permeability for the given phase β in the respective medium [-]

According to Helmig (1997), the most common used formulations for the functional correlation between saturation and relative permeability are the works of Brooks & Corey (1964) in combination with the theorem of Burdine (1953) and of Van Genuchten (1980) in combination with the theorem of Mualem (1976) for two - phase system water and non-wetting gas:

Brooks & Corey – Burdine:

$$k_{rw} = S_e^{\frac{2+3\lambda_{BC}}{\lambda}} \tag{1.15}$$

$$k_{rn} = (1 - S_e)^2 \left(1 - S_e^{\frac{2\lambda_{BC}}{\lambda_{BC}}}\right) \tag{1.16}$$

where

λ_{BC}	Brooks& Corey scaling parameters of formula 2.7 [-]
w, n	Annotations for wetting (w), non-wetting (n), here: gas

Van Genuchten – Mualem:

$$k_{rw} = S_e^{\epsilon} \left[1 - \left(1 - S_e^{\frac{1}{m_{VG}}}\right)^{m_{VG}}\right]^2 \tag{1.17}$$

$$k_{rn} = (1 - S_e)^{\gamma_{VGM}} \left(1 - S_e^{\frac{1}{m_{VG}}}\right)^{2m_{VG}} \tag{1.18}$$

where

m_{VG}	Van Genuchten scaling parameter of formula 2.8 [-]
w, n	Annotations for wetting (w), non-wetting (n), here: gas
ϵ, γ_{VGM}	Mualem parameters describing connectivity of the pores, in general $\epsilon = \frac{1}{2}$ and $\gamma = \frac{1}{3}$ (Kueper and Frind, 1991)

Stone (1970) developed a modified version for the relative permeability in a three-phase system by combining data obtained in two-phase systems, thus simplifying the process of calibration:

$$k_{rg} = \left(\frac{S_g - S_{gr}}{1 - S_{wr}}\right)^{n_s} \tag{1.19}$$

$$k_{rw} = \left(\frac{S_w - S_{wr}}{1 - S_{wr}}\right)^{n_s} \tag{1.20}$$

$$k_{rn} = \left(\frac{1 - S_g - S_w - S_{nr}}{1 - S_g - S_{wr} - S_{nr}}\right)\left(\frac{1 - S_{wr} - S_{nr}}{1 - S_w - S_{nr}}\right)\left[\frac{(1 - S_g - S_{wr} - S_{nr})(1 - S_w)}{(1 - S_{wr})}\right]^{n_s} \tag{1.21}$$

With

$$S_n = 1 - S_g - S_w \tag{1.22}$$

where

n_S Stone scaling parameter [-]

Pruess et al. (2002) modified Stone´s formulation in order to improve numerical stability, when using the TOUGH2 code for simulations: When the NAPL - saturation drops to values close to the irreducible NAPL saturation of

$$S_{nr} \leq S_n \leq S_{nr} + 0.005 \tag{1.23}$$

the relative permeability is assumed to be:

$$k_{rn}^{'} = k_{rn}\frac{S_n - S_{nr}}{0.005} \tag{1.24}$$

The varying functions for $P_c - S$ and $k_r - S$ are implemented in the numerical multiphase solver TMVOC and can be chosen according to investigated issue. The multiphase investigations performed in this thesis were calculated based on the formulation of Parker et al. (1987) for $P_c - S$ and of Stone´s (1970) modified version by Pruess et al. (2002) for $k_r - S$.

1.7.3 Influence of heterogeneities of the subsoil

Heterogeneities in the subsoil are caused by varying grain size distribution of the sediment. Layers and areas with dominant fine grained material will form naturally occurring capillary barriers for the percolating DNAPL, hindering its vertical movement (Kueper et al., 1989; Wilson et al., 1990; Kueper and Frind, 1991; Poulsen and Kueper, 1992; Kueper et al., 1993a; Dekker and Abriola, 2000). Varying grainsizes influence the relative permeability of the wetting and the non-wetting fluid (figure 1.8). Bradford et al. (2003) showed that intrinsic and relative permeability of the subsurface have a strong influence on the spatial distribution of NAPLs by affecting the historic maximum NAPL saturation. Decreasing the NAPL conductivity leads to higher NAPL saturations and, consequently, enhances NAPL retention (Bradford et al., 2003). Studies of Brusseau et al. (2000) indicate that non-uniform NAPL distribution, physical heterogeneity, and associated non-uniform flow significantly influenced the magnitude and location of NAPL dissolution. Simulation results of Lemke et al. (2003) suggest that varying sets of spatial variability in aquifer parameters strongly influence the entrapment of DNAPLs. Up until now, the greatest challenges in the simulation of DNAPL spreading are a) the unknown distribution of small- and large scale heterogeneities in the

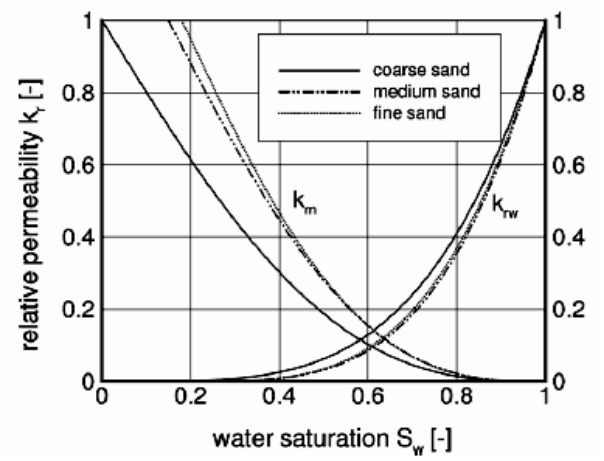

Figure 1.8 Curves of relative permeability – saturation for varying grain sizes (after Helmig, 1997)

subsoil and b) the numerical stable implementation in existing modeling software. Due to these challenges, all conducted scenarios including heterogeneities up until now are laboratory- to box-scale (Fagerlund, 2006) and / or 2D models (Mayer and Miller, 1996; Dekker and Abriola, 2000; Bradford et al., 2003; Yang et al., published online 2012) and / or 3D models with a maximum volume of 15 x 10 x 10 m (Parker and Park, 2004; Liang and Falta, 2008).

1.7.4 Influence of groundwater flow

The influence of groundwater flow on DNAPLs has been investigated in detail over the last decades. But the investigations govern mostly questions of dissolution behavior and consequently longevity of source zone and mass load. Currently it is well–known that the groundwater flow velocity significantly influences the dissolution behavior of NAPLs (Page et al., 2007; Miles et al., 2008b). Moreover, the orientation and geometry of the DNAPL source zone impacts the dissolution behavior significantly (Sale and McWhorter, 2001). Parker and Park (2004) concluded from their 3D modeling that heterogeneities in groundwater velocity and DNAPL distributions lead to field scale mass transfer coefficients that are much lower than laboratory-scale values. The influence of varying groundwater flow velocities on the cessation time of a DNAPL body in a heterogeneous aquifer on top of an impermeable, tilted aquitard was investigated by Gerhard et al. (2007) by multiphase modeling: The timescale for reaching static distribution in the subsurface directly depends on the encountered groundwater flow velocity.

Dekker and Abriola (2000) analyzed the sensitive parameters for DNAPL distribution in the subsoil, statistically comparing the impact of heterogeneous distribution of permeability, spill amount and time and groundwater velocity. They concluded that groundwater flow velocity is not among the most sensitive parameter in their investigation compared to the other aspects. But their maximum flow velocity investigated only comprised groundwater flow velocities slower than 1 m/d.

Because most of the investigations are performed on 2D and / or small scale due to restrictions of the applied numerical simulation software, it is still unknown, which impact enhanced groundwater flow will have on the travel pathway and final position of a DNAPL in the subsoil at a field scale. Moreover, it is still discussed, whether high hydraulic pressure may counter-act pooling effects in depressions.

2 Methods

2.1 Applied software

2.1.1 Multiphase modeling software TMVOC

TMVOC is a commercially available numerical simulator for multi-component, multiphase flow and dissolution processes of gases, water and volatile organic compounds. It is based on the TOUGH2 - code (Pruess et al., 2002) and includes the possibility to simulate the behavior of water, gases and NAPLs at non-isothermal conditions. It is especially designed for handling challenges of environmental contamination scenarios, such as spill of contaminations, their free phase distribution pattern, dissolution and retardation processes as well as simplified half-life biodegradation.
It is available as FORTRAN 77 – based source code (Lawrence Berkeley National Laboratory, 2012) or integrated as pre-compiled executable in the graphical user interface PetraSim (Thunderhead Engineering, 2011). In this study, the PetraSim version was applied.
TMVOC can model any combinations of the three phase system water – NAPL – gas with varying composition of several components. Necessary assumptions are that the phases are in local equilibrium and that no chemical reactions happen except interphase mass transfer, adsorption to the solid phase, and biodegradation of the dissolved contaminant. The interphase mass transfer can be modeled as evaporation, boiling, dissolution into the aqueous phase, condensation of gaseous organic chemicals to form NAPL phase, and equilibrium phase partitioning of the organic contaminant between the three phases. The chemical properties of the modeled NAPL as well as their transport behavior are computed with a very general thermodynamical formulation (Lawrence Berkeley National Laboratory, 2012), which applies the semi-empirical corresponding state methods. The parameters of the chemicals are calculated as functions of their critical properties, e.g. critical temperature and pressure. Tabulated values for most chemicals are available by Poling et al. (2007). Porosity may change as a function of fluid pressure and temperature, using simple concepts of pore compressibility and expansivity (Lawrence Berkeley National Laboratory, 2012). Several functions of $P_c - S$ and $k_r - S$ formulations are pre-installed in PetraSim, which can be chosen and / or adapted by the user.
For the mathematical-physical implementation of the various general processes of phase handling, the reader may be referred to the user manual *TMVOC, A Numerical Simulator for Three-Phase Non-isothermal Flows of Multicomponent Hydrocarbon Mixtures in Saturated-Unsaturated Heterogeneous Media* by Pruess and Battistelli (2002).
Unfortunately during the application of the software it came to attention that several main features were not implemented in the PetraSim-version yet. Creating realistic subsurface morphology, as conducted for *Chapter 6* is only possible since Petrasim v5.1.2020, which was released in a working, stable version in 2010. Bugfixes for PetraSim are released at least once per month, sometimes creating new bugs while correcting older ones (Thunderhead Engineering, 2012).

Additionally, the numerical convergence of the simulations is still handled based on the FORTRAN 77 code and the typical computer performance, which was available, when the TOUGH code was written in 1987 (Lawrence National Berkeley Laboratory, 2012):
TOUGH2 and thus TMVOC includes an internal criterion of convergence, which will abort any simulation, if the calculated results are within the relative and absolute error criteria for two consecutive iterations and if the following iteration exceeds the error criteria. Up until now, the only way of handling the internal convergence criterion is to adjust the relative and absolute error criteria, which can lead to excessive runtimes (figure 2.1).

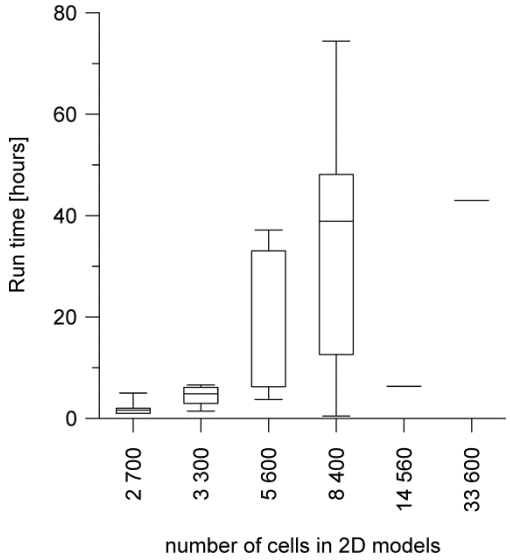

Figure 2.1 Typical runtime of simulations of the two-phase system NAPL-water in TMVOC in dependancy of discretization of model domain

2.1.2 Geological modeling software GMS

For the geological modeling of the field site Rho the commercially available software GMS – *Groundwater modeling system* (Aquaveo, 2012) was applied. GMS is a graphical user interface for performing groundwater simulations. Its modular system allows the integration of various groundwater flow and transport analysis codes, e.g. MODFLOW, UTCHEM, PEST and more, but integration of TMVOC is not yet possible. Easy integration and handling of borehole data sets, spatial information, elevations and surface maps are the basis for 3D structural geological modeling of an area.
The primary data of the available boreholes was used as input for GMS combined with an actual areal picture of the area provided by La Sapienza Rome. The structural-geological model of Rho, which was modeled with GMS, had to be data converted to the input format of TMVOC, in which groundwater flow and NAPL transport were calculated.

2.2 Primary Data

The following subchapters include the detailed description of the available and applied primary data. The information is also partly included in the publications in the follogwing chapters and the data is attached electronically in the Annex.

2.2.1 Laboratory experiments for calibration of the multiphase model

Primary data for the calibration of the models was provided by Antonella Luciano, Marco Petrangeli Papini and Paolo Viotti of La Sapienza University Rome. Luciano et al. conducted in the years 2009 - 2010 three laboratory experiments in order to investigate the DNAPL behavior at high groundwater flow velocities. They generously shared their data, so that it was possible to calibrate the multiphase model to the documented spreading behavior of the DNAPL in the laboratory experiment.

This study is published as Luciano et al. (2010) *"Laboratory investigation of DNAPL migration in porous media"* In the *Journal of Hazardous Materials*. All data presented in the following chapters are property of Antonella Luciano, Marco Petrangeli Papini and Paolo Viotti of La Sapienza University Rome.

Experimental set-up

The experimental set-up consisted of a 2D aluminium tank of 1.40 m length, 0.12 m width and 0.70 m height with a glass panel in front for observation (figure 2.2). The tank was subdivided into three parts: a) left inflow chamber, separated by stainless steel mesh from b) main chamber of investigation, separated with stainless steel mesh from c) right outflow chamber. Both flow chambers were filled with coarse grained gravel, while the main chamber was filled with two grain sizes of artificial porous media (glass beads, table 2.1) up to a height of 0.60 m. The fine grained SAND2 was used to install two impermeable lenses within the overall filling of the coarse grained SAND1.

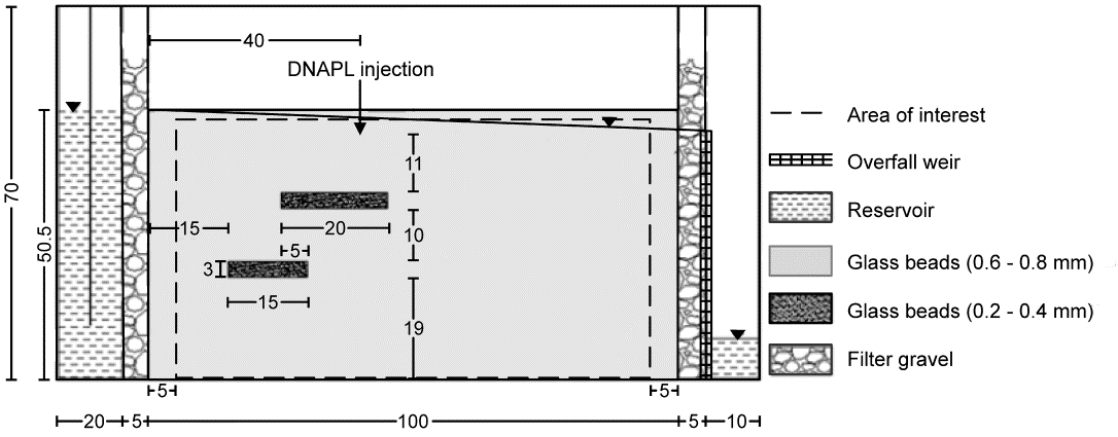

Figure 2.2 Schematic set-up of the experimental tank (Luciano et al., 2010), all length in cm

Table 2.1 Material parameters of the artificial porous media (provided by Luciano et al., 2010)

	SAND1	SAND2
Diameter of glass beads [mm]	0.4 - 0.8	0.1 - 0.2
Porosity	0.388	0.373
Density [kg/m³]	2500	2500
Bulk density [kg/m³]	1530	1570
Intrinsic permeability, horizontal [m²]	2.4×10^{-10} (a)	8.5×10^{-15} (b)
Intrinsic permeability, vertical [m²]	1.94×10^{-10} (a)	8.5×10^{-15} (b)

[a)]Calculated by means of Darcy´s law and hydraulic permeability
[(b)]No measurements, iteratively fitted during calibration process of the model

Because of the high toxicity of TCE, the non-toxic substitute HFE-7100 (3M, 2005; 2008) was used. HFE-7100 features almost identical physico-chemical properties as TCE (table 2.2) and is well established as TCE substitute in laboratory experiments (Manzello and Yang, 2002; Lee et al., 2004).

Table 2.2 Physico-chemical properties of HFE-7100 and TCE

Property	HFE-7100	TCE	PCE
Chemical formula	$C_4F_9OCH_3$	C_2HCl_3	C_2Cl_4
Relative density [kg/m³]	1500 / 1480 (dyed)	1464	1630
Relative viscosity [cP]	0.60	00.59	0.54
Surface tension [mN/m]	13.60	29.30	32.86
Interfacial tension [mN/m]	35.59	34.50	44.40
Vapour Pressure [kPa]	28.00	07.73	2.50
Water solubility [ppm]	12.00	11.00	1.40

A total amount of two liters (3.05 kg) of HFE-7100 was infiltrated below the water table with constant hydraulic head, causing variable seepage velocities in the three conducted experiments. The spreading behavior of HFE-7100 was photo-documented and analyzed using an innovative image processing technique. Calculated mass balances showed an error less than 0.6 % (Luciano et al. 2010) .
The time frame and boundary conditions of the conducted experiments are listed in table 2.3.

Table 2.3 Boundary conditions of the laboratory experiments (Luciano et al. 2010)

	Experiment 1	Experiment 2	Experiment 3
Groundwater pore velocity v_w (m/d)	0.00	21.25	40.86
Infiltrated amount of HFE-7100 (kg)	3.05	3.05	3.05
Infiltration rates in the calibration model (kg/s)	5.08 × 10-4	8.13×10-4	1.90×10-3
Seepage / infiltration time (s)	5905	3690	1580
Observation time after deactivation of infiltration = spreading time (s)	10217	1890	4325
Total time of experiments and models (h)	4.48	1.55	1.64

For the visualization and interpretation of the results, the reader may refer to Luciano et al. (2010).

2.2.2 Literature study / historical site investigation

2.2.2.1 Geology and hydrogeology

The Rho region is geologically characterized by quarternary alluvial and glaciofluvial sediments with widely varying grain sizes. Three hydraulic units of interest are present at the former industrial site Chimica di Bianchi, Rho:
An upper unconfined aquifer called *Superficiale*, an aquitard and a deeper confined aquifer called *Prima Falda*. The thicknesses of these hydraulic units range over several meters in the available literature. Figure 2.3 illustrates the variability documented in several studies on the site. For each author, minimum and maximum values for thickness of the respective hydraulic layer are drawn.

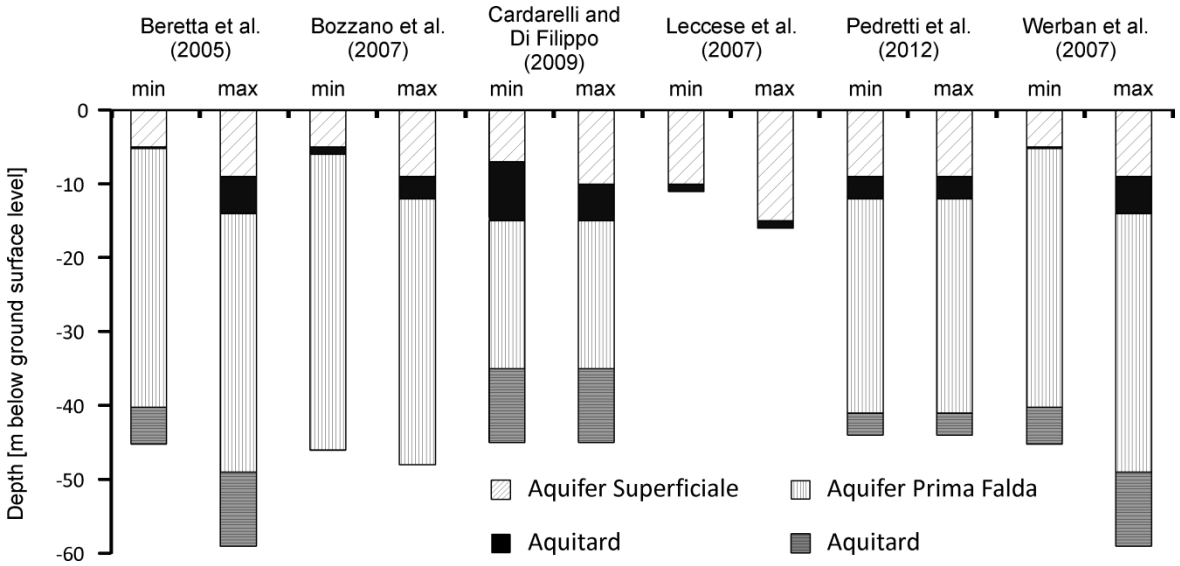

Figure 2.3 Minimum and maximum thicknesses of hydraulic units at Rho, based on values provided in literature (Beretta et al., 2005; Bozzano et al., 2007; Leccese et al., 2007; Werban et al., 2007; Cardarelli and Di Filippo, 2009; Pedretti et al., 2012)

Mean values would be an approximated thickness of ca. 8.5 m for the upper most aquifer *Superficiale*, a thickness of ca. 3 m for the aquitard and a thickness of 31 m for the *Prima Falda*. Geological properties of the varying hydraulic units (table 2.4) are only described by Beretta et al. (2005), Bozzano et al. (2007) and Leccese et al. (2007). Bozzano et al. (2007) stated furthermore that stratigraphic logtest for both aquifers exhibited huge lithological variety in vertical and horizontal direction, without mentioning specific values, but supplying relative values for logK – distribution.
The uppermost unconfined *Superficiale* consists of a mixture of gravel, sand and lenses of silty sand and clay, with a layer of anthropogenic filling (Werban et al. 2007, Pedretti et al. 2012), assumingly bricks and construction material. The following aquitard is described as an interupted clay layer by Leccese et al. (2007), Pedretti and Masetti (2009), Pedretti et al. (2012)and Werban et al. (2007) at the local scale of the industrial area.
But due to Bozzano et al. (2007) it has to be assumed, that the aquitard is continuous in the

Table 2.4 Hydrogeological parameters at the Rho Site based on literature studies (Beretta et al., 2005; Bozzano et al., 2007; Leccese et al., 2007)

Name hydraulic unit	Material	Thickness [m]	Hydraulic conductivity [m/s]	porosity [%]	Hydraulic gradient [%]
Superficiale (upper unconfined aquifer)	Silty sand, sand gravel, anthropogenic filling (bricks, cement)	10 5 – 12	1E-06 1E-02	20.0	0.4
Aquitard	Silty clay clay	1 – 4	1E-09 1E-07	na	na
Prima Falda (lower confined aquifer)	silty-clayey layers sand gravel	20 – 45 15 – 40	1E-06 1E-03	20.0 45.0	0.4 0.6

area of Chimica di Bianchi, but missing north east of the industrial area, creating a hydraulic connection between the aquifers *Superficiale* and *Prima Falda* on regional scale. The thickness of the aquitard ranges between 0.5 m (Beretta et al., 2005; Werban et al., 2007) and a few meters (Bozzano et al., 2007). The deeper aquifer *Prima Falda* is described to be similar in its geological composition to the Superficale, but to reach a thickness of 35 - 45 m. According to Bozzano et al. (2007)*Prima Falda* is even ten times thicker than the aquifer *Superficiale*, which would result in a mean thickness of 55 – 90 m.

Hydraulic conditions are described with a general groundwater flow from NNW to SSE for the *Superficiale* and from NNE to SSW for the *Prima Falda* in Bozzano et al. (2007) and Beretta et al. (2005). Whereas Cardarelli and Di Filippo (2009) describe a general groundwater flow direction in *Prima Falda* from NE to SW. Leccese et al. (2007) state that general groundwater flow direction is assumed to be NW to SE without mentioning of the respective aquifer. But it is fitting to assume that this statement refers to the aquifer *Superficiale*.

2.2.2.2 History of contamination and remediation actions

The industrial facility Chimica di Bianchi mainly produced dyes over a time period of at least 70 years (Leccese et al, 2007). It was registered from 1907 - 1979 as Societa Chimica Bianchi. In the beginning they produced only ink and glue with approximately 1500 tons per year. Production of industrial dyes followed shortly after (no year available) with equal and higher production rates in later years (personal communication M. Petrangeli Papini and P. Viotti). First evidence of contaminations with chlorinated solvents, as PCE and TCE, were documented in the late 1970s (Pedretti et al., 2012). The most probable leakage point seemed to be a former disposal basin of 10 m x 10 m, leading to a contamination of up to 180 mg/l TCE and 50 mg/l 1,1,2,2-tetrachloroethane as dissolved phase in the underlying aquifers (Leccese et al., 2007; Werban et al., 2007).

The supposed main source of contamination was encapsulated immediately (Pedretti et al., 2012) or in 1982 (Leccese et al., 2007). According to Perdetti et al. (2012) the method of encapsulation was the installation of vertical slurry cut-off walls around the former disposal basin, meanwhile Bozzano et al. (2007) describe the installation of an impermeable annular

diaphragm. Impermeable steel piling walls are also mentioned (personal communication M. Petrangeli Papini, P. Viotti). But all authors agree on the footing of the system in the aquitard between *Superficiale* and *Prima Falda*. The exact position, installation method and material composition of the encapsulation system are not documented in the literature, but Bozzano et al. (2007), Leccese et al. (2007) and Pedretti et al. (2012) suspect an increasing conductivity of the assumed impermeable encapsulation system.
Due to Perdetti et al. (2012) the encapsulation system was never coupled with any other kind of remediation system until the installation of a hydraulic barrier in the year 2006, being consistent with personal communication with M. Petrangeli Papini and P. Viotti.
The 2006 installed hydraulic barrier consists of 19 wells in row, 375 m to the SSE of the former industrial area. Fifteen of the wells are only connected to the aquifer *Superficiale*. Four wells should only have been installed in the aquifer *Prima Falda*, but possibly have an additional connectivity to *Superficiale*. Currently only two wells operate at the former industrial site. The approximate pumping rate is 1.61 m^3 per day (personal communication M. Petrangeli Papini and P. Viotti; La Sapienza, Rome). One of the wells operating is not even part of the well arch but is positioned closer to the encapsulation system.
In 2007 an almost stable high concentration of 110 - 180 mg/l TCE in the deeper aquifer *Prima Falda* was confirmed by monitoring data over the previous fifteen years (Leccese et al., 2007; Pedretti et al., 2012), whereas the shallow aquifer *Superficiale* showed quite low concentrations. This would imply a still functioning lateral impermeable encapsulation, but also an enhanced or artificially created vertical conductivity at the former source zone, which Pedretti et al. (2012) assumed due to numerical modeling of seepage and groundwater flow between encapsulation system and aquifers.
Cardelli and Di Filippo (2009) conducted several 2D and 3D measurements applying electrical resistivity and induced polarization tomography at the site. Their data exhibits anomolies in the subsoil which indicate the possible presence of DNAPLs in depth of 15 – 18 m bgs. to the SW of the former source zone, which would locate them in the deeper aquifer Prima Falda.

2.2.3 Borehole data set of former site investigation campaigns

The borehole data set was provided by Antonella Luciano in 2010 in an Italian and 2011 in an English version. It is compiled as MS Access data base, containing gathered borehole and well information from the following sources:
Acquedotto Comunale, Acquedotto di Rho, Acquedotto Pregnana Milanese, AGIP Petroli S.p.A., AGIP Raffinazione S.p.A., AMSA, Bogophane S.p.A., Cambiaghi S.p.A., Centro commerciale, Comune di Rho, Costruzioni Meccaniche di Rho, COVENGAS, Cromatura Rhodense s.r.l., Ditta Bogophane S.p.A., ditta Maestri Ernesto, EDAM s.r.l., Edera Immobiliare s.r.l., Elf Atochem Italia s.r.l., Estrazioni Lapidei Bossi, Ex-Chimica Bianchi, Ex-Chmica Bianchi, FIAT Auto S.p.A., Fosfantartiglio LEI, Fosfantartiglio S.p.A., Foster Wheeler, Hydron Italia, I.CO.SEM., Industria ISA SAVA, Montecatini Edison Milano, Ospedale di Rho, Panificio Pastori, PIBIGAS - Idrocarburi ed Affini S.p.A, Pozzo in Cerchiate, Provincia di Milano, Regione Molinello, Salumificio Citterio, SNAM, Società Chatillon, Spett. Cont. Scheibler in Gallarati Scotti, Stabilimento M.T.M., Tintoria Bonecchi, Unione Manifatture Nerviano, Università La Sapienza, Viallaggio Paolucci.

The database contains 296 wells and includes information about:

- Name of well / borehole and owner
- Coordinates of wells in Gauss-Boaga coordinate system
- Occasional data available:
  - Description of geological material
  - Classification of geological material based on Unified Soil Classification System (ASTM, 2011)
  - Top and Bottom elevation of geological units
  - Name of the hydraulic units (*Superficiale, Aquitard, Prima Falda, Aquitard, Secunda Falda*, Terza Falda) for 160 boreholes
  - Transmissivity
  - Water table elevation and date of measurement (2004, irregular interval between 2004 – 2006)
  - Monitoring values of tetrachloroethane (TeCA), TCE, dichloroethane (DCA), CA, PCE, TCE, cis-DCE, t-DCE, VC, ethane, methane, sum of chlorinated solvents, pH, conductivity, temperature, dissolved oxygen, oxidation / reduction potential, turbidity, chloride, nitrate, sulfate, chemical oxygen demand, Fe^{2+}, Fe^{3+}, Fe^{total}, sulfide (sparse or no data before 2001, irregular interval between 2001 – 2007)
  - depth and date of samples (sparse or no data before 2003, irregular interval between 2003 – 2007)

The contained information differs in level of accuracy. Over 50 % of the boreholes only contain incomplete geological descriptions. Additionally 10 % of the remaining boreholes only reach a depth of 1 m. Therefore only 161 boreholes were applicable to the geological modeling, resulting in an average data density of nine boreholes per square kilometer (figure 2.4).
For the hydraulic 3D models, only 129 boreholes contained information about the hydraulic units at the site, resulting in an average data density of seven boreholes per square kilometer (figure 2.5).
Moreover, the distribution of the aquitard between *Superficiale* and *Prima Falda* which is the funding for the encapsulation system is only documented in four of the total amount of 296 boreholes. Additionally, measurements of water table elevation and of hydrochemistry are only available for some wells and only for the time period 2004 – 2007 in best cases.
The provided data was used to obtain the structural geological model of the field site, to deduct properties as porosity and hydraulic conductivity and to calibrate water table elevation of the unconfined aquifer *Superficiale*.
Additionally to the MS-access database of the primary data, master students of Paolo Viotti and Antonella Luciano conducted a Modflow model of the area of the former industrial site. The Modflow model includes the spatial distribution of the three relevant hydraulic units *Superficiale*, aquitard and *Prima Falda*. The distribution files of the ModFlow model were also included in the dataset.

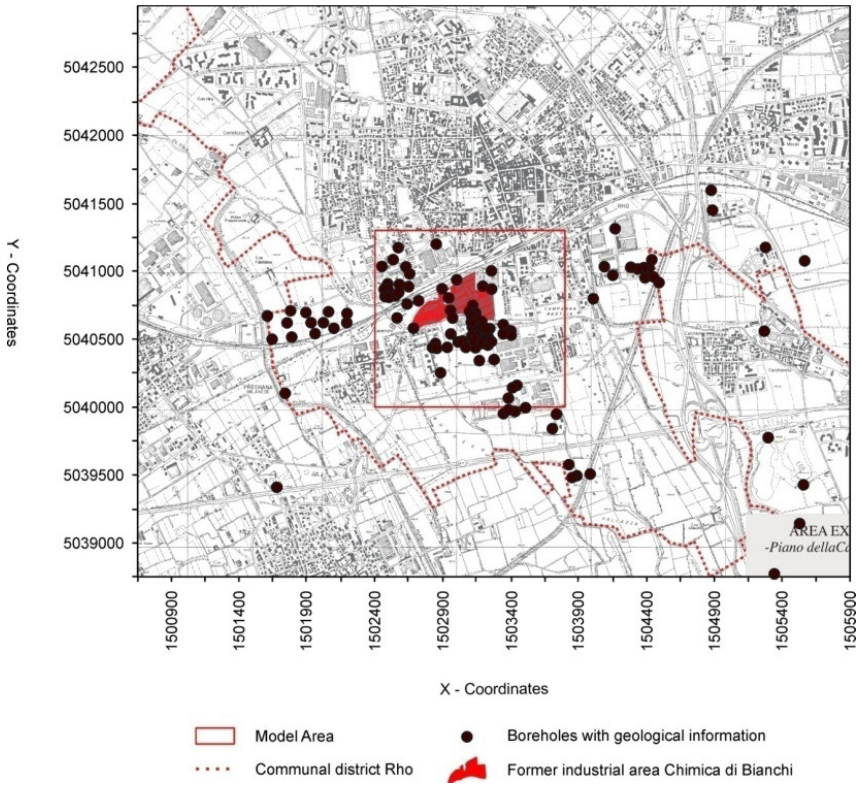

Figure 2.4 Position of boreholes (dots) with geological descriptions used for 3D modeling

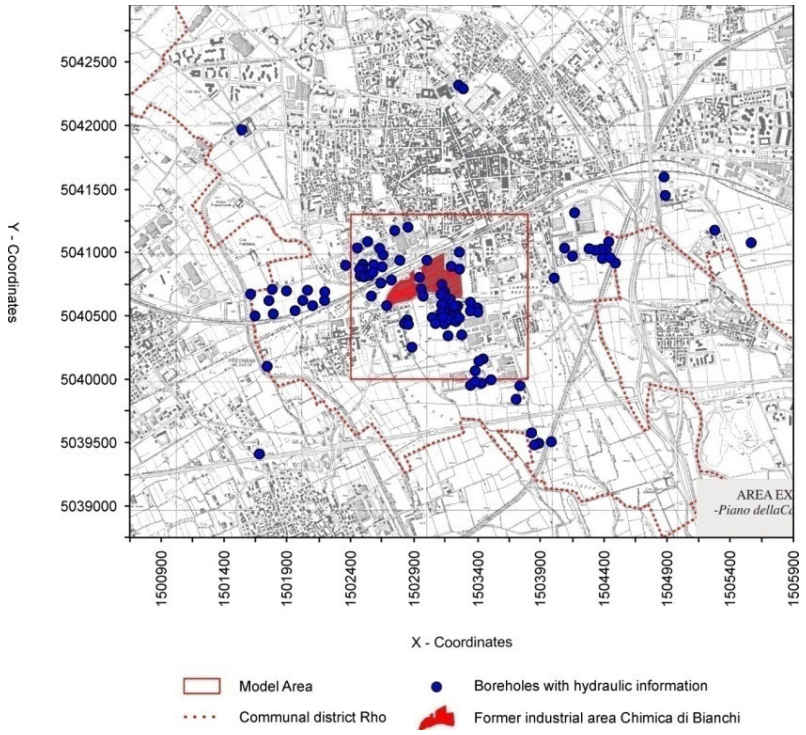

Figure 2.5 Position of boreholes (dots) with hydraulic descriptions used for 3D modeling

2.3 Structural 3D models of Rho, Italy

The dimensions of all conducted 3D models are 1.8 km² (figure 2.6) and include the former industrial area Chimica di Bianchi in the middle of the domain, the installed wells south-east of the former industrial site and the surrounding area by approx. 750 m in each direction.

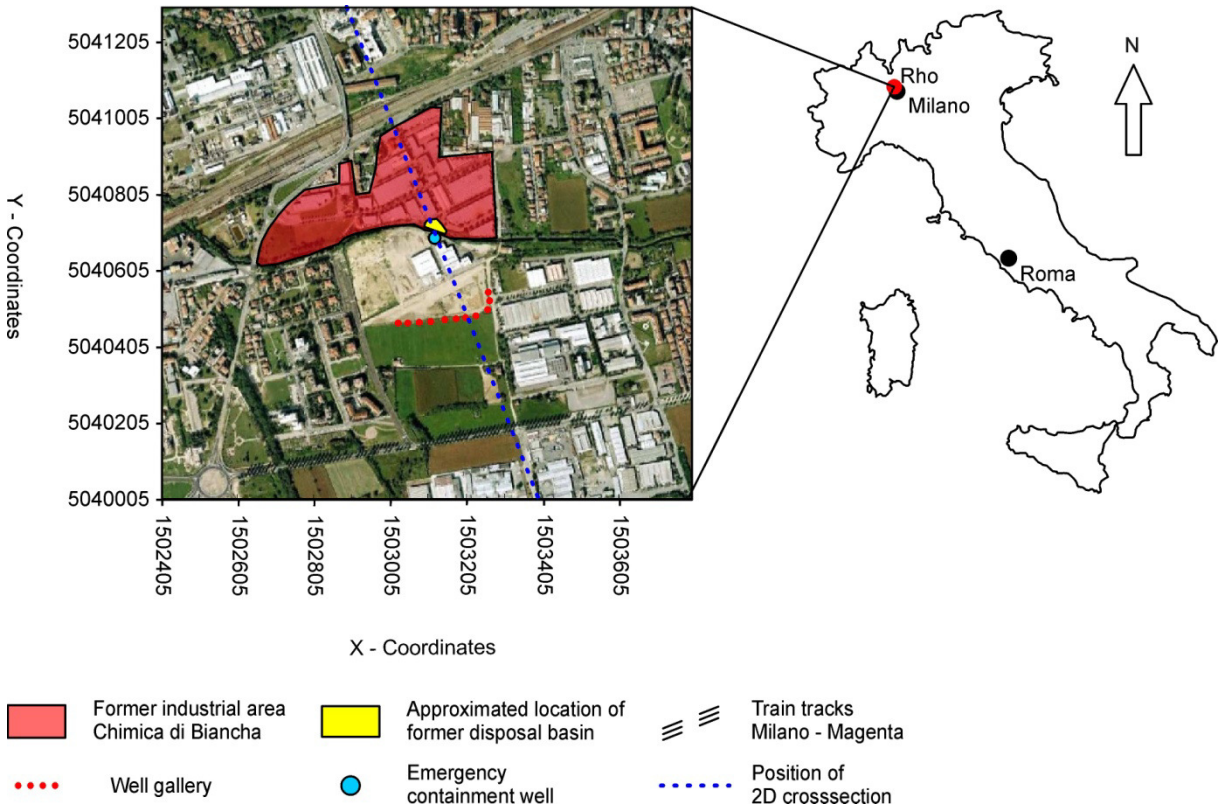

Figure 2.6 Area of interest, overlaid by aerial picture (adapted from Google Earth, 2010), coordinates in Gauss-Boaga, extension of all conducted structural, geological and hydraulic models

Based on the available primary data, three different models of the subsurface of Rho were created. Main focus in all models was set on the distribution of the aquitard at the field site, its position in depth and its spatial shape, assumed as barrier and hindrance for the DNAPL movement.

2.3.1 Model 1 – Structural hydraulic 3D model based on layers of the Modflow –model

The first model is the reconstruction of the Modflow-Model of La Sapienza Rome. For Modflow modeling, it was assumed that the three relevant hydraulic units are omnipresent in the area (figure 2.7). The three units *Superficale*, *Aquitard* and *Prima Falda* dip from north to south by approx. 0.4 %. Average thicknesses are ca. 7 – 9 m for Superficiale, 1 – 8 m for the aquitard and approx. 45 m for the deeper aquifer Prima Falda. While the top of Superficiale shows only minimal morphology, the top of the aquitard is characterized by trenches and depressions. The first trench elongates from NW to SE through the former industrial site. The second trench with E – W orientation interconnects below the industrial site with the first one and forms a depression basin directly below the former disposal bassin (figure 2.8). This bassin is separated from the first trench in south eastern direction by a small ridge with

a relative height of 4 m compared to the trench. The northern half of the aquitard forms a slight plateau, caused by the east-west trench (figure 2.9). The morphology of the top of the deeper aquifer Prima Falda partly follows the topography of the aquitard, inversely showing the main features of trenches and depressions.

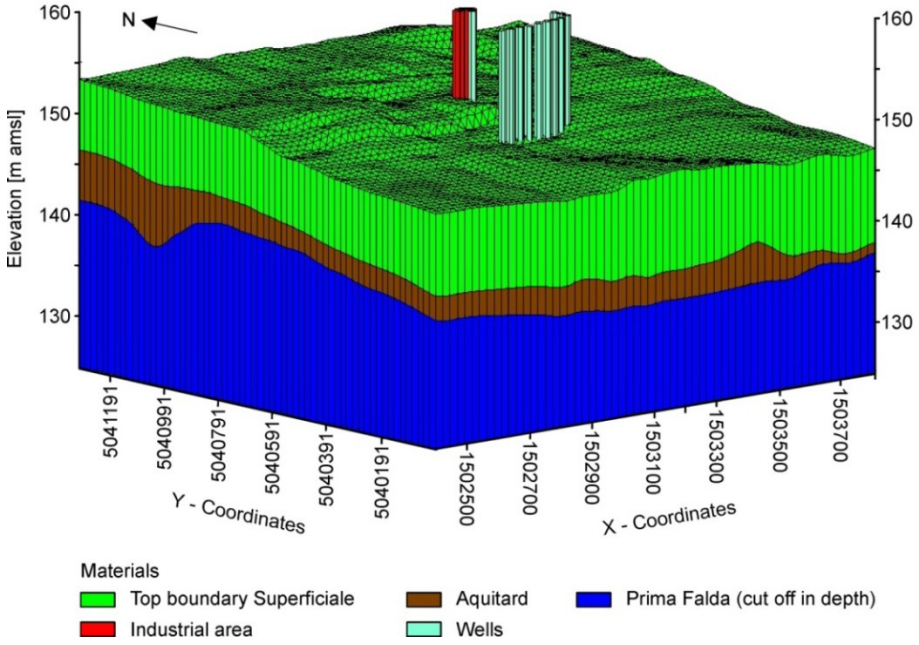

Figure 2.7 Perspective view of Modflow model, all hydraulic units, z-magnification 1 : 25

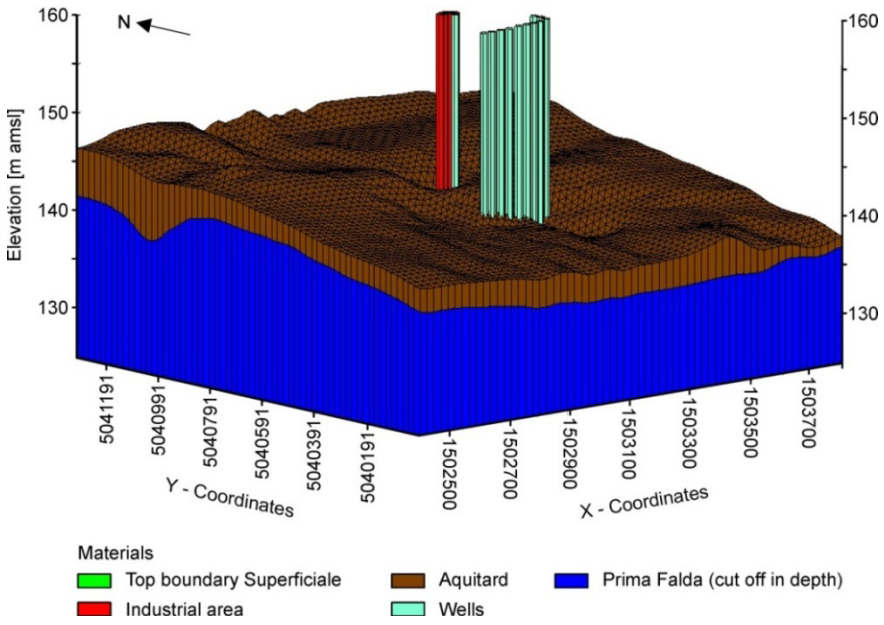

Figure 2.8 Perspective view of top of aquitard, modflow model, z-magnification 1 : 25

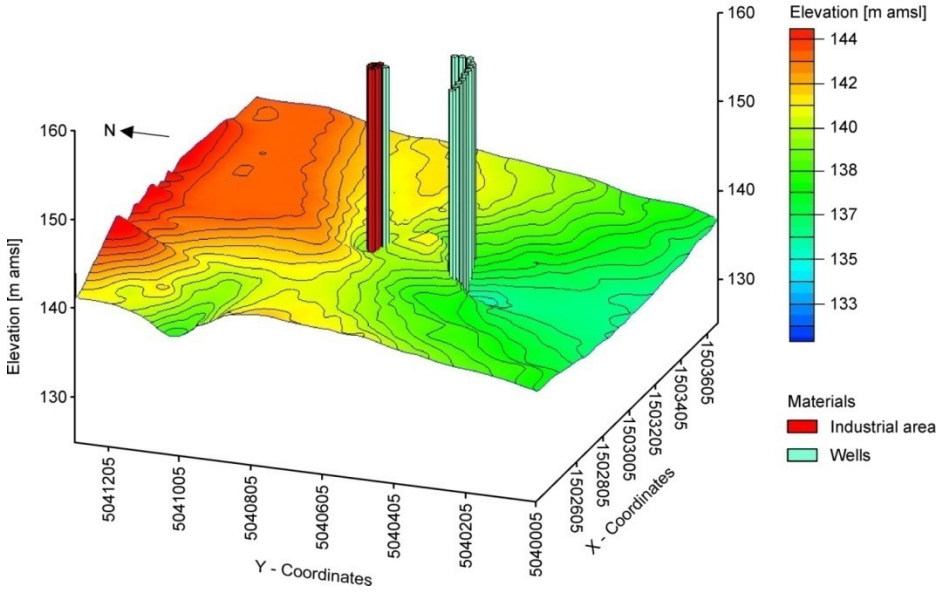

Figure 2.9 Topographic surface map in perspective view of top of aquitard of model 1 – Modlfow layer based, z-magnification 1 : 25

The Modflow-based model is a first, very rough approximation of the subsurface of the area Chimica di Bianchi. Hydraulic connections created by erosion of the aquitard are not defined by restricted extension of the Aquitard-layers, but later on implemented by adjustement of the permeability in the Modflow model. In order to identify gaps in the aquitard as well as its resulting topography, Model 2 was set up, using the available information about hydraulic units included in the borehole data base.

2.3.2 Model 2 – Structural hydraulic 3D model based on boreholes

The primary data for the second model was the included hydraulic characterization of the geological material of the boreholes. In the data base, four aquifers are characterized as Superficiale, Prima Falda, Seconda Falda and Terza Falda. Information about thickness and depth of bottom of the aquifers allow the calculation of the presence and the resulting depth position and thickness of the seperating aquifers. Depending on the predefined handling of missing data points, two varying results were calculated. The first model allows to represent missing points implicitly, which results in an almost omnipresent aquitard, which is characterized by varying missing spots (figure 2.10). Northeast of the industrial area, the aquitard layer is heightened to 151 m amsl, whereas the deepest location of the aquitard is at 132 m amsl. Within a distance of ca. 400 m south of the industrial area there is a north-south elongated trench in the aquitard (figure 2.11), which would probably create a preferential flow path for the DNAPL.

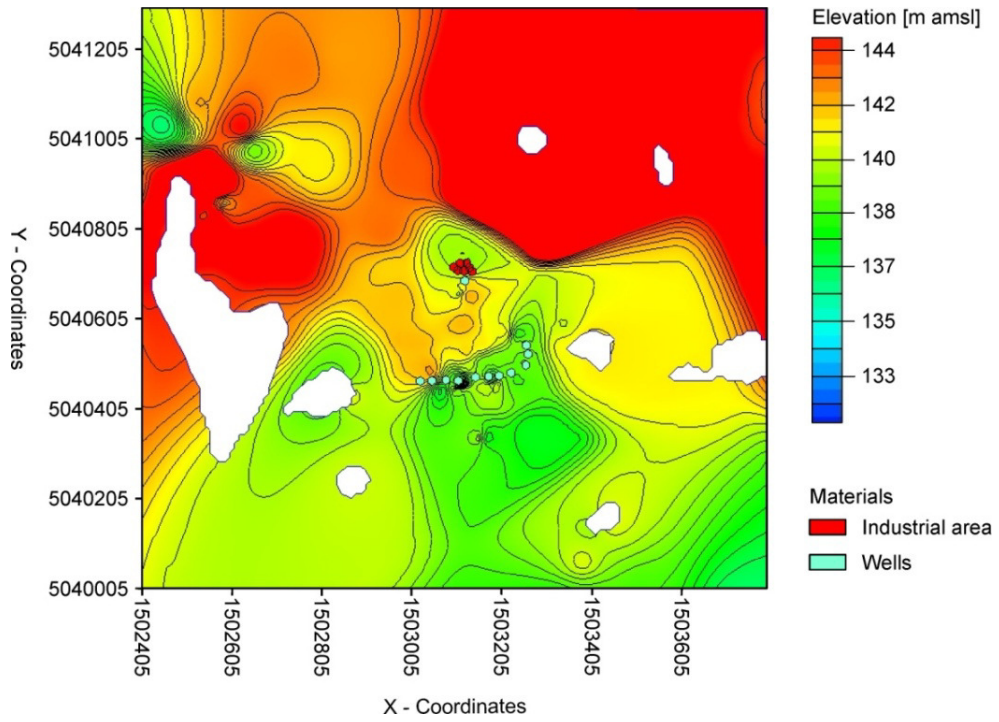

Figure 2.10 Topographic surface map of top of aquitard of model 2 - version 1

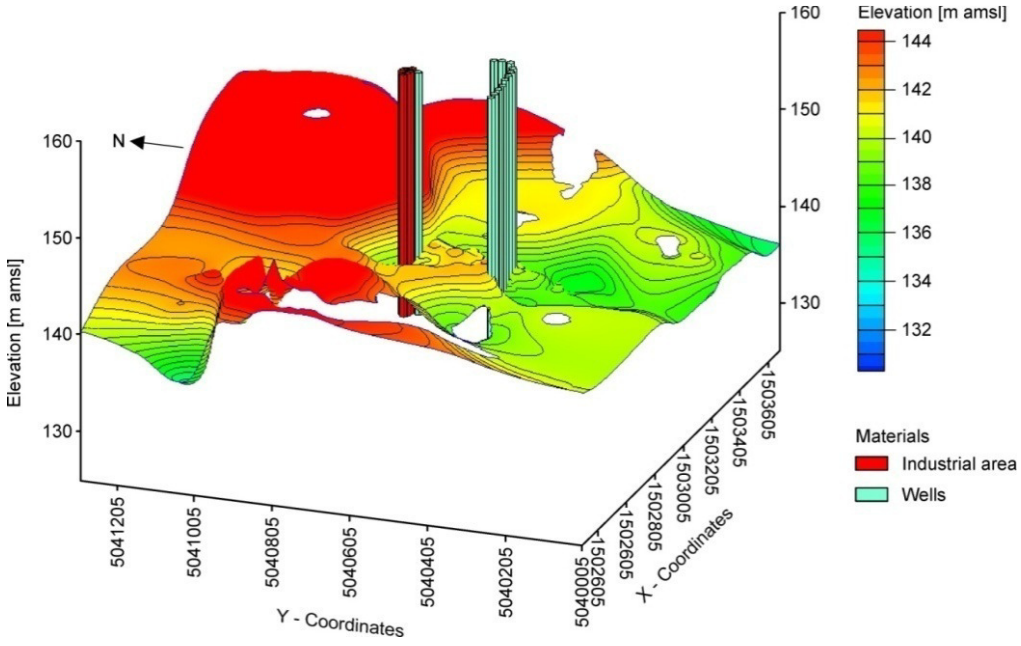

Figure 2.11 Topographic surface map in perspective view of top of aquitard of model 2 - version 1, z-magnification 1 : 25

Version 2 of the structural hydraulic model was defined as only applying the available data points of the borehole database. As result, the distribution of the aquitard is much more restricted (figure 2.12).

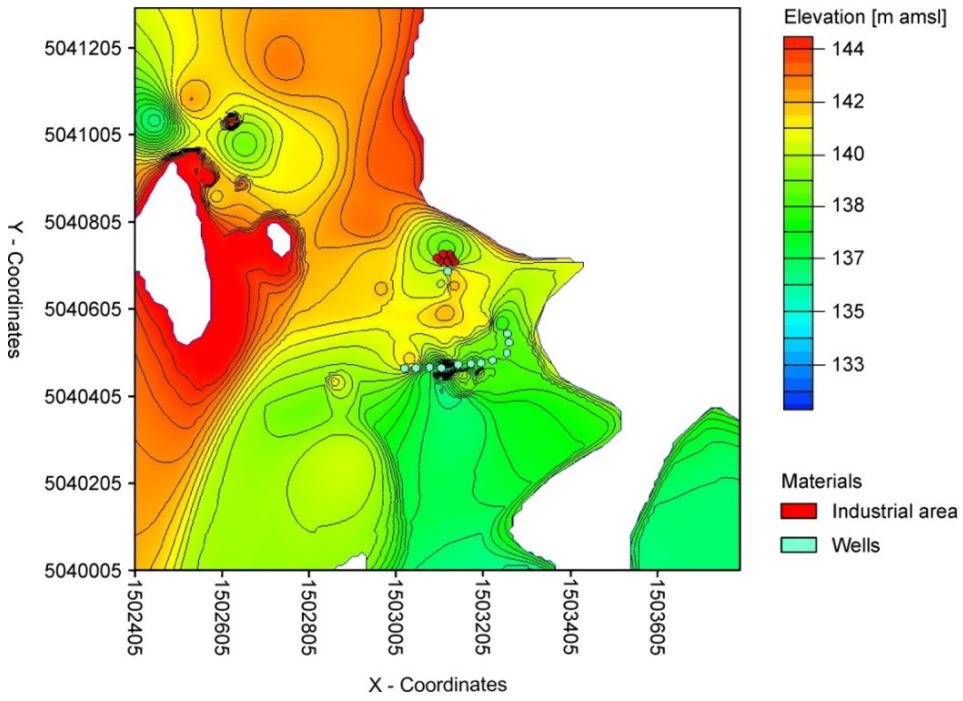

Figure 2.12 Topographic surface map of top of aquitard of model 2 - version 2

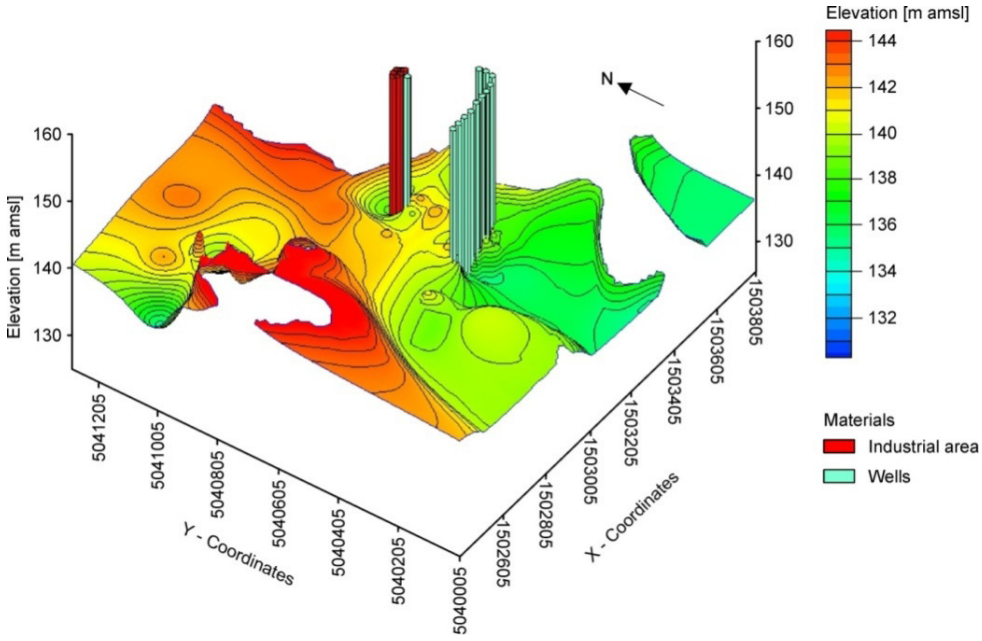

Figure 2.13 Topographic surface map in perspective view of top of aquitard of model 2 - version 2, z-magnification 1 : 25

Due to the sparse distribution of boreholes, the aquitard is not present in the northeastern part of the model. To the west and to the south east of the industrial area, an occurrence is not proved by data. To the south of the industrial area, the same morphological structure as in version 1 is exhibited, forming a north-south elongated depression (figure 2.13). The general depth of the aquitard ranges between 135 m amsl and 145 m amsl.

2.3.3 Model 3 – Structural geological 3D model based on boreholes

The third model consists of the geological description and characterization of the borehole data set according to USCS. There are 19 USCS classes present in the database overall. The geological classes were combined and reduced to four geological materials, based on their main components and resulting hydrauclic conductivity:

- RIP anthropogenic filling
- TV green area, vegetation
- G gravel with minor amounts of sand, silt and clay
- S sand with minor amounts of gravel, silt and clay
- C silt and clay, with minor amounts of sand and gravel

Units G and S represent hydraulic permeable layers, whereas unit C comprises all hydraulic impermeable layers. The surface units RIP and TV were not taken into account for the modeling.

The silt and clay layers form three main units: a raised plateau in the Northwest of the model domain, an elongated EW- trench through and south of the former disposal bassin and a second increased plateau at the industrial area (figure 2.14).

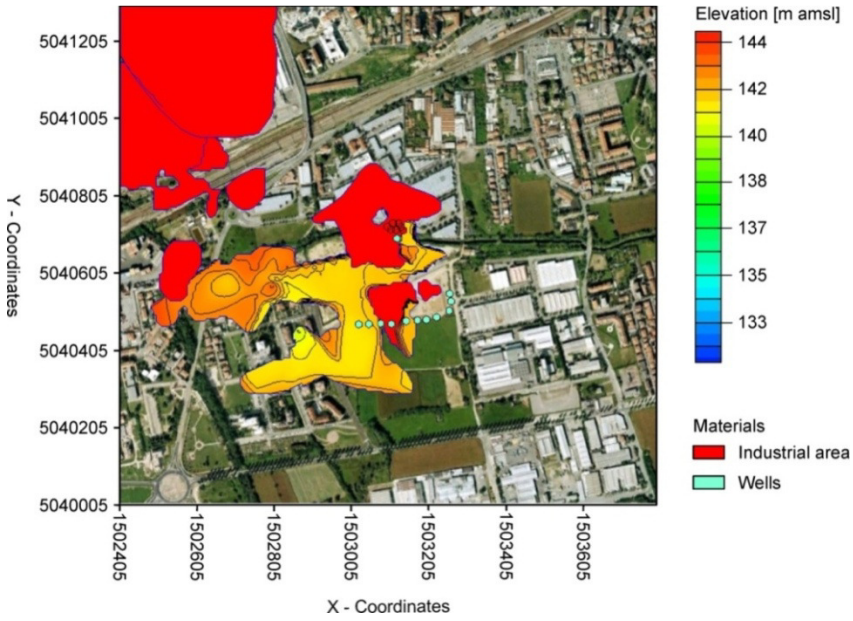

Figure 2.14 Topographic surface map of top of aquitard of model 3, on top of surface map of Rho

Although it may seem like one continuous layer at the former industrial site, it is formed by several lenses in varying depth. The layers are overlapping with a depth variance of approx. 10 m in a stepladder-like system of clay and silt layers, creating possible pathways for the DNAPLs (figure 2.15). Moreover, the top of the aquitard is five to ten meters closer to the surface than in the ModFlow model, which actually results in an impermeable layer within the Superficiale (figure 2.16).

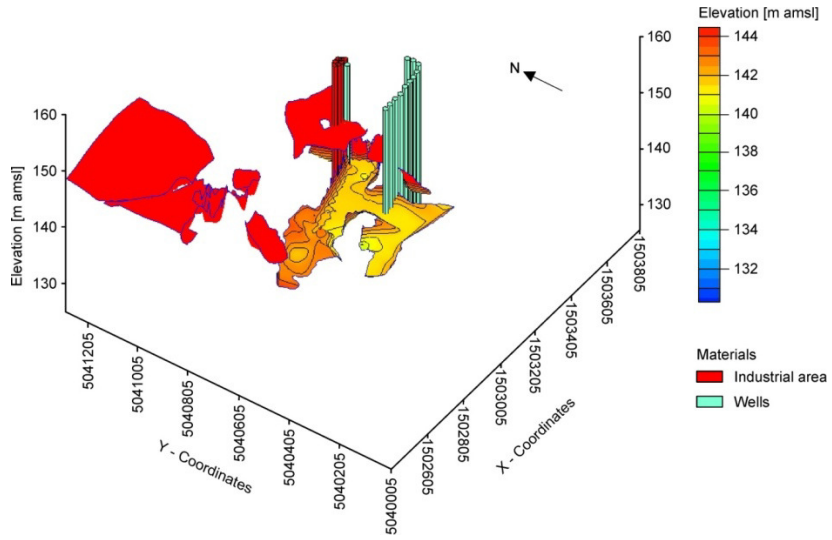

Figure 2.15 Topographic surface map in perspective view of top of aquitard of model 3, z-magnification 1 : 25

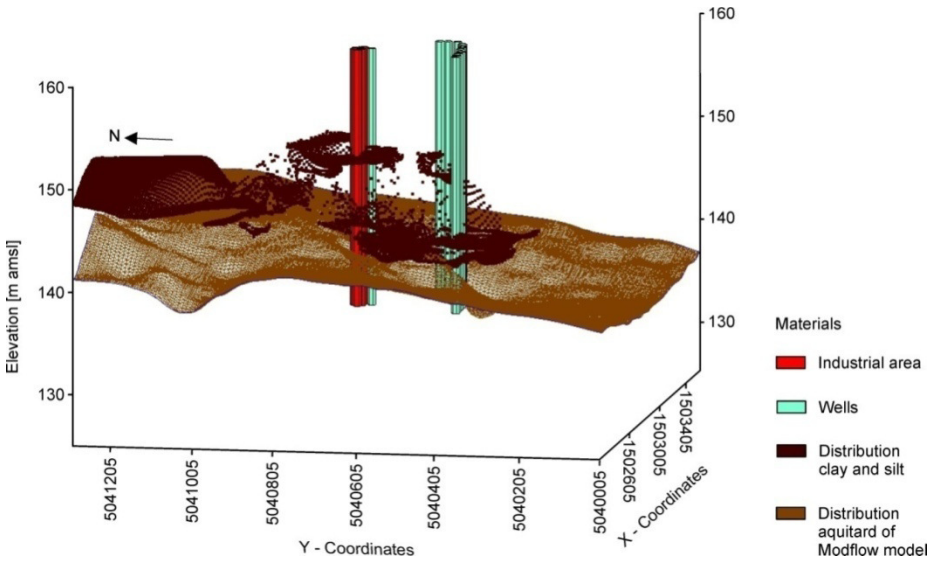

Figure 2.16 Surface of aquitard in model 3 (dark brown dots) in comparison to aquitard of model 1 (light brown dots) in perspective view, z-magnification 1 : 25

Some differences may be explained by a potentially oversimplified soil classification during drilling, maybe small layers of silt and clay were ignored and handled as minor aspects of the aquifer. Moreover, the grouping of materials into four groups based on their main components probably has been too simplified. But still, the geological data of the available borehole data base does not support a regular or even continuous distribution of impermeable, clayey and silty material at the field site.

Unfortunately no information exists about the process of classification of geological material as hydraulic units. In the available borehole data set, no additional occurrence of silt and clay can be found. The discrepancy between geological material description and definition as aquifer or aquitard at the site can not be explained, because no informations were available at La Sapienza about the process of classification and transformation.

In order to address *Issue 3 – "Is it possible that the DNAPL migrated through a gap in the aquitard to the deeper aquifer?"* and *Issue 4 – "What are the influences of subsurface morphologies on the DNAPL movement and its final position?"* a 2D cross section parallel to the

documented groundwater flow was cut through the Modflow-based model 1 (figure 2.17). Groundwater flow in the modflow model is calibrated by well head information and documented as NNW to SSE in direction. The 2D cross section runs through the position of the former disposal basin, the emergency well 50 m downstream and the well gallery (figure 2.18). The unsaturated zone was neglected for multiphase modeling. The hydraulic units were reconstructed concerning material parameters as porosity and permeability as far as values were present in the borehole data base. Missing values were complemented by documented values in the literature. For details of the multiphase implementation, please refer to *Chapter 6*.

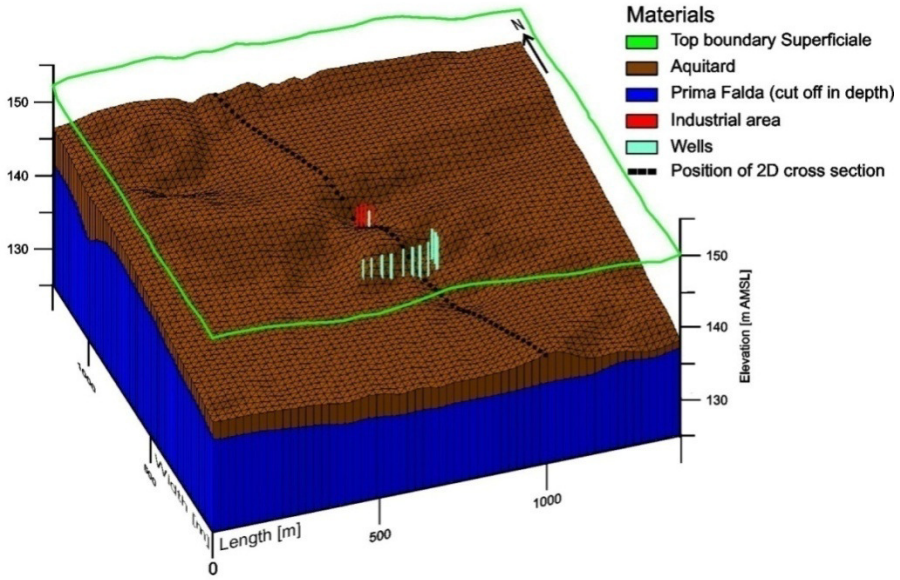

Figure 2.17 Perspective view of Aquitard and Prima Falda (Superficiale not shown), z-magnification 1 : 25

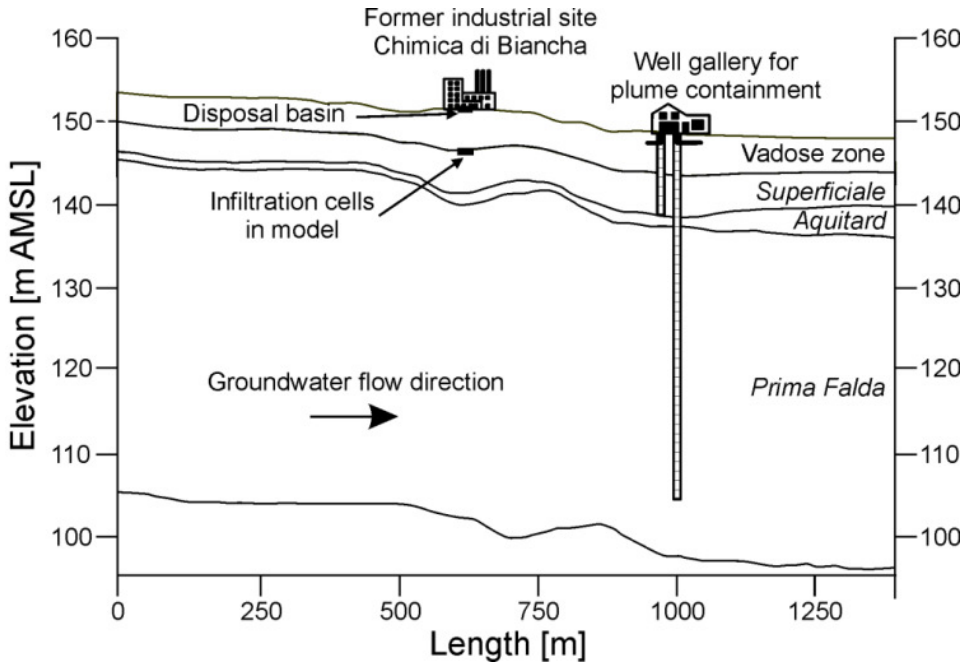

Figure 2.18 2D cross section converted for multiphase modeling, z-magnification 1 : 25

3 Simulation of DNAPL distribution depending on groundwater flow velocities using TMVOC

Published as

Erning, K., Schäfer, D., Dahmke, A., Luciano, A., Viotti, P. and Petrangeli Papini, M. (2010a): Simulation of DNAPL distribution depending on groundwater flow velocities using TMVOC. In: M. Schirmer, E. Hoehn and T. Vogt (Editors). IAHS Publication: Groundwater Quality Management in a Rapidly Changing World. Proceedings of the 7th International Groundwater Quality Conference held in Zurich, Switzerland, 13-18 June 2010. Red Books. IAHS. Oxfordshire. pp. 128-131.

Abstract

Remediation actions on groundwater contaminations are based on the knowledge of the position, the size and the mass of the source zone. We focus in our research on the question, whether high groundwater flow velocities can cause a displacement of a DNAPL source zone. Additionally, the impact of high groundwater flow velocities on the development of the DNAPL body is investigated. The tool for these investigations is multiphase modeling of different flow scenarios with TMVOC. The simulation revealed that even low groundwater flow velocities affect the DNAPL movement and distribution in the saturated zone and should thus be taken into account by site investigation.

Keywords DNAPL infiltration; lateral displacement; groundwater flow velocities; multiphase flow modeling; TOUGH; TMVOC

3.1 Introduction

Chlorinated solvents, like tetrachloroethylene (PCE) and trichloroethylene (TCE), are among the most widespread groundwater contaminants worldwide and are often released into the subsurface as Dense Non-Aqueous Phase Liquids (DNAPL).
DNAPL as a distinct phase is commonly observed not only straight below, but also downstream of the surface contamination area. General explanations for this phenomenon are the existence of an undocumented, second point source downstream of the main source, or a DNAPL displacement through preferential flow paths due to hydraulic heterogeneities within the aquifer. Apart from these aspects, the displacement of the DNAPL may be influenced by high groundwater flow velocities (pore velocity of water v_w), which can occur in gravel-sandy aquifers at the foothill of mountain ranges or in aquifers which are influenced by human activities, such as active pump and treat remediation actions.

In this study the behaviour of the DNAPL TCE is analysed on a small scale and in homogeneous conditions by investigating laboratory experiments with 2D multiphase modeling with the software TMVOC (Pruess and Battistelli, 2002) and PetraSim (Thunderhead Engineering, 2011). The focus of this investigation is set on the question whether a minimum groundwater flow velocity, a so-called threshold value, is required to displace a DNAPL within a homogeneous environment. Additionally, the influence of the water flow velocities on the DNAPL spatial position is analysed and quantified.

3.2 Influence of Groundwater flow velocities on DNAPL movement

3.2.1 Methodology

In order to investigate the spatial movement of TCE under high groundwater flow velocities, a coupled approach of 2D laboratory tank experiments (performed at La Sapienza University, Rome) and 2D multiphase modeling with TMVOC and PetraSim was used. The experimental tank measured 1.0 × 0.12 × 0.7 m (L × W × H) and was filled with coarse grained glass beads (grain size: 0.4 - 0.8 mm, porosity: 39 %, intrinsic permeability: 2.45×10^{-10} m^2) up to a height of 0.7 m. Via a fixed hydraulic head in the inflow chamber and a weir at the outflow chamber, constant hydraulic gradients of 0.0 %, 0.4 % and 0.8 % were obtained, corresponding to groundwater flow velocities of approx. 0.00 m/day, 20.00 m/day and 40.00 m/day. A total amount of 2 L of the dyed, non-toxic TCE substitute HFE-7100 (3M, 2005) was infiltrated with constant entry pressure. The spreading behaviour of HFE-7100 was documented and processed via an image analysis method (Luciano et al., 2010). The results of the laboratory experiments were used to calibrate the multiphase model within TMVOC (Erning et al., 2009). After calibration of the model to HFE-7100, a verification run using TCE was performed, showing no differences in the DNAPL distribution. As a next step, the model domain was elongated to a total length of 5 m and 10 m, respectively. Thirteen different groundwater flow velocities ranging from 0.00 m/day to 40.00 m/day were applied using first order boundary conditions regarding hydrostatic pressure at the inflow and outflow of the model. In the model a total amount of 2 L of TCE was infiltrated with a constant rate over 6000 s. After 6000 s simulation time, the TCE source was deactivated in order to observe the spreading behaviour after removal of the contamination source for additional 5 hours.
The spatial distribution was analysed for every groundwater flow velocity at constant time steps with regard to five different features: (1) inclination of the percolation path, (2) position of the pooling DNAPL, (3) length of the pooling DNAPL, (4) maximum contaminated area and (5) maximum saturation of the TCE phase in comparison to a base case scenario without groundwater flow (figure 3.1).

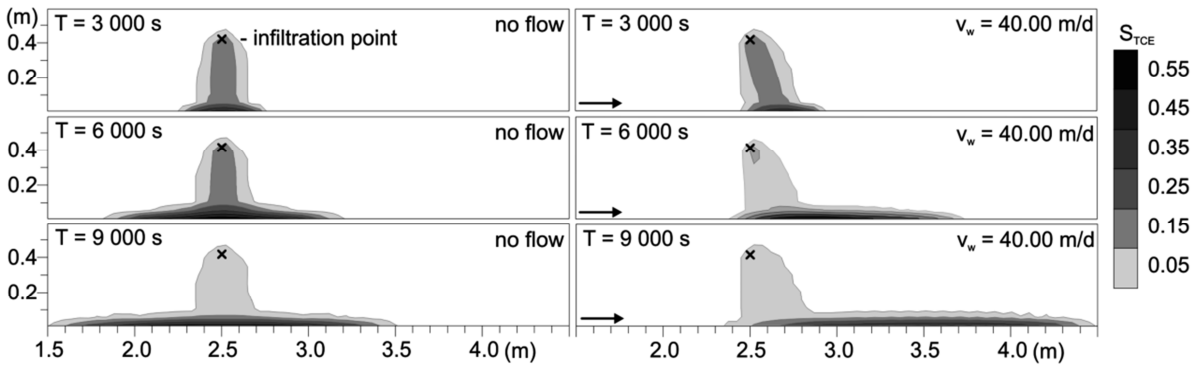

Figure 3.1 Simulated TCE saturation at $v_w = 0.00$ m/day (base case scenario) and $v_w = 40.00$ m/day. Small differences in the lateral distribution of the base case scenario are due to the resolution of the model and the interpolation method (kriging)

3.2.2 Results

The simulations ranging from $v_w = 0.05$ m/day to $v_w = 40.00$ m/day revealed that no minimum groundwater flow velocity is required to affect the movement and position of a DNAPL body in the saturated zone. However, the impacts on the geometry and position are absolutely and relatively small as long as flow velocities of 5.00 m/day are not exceeded in our model (table 3.1). The obtained results are exemplarily described for the highest groundwater flow velocity of 40.00 m/day, where changes are most visibly prominent.

Table 3.1 Impacts of groundwater flow velocities on DNAPL distribution in the saturated zone at t = 24 000 s

	Groundwater flow velocity (m/day)								
	0.00	0.05	0.25	0.50	1.00	5.00	10.00	20.00	40.00
Inclination of the percolation path (°) at $t = 6\,000$ s	0	–0.01	–0.15	–0.21	–0.41	–3.52	–6.62	–11.31	–18.57
Downstream translocation of the pool (cm)	0.00	1.00	4.30	5.50	8.20	37.80	75.40	114.80	145.0
Length of the pool (cm)	293.30	292.60	290.40	290.60	293.60	294.40	294.70	318.80	399.20
Max. DNAPL saturation (%)	42.70	42.60	42.70	42.70	42.70	42.70	42.00	39.00	33.00
Percental area (%)	100.00	100.32	99.64	99.02	100.00	97.78	95.05	96.37	73.55
DNAPL mass (kg)	3.0389	3.0389	3.0388	3.0386	3.0381	3.0339	3.0281	3.0157	2.9894

At flow velocities of 40.00 m/day the percolation path of TCE is inclined by a mean average of 18.57° to the downstream direction, resulting in a translocation of the pool at $t = 6\,000$ s of 0.51 m to the outflow. While at no flow conditions (base case scenario) the DNAPL pool starts 0.64 m "upstream" of the infiltration point, it begins only 0.13 m upstream at $v_w = 40.00$ m/day. At $t = 24\,000$ s, the translocation reaches 1.45 m in downstream direction. The length of the pool is enlarged by 1.06 m compared to the base case scenario at $t = 24\,000$ s, while the area is reduced by 26.45%. The maximum DNAPL saturation decreases to $S_{DNAPL(vw = 40.00\ m/d)} = 0.33$ compared to $S_{DNAPL(base\ case)} = 0.43$ at the end of the simulation time.

3.3 Discussion

Two different aspects of the groundwater flow velocity influence the spatial distribution of the DNAPL. The first factor is the kinetic force and thus the hydrodynamic pressure of the streaming water. This leads to an inclination of the percolation path and a translocation of the DNAPL pool. Following the way of least resistance, i.e. least pressure, the DNAPL is transported downstream by erosion of the surface layers of the pool and relocation in the depressurized zone downstream.
The second aspect is the enhanced mass flux (M) of TCE dissolved in groundwater ($C_{TCE,dissolved}$) with larger flow velocity:

$$M = q_w \times C_{TCE,dissolved} \times A \tag{3.1}$$

with q_w being the Darcy flow velocity and A the area.
As TMVOC is only able to calculate the dissolution of the DNAPL phase assuming instantaneous solution and saturation up to maximum solubility, the mass transfer rate in the model is enhanced by increased groundwater flow velocities and therefore probably overestimated at high groundwater flow velocities. Effects of translocation processes and of enhanced dissolution processes are intermingled and counterbalanced at low flow velocities, while at high flow velocities, the translocation processes dominate in our set-up.

3.4 Conclusion

A threshold value for groundwater flow velocities required to affect the distribution of a DNAPL in the subsurface does not exist in our homogenous model set-up. The streaming water even impacts at $v_w = 0.05$ m/day the position, the size and the mass transfer rates of the DNAPL body, although the influence remains small for $v_w \leq 5.00$ m/day on the chosen spatial and temporal scale. However, transferring the results of the simulations to a homogeneous field scale problem, the DNAPL could be transported at $v_w = 1.00$ m/day and t = 50 years over a length of approx. 5.4 km, assuming a permanent DNAPL injection and same geological conditions as in the small scale investigation.
But, as was observed during the laboratory experiments, the influences of high groundwater flow velocities can be superimposed by heterogeneities of the material parameters. Smallest variances in permeability can produce preferential flow paths and thus change the position and geometry of the DNAPL body significantly.

3.5 Further prospects

In the next work step, the influence of heterogeneities and preferential flow paths will be investigated on small scale model scenarios, in order to evaluate the effects of material parameters vs. groundwater flow velocities. The heterogeneous model will then be upscaled and adapted to a real field site.

Acknowledgements

The research leading to these results has received funding from the European Community's Seventh Framework Programme (FP7/2007-2011) under grant agreement no. 213161 (ModelPROBE).

References

3M (2005): 3M Novec TM 7100 - Engineered Fluid. Product Information. 3M Electronics. St. Paul, MN, USA. pp. 8.

Erning, K., Schäfer, D., Dahmke, A., Luciano, A., Viotti, P. and Petrangeli Papini, M. (2009): Simulation of DNAPL infiltration into groundwater with differing flow velocities using TMVOC combined with PetraSim. TOUGH Symposium 2009. Proceedings TOUGH Symposium. LBNL. Berkeley, CA, USA.

Luciano, A., Viotti, P. and Petrangeli Papini, M. (2010): Laboratory investigation of DNAPL migration in porous media. Journal of Hazardous Materials 176: 1006-1017.

Pruess, K. and Battistelli, A. (2002): TMVOC, A Numerical Simulator for Three-Phase Non-isothermal Flows of Multicomponent Hydrocarbon Mixtures in Saturated-Unsaturated Heterogeneous Media. Report LBNL-49375. Berkeley.192 pp.

Thunderhead Engineering (2011): PetraSim - Interactive Model Creation for Advanced Flow, Transport and Heat Transfer Models. In: T.E.C. Inc. (Editor). Manhattan, USA.

4 Simulation of DNAPL infiltration and spreading behaviour in the saturated zone at varying flow velocities and alternating subsurface geometries

Published as

Erning, K., Grandel, S., Dahmke, A. and Schäfer, D. (2012): Simulation of DNAPL infiltration and spreading behaviour in the saturated zone at varying flow velocities and alternating subsurface geometries. Environmental Earth Sciences 65(4): 1119-1131.

Abstract

The influence of varying groundwater flow velocities on DNAPL infiltration and spreading behaviour was investigated by multiphase modeling using TMVOC & PetraSim. The multiphase models were calibrated by results of previously conducted laboratory experiments for the complete spatio-temporal range of the experiments. The small scale 2D scenario modeling was applied to qualify and quantify changes in position, architecture, geometry and dissolution of a TCE body in a fully saturated homogenous sandy medium. The applied flow velocities ranging from 0.05 m/d up to 40.00 m/d exhibited that the DNAPL TCE is affected even at the lowest flow velocity in its position, its size and its architecture. Additionally, several impermeable lenses with simple geometry were assumed in the model, to investigate the influence of stratified subsoil. In the experimental set-ups, the DNAPL body reacts more sensitive to the applied groundwater flow velocities than to the geometrical set-up of the scenarios. A possible consequence can be the transportation and displacement of a DNAPL pool due to natural or anthropogenic induced high groundwater flow velocities, as by Pump & Treat facilities, complicating site investigation process and planning of remediation activities.

Keywords: DNAPL, source zone architecture, groundwater flow velocities, TMVOC, modeling

4.1 Introduction

Chlorinated solvents like tetrachloroethylene (PCE) or trichloroethylene (TCE) are among the most widespread groundwater contaminants worldwide and are often released into the subsoil as Dense Non-Aqueous Phase Liquids (DNAPL). Once released to the subsoil the DNAPL moves vertically through the vadose zone and the saturated zone, steered by its physico-chemical properties as high density and low viscosity. When the DNAPL encounters formations with reduced permeability it will accumulate on top of them. In cases where the DNAPL mass exceeds the entry pressure of the respective material, it infiltrates the low permeability zone. Alternatively, the DNAPL follows gravity-driven the inclination of the

respective barriers, leading to complex distribution patterns of DNAPL fingers and pools in the subsoil. At site investigations of contaminated areas, DNAPLs are sometimes not only observed straight below the original surface contamination area, but also in considerable downstream direction. Possible explanations are the existence of an undocumented second point source or preferential flow paths in the subsurface due to high permeable geological layers. Additionally, transport of the DNAPL as free phase with the streaming groundwater could be possible. The identification of the exact or at least approximated position of a long-term DNAPL source zone is essential for any kind of groundwater remediation purposes, as otherwise the planning of remediation and / or containment facilities is hardly possible.

Although a lot of research has been done on the topic of DNAPL migration in the saturated zone with respect to small and large scale heterogeneities (Kueper and Frind, 1988; Illangasekare et al., 1995; Dekker and Abriola, 2000; Saenton et al., 2002; Bradford et al., 2003; Bao et al., 2004; Broholm et al., 2005; Jawitz et al., 2005; Rivett and Feenstra, 2005; Fagerlund et al., 2006a; Page et al., 2007), dissolution processes (Zhu and Sykes, 2000; Falta, 2003; Bao et al., 2004; Falta et al., 2005a; Rivett and Feenstra, 2005; Fure et al., 2006; Li et al., 2011) and mass flux (Jellali et al., 2003; Soga et al., 2004; Fure et al., 2006; Illangasekare et al., 2006; Page et al., 2007; Christ et al., 2009), there has to the knowledge of the authors, not yet been a distinct focus on enhanced groundwater flow velocities (v_w). The effects of v_w up to 1.0 - 1.5 m/d in combination with heterogeneities has already been investigated with numerical simulations by several research groups. Dekker and Abriola (2000) for instance stated no significant influence on the DNAPL behaviour in the range of $0.0 \text{ m/d} < v_w < 1.0 \text{ m/d}$ compared to alternative dominating factors like spatial variance of permeabilities in the subsoil and spill rate of the DNAPL. Gerhard et al. (2007) investigated the controlling factors of the cessation time for movement of five different DNAPLs and concluded that groundwater flow velocities in the range of $v_w < 1.3$ m/d have no significant influence on the time scale for the DNAPL movement. But they determined that the position of the main DNAPL body is influenced by the ambient groundwater flow velocities up until $v_w \leq 1.5$ m/d. Furthermore they concluded that higher impacts have to be expected in the surroundings of drinking water production facilities, where the groundwater flow is artificially enhanced.

Natural groundwater flow velocities are generally considered to vary in most aquifers between a few centimetres and a maximum of one meter per day. Although this is an acceptable assumption for most of the investigated areas in the lowlands, these values can easily be exceeded in hilly countryside or at the foothills of mountains.

In gravely aquifers at the foothills of mountains or in narrowing river valley aquifers, flow velocities of more than one meter per day are often encountered. The river valley Glatt in Switzerland for instance is characterized by natural groundwater flow velocities of 3.5 m/d to 5.0 m/d (Hoehn and Santschi, 1987; Hoehn and Von Gunten, 1989; Von Gunten et al., 1991) due to riverbank infiltration. The narrowing valley aquifers of Stuttgart, Germany exhibit natural groundwater flow velocities up to 5.0 m/d (Herfort and Ptak, 2002), which can reach approx. 10 m/d on a local scale due to influences of topography and morpho-geology (Herfort et al., 1998). The same factors affect the groundwater flow in Darmstadt, Germany (Greifenhagen, 2000).

Moreover, the groundwater flow velocities in these highly permeable quaternary alluvial sediments can further be increased in the surroundings of drinking water production, hydraulic containments and Pump & Treat facilities for remediation purposes.
This is the case at a former industrial site in Rho, in the proximity to Milan, Italy.
The site is characterized by a quaternary multi-aquifer formation with a natural groundwater pore velocity of one to two meters per day. The aquitard between the two aquifers of interest consists of clay and silty clay. Based on the geological investigation of the area, the aquitard is probably not omnipresent in the area, but characterized by gaps of varying size, creating hydraulic connections between the aquifers.
During an operational time of approximately 75 years, the chlorinated solvents TCE and PCE were disposed via an open basin. Groundwater sampling campaigns over the last decades revealed high concentrations of dissolved TCE and PCE in the uppermost and in the deeper aquifer. The concentration profiles suggest the occurrence of a free DNAPL phase in both aquifers. In approx. 2005 a Pump & Treat facility was installed, extracting from both aquifers and furthermore increasing the groundwater flow velocity.
Since the already installed remediation facilities are neither effective nor efficient regarding time and costs, the installation of a permeable reactive barrier (PRB) is considered. For the planning and installation of any PRB, the knowledge of the position of the contaminants is essential.
The working hypothesis for the field site is a transportation of the free phase DNAPL with the streaming groundwater in the uppermost aquifer to a hydraulic connection and further passage to the deeper aquifer. The possible location in the deeper aquifer is still unknown.
In this paper, which is the first in a serial about the influence of high groundwater flow velocities on the behaviour of DNAPLs, the physical principles are investigated by numerical multiphase modeling on laboratory scale.
The simulations are conducted with the multiphase modeling software TMVOC (Pruess and Battistelli, 2002) via the graphical user interface PetraSim (Thunderhead Engineering, 2011) on 2D small scale, calibrated by laboratory experiments. Thirteen different groundwater flow velocities ranging from centimetres per day up to several tens of meters and four different realizations of geometrical set-up of the subsoil are investigated, resulting in a total of 28 scenarios.
The main points of interest in this first study are the qualification and quantification of the transport of a TCE DNAPL pool as a result of varying groundwater flow velocities.
Furthermore the influence of small scale heterogeneities is investigated as well as the changed geometry of the free phase DNAPL body in the saturated zone, since dissolution behaviour and therefore mass flux are directly dependent on the orientation and the geometry of a NAPL pool within the saturated zone, as investigated by Sale and McWhorter (2001), Fure et al. (2006) and Miles et al. (2008a).
These small scale investigations will give a first approximation for the behaviour of DNAPLs at the real field site in Italy, at geological - hydrogeological similar field sites and for hydraulic flushing scenarios.

4.2 Methodology

4.2.1 Calibration model

Laboratory experiment for computer model calibration

The primary data set for the calibration of the multiphase model was provided by Luciano et al. (2010), who conducted the laboratory experiments. The documented spreading behaviour of the DNAPL in the experiments was used to identify the scaling parameters of the multiphase formulations of the relationships of capillary pressure – saturation (P_c - S) and relative permeability – saturation (k_r - S), two primary controlling factors for the spreading behaviour of NAPLs (Pankow and Cherry, 1996; Dekker and Abriola, 2000; Fagerlund et al., 2006b; Chang et al., 2009). The tank experiment measured 1.33 m × 0.12 m × 0.70 m (L × W × H) and was filled with coarse glass beads (SAND1) up to a height of 0.50 m (table 4.2). Two low permeable lenses of fine grained glass beads (SAND2) were installed at different heights within the coarse grained stratum (figure 4.2).

Table 4.1 Material parameters of the artificial porous media (provided by Luciano et al. 2010)

	SAND1	SAND2
Diameter of glass beads [mm]	0.4 - 0.8	0.1 - 0.2
Porosity	0.388	0.373
Density [kg/m³]	2500	2500
Bulk density [kg/m³]	1530	1570
Intrinsic permeability, horizontal [m²]	2.4×10^{-10} (a)	8.5×10^{-15} (b)
Intrinsic permeability, vertical [m²]	1.94×10^{-10} (a)	8.5×10^{-15} (b)

(a) calculated by means of Darcy´s law and hydraulic permeability
(b) no measurements, iterativey fitted during calibration process of the model

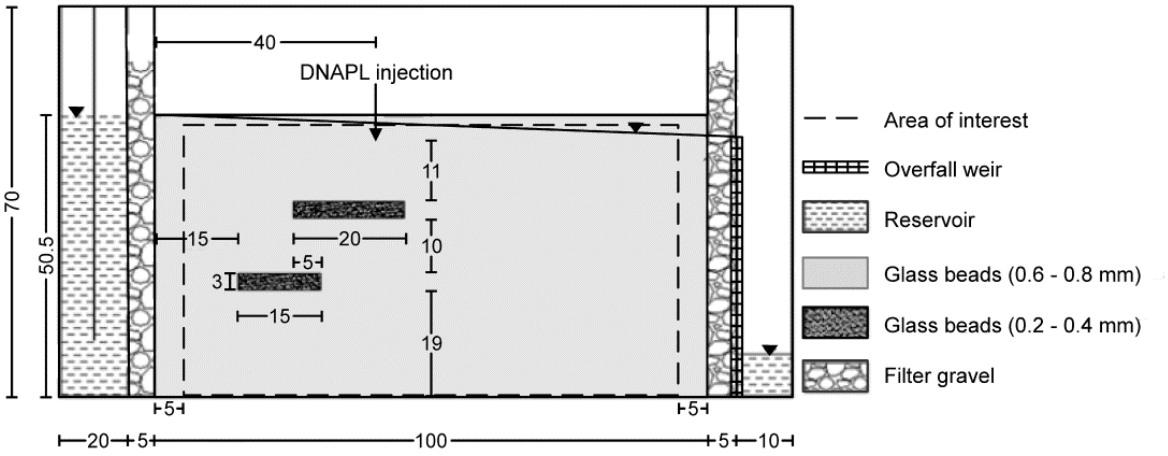

Figure 4.1 Schematic set-up of the experimental tank (Luciano et al., 2010), all length in cm

Via a fixed hydraulic head in the inflow chamber and an adjustable overfall weir at the outflow chamber groundwater pore velocities (v_w) of 0.00 m/d, 21.25 m/d and 40.86 m/d were obtained.

HFE-7100 (3M, 2005) was used as DNAPL substitute, being well established as non-toxic alternative to TCE in laboratory experiments (Lee et al., 2004).

A total amount of 2 litres (3.05 kg) of dyed HFE-7100, featuring similar physico-chemical properties as TCE (table 4.3), was infiltrated below the water table with a constant entry pressure. The spatio-temporal spreading behaviour of HFE-7100 in the laboratory tank was photo documented for each flow velocity at predefined time steps and processed via an image analysis procedure. Thus it was mapped only visually, since the measurement of saturation profiles is extensively time and cost consuming and for this investigation of minor interest. Saturation profiles are essential for investigations regarding the mass flux and longevity of source zones, but the focus of this investigation is on the position of source zones, in order to improve site investigation and planning of remediation facilities.
For additional details concerning the set-up, the analysis and the applied boundary conditions the reader is referred to Luciano et al. (2010).

Table 4.2 Physico-chemical properties of HFE-7100 and TCE

Property	HFE-7100	TCE
Chemical formula	$C_4F_9OCH_3$	C_2HCl_3
Relative density [kg/m³]	1500 / 1480 (dyed)	1464
Relative viscosity [cP]	0.60	0.59
Surface tension [mN/m]	13.60	29.30
Interfacial tension [mN/m]	35.59	34.50
Vapour Pressure [kPa]	28.00	7.73
Water solubility [ppm]	12	1100

Calibration of the computer model

The size of the calibration model within TMVOC was 1.00 m × 0.12 m × 0.60 m (L × W × H), corresponding to the volume of the laboratory experiment filled with glass beads, having a resolution of 75 cells in length, 1 cell in width and 44 cells in height and creating a 2D model domain of 3 300 cells. The resolution was refined from 4 cm² to 1 cm² in the surroundings of the low permeable lenses and the infiltration point (figure 4.3).
The geometry of the lab experiments was rebuilt in the model regarding the geometry of infiltration point and low permeable lenses, applying the physical properties of the two types of glass beads (cf. table 4.2).
The model was initialized as fully water saturated with first order boundary conditions regarding hydrostatic pressure and water saturation for the inflow (left side) and the outflow (right side) of the model domain. Top and bottom of the model were defined as impermeable, implying a confined aquifer although the laboratory experiments were unconfined. These simplifications were chosen since the simulation and calibration of the capillary fringe is excessively runtime consuming and since the DNAPL infiltration in the laboratory experiments took place below the water table. Thus the vadose zone had no effect on this investigation and could be neglected for the simulations.

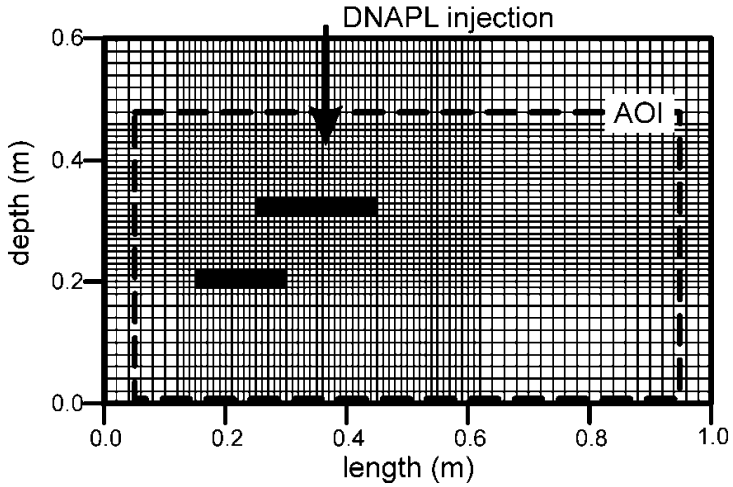

Figure 4.2 Model domain in TMVOC, low permeable lenses in black, overlaid by discretization grid, groundwater flow from left to right (AOI = area of interest of the laboratory experiments)

The location of the infiltration point, the amount of the infiltrated DNAPL HFE-7100, the infiltration rates (kg/s) and the observation times corresponded to the measurements in the laboratory experiments and are listed in table 4.4. The enhanced infiltration of the DNAPL in the laboratory experiments with increasing groundwater flow velocities already shows the influence of the streaming water on the DNAPL body and are analyzed in Luciano et al. (2010).

Table 4.3 Boundary conditions of the laboratory experiments (Luciano et al. 2010)

	Experiment 1	Experiment 2	Experiment 3
Groundwater pore velocity v_w (m/d)	0.00	21.25	40.86
Infiltrated amount of HFE-7100 (kg)	3.05	3.05	3.05
Infiltration rates in the calibration model (kg/s)	5.08×10^{-4}	8.13×10^{-4}	1.90×10^{-3}
Seepage / infiltration time (s)	5905	3690	1580
Observation time after deactivation of infiltration = spreading time (s)	10217	1890	4325
Total time of experiments and models (h)	4.48	1.55	1.64

Different sets of functions for P_c - S and k_r - S functions were tested regarding their accuracy in simulating the spreading behaviour of the DNAPL as well as their applicability, roughness and runtime performance. Due to best performance and most accurate results, Parker and Lenhard ´s three-phase formulation of P_c – S(Parker and Lenhard, 1987) and Stone´s three phase formulation of k_r – S(Stone, 1970) were finally chosen. Both formulations are originally for the three phase system water -gas - NAPL, but can easily be adapted to the two phase system water - NAPL. The scaling parameters of the chosen formulations were iteratively fitted from provided literature values (Falta et al., 1995; Pruess and Battistelli, 2002) to the documented spreading behaviour of all the laboratory experiments, thus that one set of parameters fitted the DNAPL behaviour at all flow velocities at the same time. The fitted parameters are listed in table 4.4, with S_{wr} being the residual water saturation, S_{nr} the residual NAPL saturation, S_{gr} the residual gas saturation, and n, a_{gn} and a_{nw} as scaling factors.

Table 4.4 Determined parameters for capillary pressure and relative permeability.

	P_c – S – formulation (Parker and Lenhard, 1987)	k_r – S – formulation (Stone, 1970)
S_{wr}	-	0.1
S_{nr}	-	0.1
S_{gr}	-	0.0
n	2.5	2.5
S_m	0.1	-
α_{gn}	100	-
α_{nw}	50	-

4.2.2 Scenario Modeling

The calibration model was used to investigate additional scenarios that were not investigated in the laboratory experiments. Therefore the calibration model was adapted in its size, resolution and geometrical set-up for the scenario modeling to avoid any interaction of the DNAPL with the model boundaries. The specific values are listed in the description of the different scenarios. The material properties, the boundary conditions and the amount of injected DNAPL were identical to the parameters of the calibration model, but the simulations were performed using TCE instead of HFE-7100.
The infiltration point was set to the coordinates X = 2.50 m and Z = 0.42 m. For the highly permeable areas the physical properties of SAND1 were applied (cf. table 4.2 and table 4.5). For the layered scenarios a new material was introduced, reflecting impermeable clay, named IMPER.

Table 4.5 Material parameters of the model domain

	SAND1 (= coarse grained glass beads)	IMPER (newly defined)
Density (kg/m³)	2500	2900
Effective porosity	0.39	0.10
Intrinsic permeability, horizontal (m²)	2.43×10^{-10}	8.50×10^{-21}
Intrinsic permeability, vertical (m²)	1.94×10^{-10}	8.50×10^{-21}

In the models a total amount of 3.05 kg of TCE was infiltrated at a constant rate over 6 000 s. After 6 000 s the TCE infiltration was deactivated in order to observe the spreading behaviour of the DNAPL body after removal of the original source zone for additional 5 hours, resulting in an overall simulation time of 6.67 hours. The spatial distribution of TCE as DNAPL body was analyzed at 14 predefined time steps for all applied flow velocities. The size of the DNAPL body was defined by the area with a saturation of TCE (S_{TCE}) higher than the residual saturation ($S_{TCE\,r} > 0.1$). Any flow induced changing in the position of the pooling DNAPL on the bottom of the model domain was defined as displacement, compared to the position of the pool in the base case scenario without groundwater flow. The starting position of the pool was defined by the first left-hand / upstream cell on the bottom of the model domain, which encounters DNAPL saturation of $S_r > 0.1$. Furthermore, the changes of occupied area were analyzed for the homogeneous scenario in order to approximate the potential changes in contaminated soil volume. The occupied area in the base case scenario corresponds hereby to a percentage of the area of 100 %.
Homogenous scenarios

In order to investigate the influence of the groundwater flow velocity on the DNAPL behaviour, a homogenous model only consisting of SAND1 was created. The domain was set to 5.00 m × 0.12 m × 0.60 m (L × W × H = X × Y × Z) and 10.00 m × 0.12 m × 0.60 m, respectively, depending on the applied flow velocities. Discretisation was defined as 90 cells and 140 cells, respectively, in length, 1 cell in width and 30 cells in height, with a high resolution zone from X = 2.0 m to X = 3.0 m, resulting in refined cell sizes of 0.02 m × 0.02 m in the surroundings of the infiltration point. Thirteen different pore velocities were applied to the model, including 0.00 m/d, 0.05 m/d, 0.10 m/d, 0.25 m/d, 0.50 m/d, 0.75 m/d, 1.00 m/d, 2.00 m/d, 2.50 m/d, 5.00 m/d, 10 m/d, 20 m/d and 40 m/d covering the whole range of the calibration model.

The spatial distribution of TCE was analyzed regarding five different features: (1) inclination of the percolation path, (2) position of the pooling DNAPL on the bottom of the model domain, (3) length of pooling DNAPL, (4) maximum contaminated area and (5) maximum saturation of the TCE phase in comparison to a base case scenario without groundwater flow.

Layered scenarios

The dimensions of the layered scenarios were 10.00 m × 0.12 m × 0.60 m (X × Y × Z), based on the size of the previous experiments. The domains were discretized in 140 cells in length, 1 cell in width and 60 cells in height, resulting in general cell sizes of 0.10 m × 0.01 m with a high resolution zone from X = 2.0 m to X = 3.0 m with a cell size of 0.02 m × 0.01 m.

Three different geometrical set-ups (figure 4.4) were investigated, constructed by SAND1 and IMPER (geometries A – C). Based on the results of the homogeneous scenarios, only five pore velocities of water (0 m/d, 5 m/d, 10 m/d, 20 m/d and 40 m/d) were investigated for each geometrical set-up regarding the position and the length of the DNAPL pool on the bottom of the model as well as the maximum contaminated area.

After using a resolution of millimetres for the data analysis in the homogenous scenarios in order to identify even smallest changes at low flow velocities, the scale was changed for the layered simulations to centimetre scale. Since the differences between the different layered scenarios are in the range of centimetres instead of millimetres as in the homogeneous settings, this simplification seems acceptable. A rerun of selected homogenous scenarios (results not shown) with refined discretisation showed no significant difference in the distribution and the behaviour of the DNAPL, thus the scenarios were comparable even with differing discretisation.

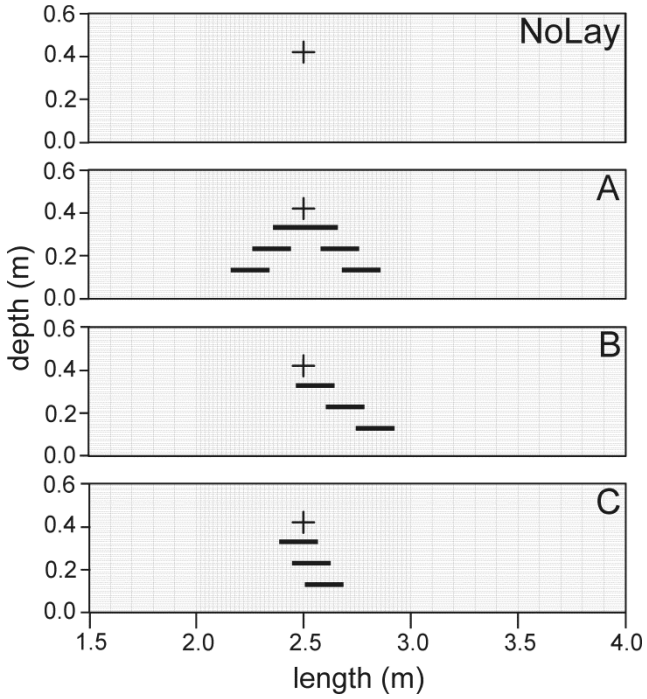

Figure 4.3 Geometrical set-ups of the different scenarios (detail of model domain from 1.5 m < X < 4.0 m), the cross marks infiltration point, black horizontal bars mark impermeable layers, overlaid by discretisation grid

4.3 Results and discussion

4.3.1 Calibration model

The computer model was calibrated for all three pore velocities of the laboratory experiments at every documented time step, thus fitting with one calibration-set the complete spatio-temporal behaviour of the DNAPL at the whole range of 0.0 m/d $< v_w <$ 40.0 m/d.
The results of the calibration process are illustratively shown for $v_w = 21.25$ m/d at $t = 3\,690$ s (figure 4.4). In general the model results of position and spreading behaviour of the DNAPL over time correspond well to the laboratory observations. However, there are small differences between the results of the laboratory experiments and the model calibration. For example, the DNAPL in the simulation passes the first lens in larger amounts on the upstream side, thus resulting in lower DNAPL saturations in the downstream area. Such differences can be explained firstly by the fact that porosity and permeability of the coarse grained glass beads in the model are homogeneously distributed, while in reality there are always small scale heterogeneities due to the filling process of the tank, creating preferential flow paths within the medium. Secondly, between experiment and simulation there are small differences in the geometry of infiltration point and fine sand lenses due to the discretisation of the model, influencing the distribution of the DNAPL. Thirdly, it is possible that the DNAPL within the laboratory experiments is distributed irregularly over the tank width, while in the 2D model there is no distribution in width. Moreover, small differences are created by the interpolation of the results to the model domain. However, considering all the time steps and experimental set-ups, there is a good agreement between observations and

simulated results with respect to DNAPL distribution in dependency of high groundwater flow velocities.

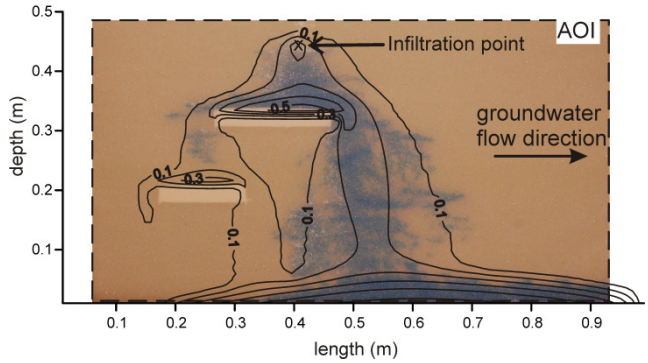

Figure 4.4 Area of interest (AOI) of laboratory experiment with $v_w = 21.25$ m/d overlaid by results of model calibration (isolines showing modelled DNAPL saturation of the model domain) at $t = 3\,690$ s

After calibrating the model with HFE-7100, a verification run using TCE in same amounts and at same boundary conditions was performed. The results of the TCE simulations showed no difference in the spatio-temporal distribution of the DNAPL body to the documented spreading behaviour of HFE-7100, thus the calibration was also valid for TCE.

4.3.2 Homogeneous scenario

The simulations ranging from $v_w = 0.05$ m/d to $v_w = 40.00$ m/d revealed that even lowest groundwater flow velocities affect the movement and position of a DNAPL body in the saturated zone (table 4.7). However, the simulated impacts on the geometry and position are relatively small in the model as long as flow velocities of 5.00 m/d are not exceeded. Higher flow velocities significantly affect the movement and position of TCE. The obtained results are illustratively described for the highest groundwater flow velocity of 40.00 m/d, where changes are most prominent (figure 4.5):
At flow velocities of 40.00 m/d the percolation path of TCE is inclined by an average angle of 18.57° to the downstream direction, resulting in a displacement of the pool at $t = 6\,000$ s of 0.51 m to the outflow. While at no flow conditions (base case scenario) the DNAPL pool starts 0.64 m left ("upstream") of the infiltration point, it begins only 0.13 m upstream at $v_w = 40.00$ m/d. At $t = 24\,000$ s, the displacement reaches 1.45 m in downstream direction.

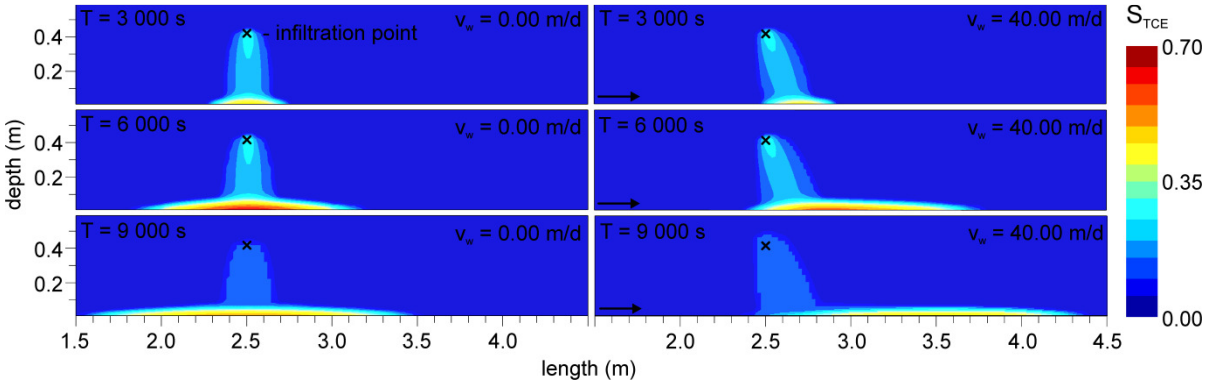

Figure 4.5 Simulated TCE saturation at $v_w = 0.00$ m/d (base case scenario) and $v_w = 40.00$ m/d. The uneven spreading front of the percolation path is caused by the discretization of the model domain (Erning et al., 2010)

Table 4.6 Impacts of groundwater flow velocities on DNAPL distribution in the saturated zone at $t = 24\,000$ s (Erning et al., 2010a)

	Groundwaterflowvelocity (m/d)								
	0.00	0.05	0.25	0.50	1.00	5.00	10.00	20.00	40.00
Inclination of the percolation path (°) at $t = 6\,000$ s	0	-0.01	-0.15	-0.21	-0.41	-3.52	-6.62	-11.31	-18.57
Displacement of the pool (cm)	0.0	1.0	4.3	5.5	8.2	37.8	75.4	114.8	145.0
Length of the pool (cm)	293.3	292.6	290.4	290.6	293.6	294.4	297.7	318.8	399.2
Max. DNAPL saturation (%)	42.7	42.6	42.7	42.7	42.7	42.7	42.0	39.0	33.0
Percental area with $S_{TCE} > 0.1$ (%)	100.00	100.32	99.64	99.02	100.00	97.78	95.05	96.37	73.55
DNAPL mass (kg) in the whole model domain	3.039	3.039	3.039	3.039	3.038	3.034	3.028	3.016	2.989

Moreover, the DNAPL pool is enlarged to a length of 399.2 cm at $v_w = 40$ m/d, while it covers only 293.3 cm at $v_w = 0$ m/d. Meanwhile the area with $S_{TCE} > 0.1$ is reduced by 26.45 % compared to the no flow base case scenario, because of enhanced dissolution processes and higher amounts of dissolved TCE in the aqueous phase. At the end of the simulation time, the maximum DNAPL saturation decreases to $S_{DNAPL(vw\,=\,40.00\ m/d)} = 0.33$ compared to $S_{DNAPL(base\ case)} = 0.43$.

Two different aspects of the groundwater flow velocity influence the spatial distribution of the DNAPL. The first factor is the kinetic force and thus the hydrodynamic pressure of the streaming water. While the DNAPL infiltrates the subsoil, the potential area for water flow is reduced. Thus the groundwater flow velocity is enhanced the deeper the DNAPL migrates. The hydrodynamic pressure of the streaming water pushes and transports the DNAPL within the porous medium in downstream direction, hinders upstream spreading against the hydrodynamic pressure gradient and leads to a thinning and an elongation of the pool: DNAPL in high hydrostatic pressure zones, e.g. upstream face and top of the DNAPL pool, will be transported along the hydrostatic pressure gradient. DNAPL reaching low hydrostatic pressure zone, e.g. the end of the DNAPL pool, will accumulate at the end of the pool, where the influence of gravity exceeds the influence of the hydrodynamic pressure.

The second aspect influencing the spatial distribution is the enhanced mass flux (M) of TCE dissolved in groundwater ($C_{TCE,dissolved}$) with increasing flow velocity:

$$M = q_w \times C_{TCE,dissolved} \times A \tag{4.1}$$

with q_w being the Darcy flow velocity and A the contact area between water and NAPL.
Enhanced dissolution processes increase mass transfer from the source zone to the aqueous phase, resulting in a smaller source zone. Since the dissolution processes are highest at the upstream side and edges of the DNAPL body, where concentration gradients are highest (Sale and McWhorter, 2001), upstream positioned DNAPL will dissolute faster, enhancing the apparent visual effect of lateral displacement in downstream direction.
As TMVOC is only able to calculate dissolution of DNAPL phase assuming instantaneous solution and saturation up to maximum solubility, the mass transfer rate in the model is enhanced by increased groundwater flow velocities and therefore probably overestimated at high groundwater flow velocities. Effects of displacement processes and of enhanced dissolution processes are intermingled and hard to distinguish at low flow velocities, while at high flow velocities, the displacement processes dominate in these set-ups, in the homogenous as well as in the layered scenarios.

4.3.3 Layered Scenarios

A short graphical overview of the simulation results for the layered settings is given in figure 4.6, showing the end of the infiltration process ($t = 6\ 000$ s). The results are illustratively described for the base case scenario and for the effects of $v_w = 40.00$ m/d.
In the base case scenario (NoLay_0m/d), TCE percolates vertically through the homogeneous environment and pools symmetrically to the left and to the right of the infiltration point. In the symmetrical setting A, the percolating DNAPL spreads at $v_w = 0$ m/d evenly to both sides of the upper impermeable lens as well as on the following ones, resulting in a wider percolation path. Considerable amounts of TCE are stored as smaller pools on top of the lenses, resulting in a reduced mass reaching the bottom of the domain at $t = 6\ 000$ s and thus a reduced and shortened pool.The setting B influences the percolation path only slightly for $v_w = 0$ m/d. The main TCE mass passes the lenses on the left side and only minor amounts are stored on the lenses.
In the set-up C, the DNAPL proceeds the lenses nearly equally distributed on the left and right side, forming two pools on the bottom of the domain at $t = 3\ 300$ s, which merge to one pool at $t = 3\ 750$ s.
Applying enhanced flow velocities, figure 4.7 illustrates that the percolation paths are generally inclined to the downstream area of the infiltration point. This leads to preferential flow paths regarding the passing of the lenses. At flow velocities of $5\ \text{m/d} < v_w < 20\ \text{m/d}$, the main DNAPL body passes the lenses at the downstream (right) side with smaller amounts still migrating on the upstream side of the lenses.
At flow velocities of 40 m/d, small amounts of TCE pass only in setting B on the upstream side of the lenses, while in settings A and C the complete percolation path is shifted to the downstream area of the infiltration point.
The flow enhanced preferential flow paths lead to different positions and lengths of the DNAPL pool at the bottom of the model domain at later time steps. The range of the displacement regarding starting position and length of the TCE pool at the aquifer base depends on the applied groundwater flow velocities and geometries (figure 4.7).

In the base case scenario (*NoLay_ 0m/d*) the DNAPL pool at the bottom of the model domain starts at X = 1.05 m and reaches a length of 2.90 m at $t = 24\,000$ s. Due to the elongated percolation path, which TCE encounters in geometry A (*A_ 0m/d*), the overall pool length at the bottom of the model domain is shortened by 0.20 m (= 6.9 %), because more DNAPL mass is stored on top of the impermeable lenses. Geometry B and C seem to have no influence on the pooling DNAPL at $v_w = 0$ m/d or the influences are smaller than the spatial resolution of the model.
A flow velocity of $v_w = 5.00$ m/d causes a downstream displacement of 0.40 m of the TCE pool, but does not influence the length of the pool in the homogenous setting (*NoLay_ 5m/d*). The displacement can be enhanced as well as diminished by a layering of the subsoil. Geometry B (*B_ 5m/d*) causes a smaller downstream displacement, *A_ 5m/d* a larger displacement of the DNAPL pool compared to the base case (*NoLay_ 0m/d*).
At $v_w = 10$ m/d, the pooling DNAPLs in the scenarios A - C is transported 0.70 - 0.90 m compared to the base case scenario. The pool length ranges between 2.70 m in scenario *A_ 10m/d* to 3.00 m in scenario *C_ 10m/d,* resulting in an increased pool length of max. 0.10 m compared to the base case scenario *NoLay_ 0m/d.*
The displacement of the pool at $v_w = 20$ m/d varies from 1.04 m (*NoLay_ 20m/d*) to 1.24 m (*A_ 20m/d*). The pool length is elongated to 3.16 m (*A_ 20m/d*) - 3.34 m/d (*C_ 20m/d*).

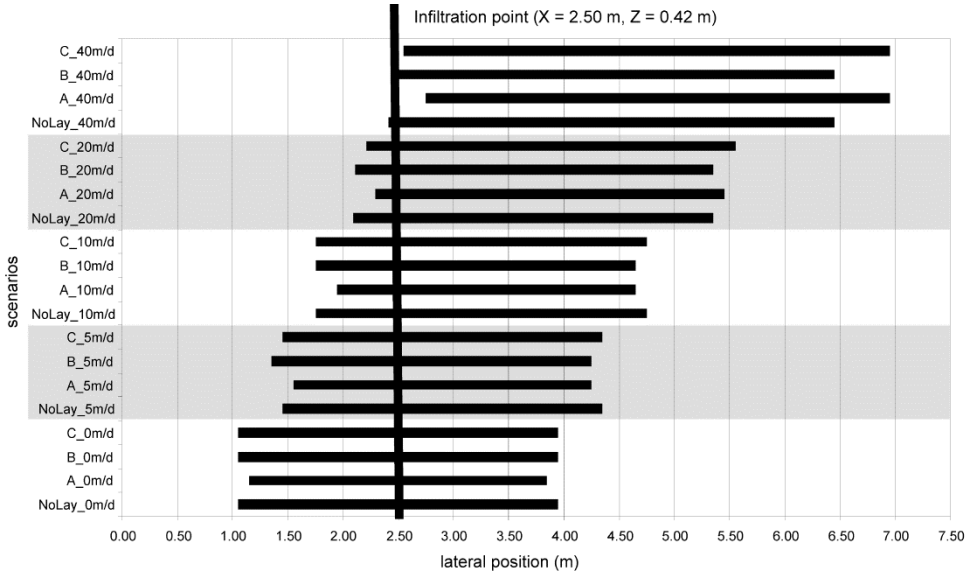

Figure 4.7 Spatial position and length of the DNAPL pool at $t = 24\,000$ s

The same trend for the displacement can be observed for $v_w = 40$ m/d. The starting position of the pool is in close proximity to the infiltration point with the displacement ranging between 1.36 m (*NoLay_ 40m/d*) and 1.70 m (*A_ 40m/d*). The TCE pool is enlarged to 4.04 m (*NoLay_ 40m/d*) - 4.40 m/d (*C_ 40m/d*), corresponding to an elongation by a factor of 1.52 compared to the no flow base case scenario (*NoLay_ 0m/d*).
As observed, the starting position and the length of the DNAPL pool vary with alternating flow velocities and with alternating geometries. Nevertheless, the same starting positions and the same length of the DNAPL pool can be obtained by different combinations of flow velocity and geometry, complicating the identification of the more sensitive factors influencing the DNAPL pool distribution.

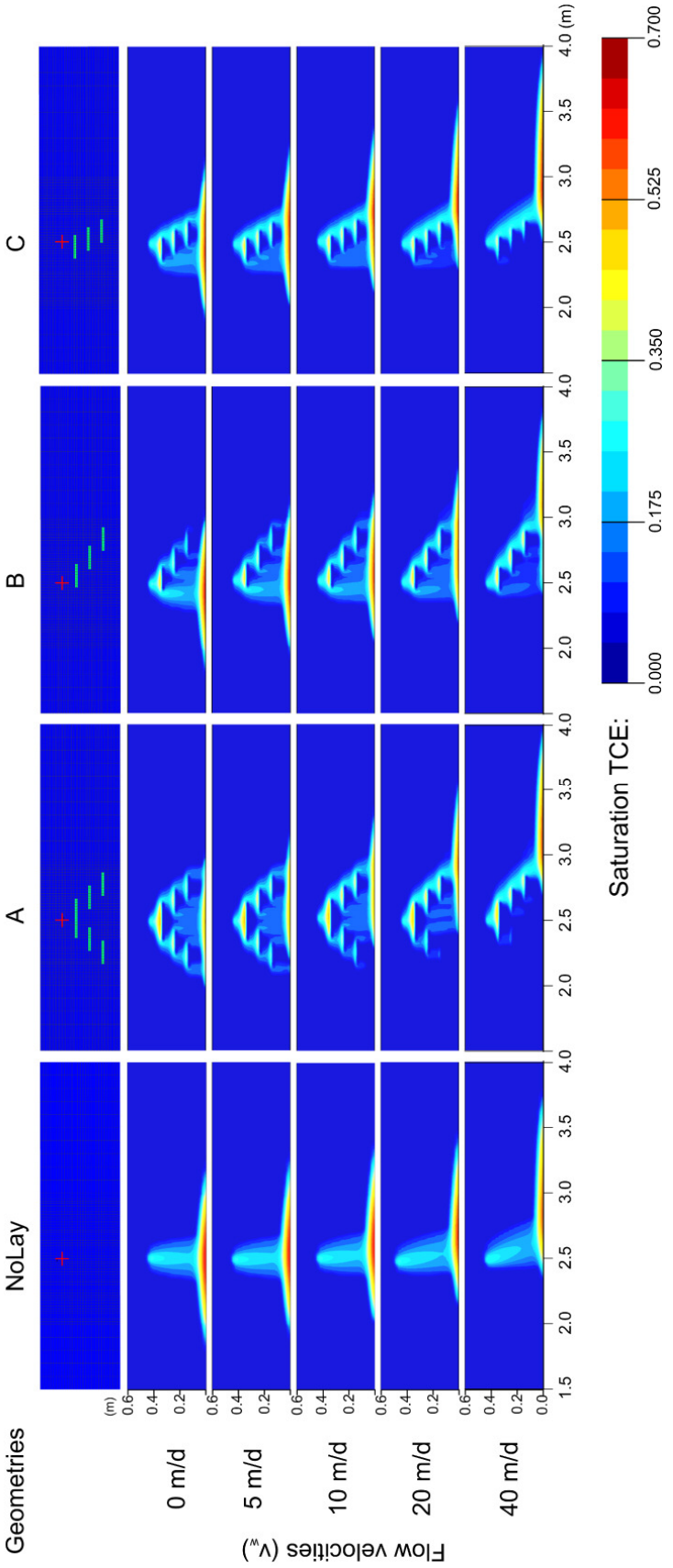

Figure 4.6 Spatial position of TCE at $t = 6\,000$ s (end of infiltration period) for alternating groundwater flow velocities and subsurface geometries, cross marks infiltration point, detail of model domain (1.5 m < X < 4.0 m), applied geometries in columns, applied flow velocities in rows.

In order to distinguish between influences of groundwater flow velocity and influences of the applied geometrical set-up, the results of the scenarios were classified into two categories:

- Position and length of TCE pool for one given flow velocity, analyzed for all applied geometries, for instance v_w = *0m/d & all geometries* (four scenarios for each v_w),
- Position and length of the TCE pool for one given geometry, analyzed for all applied flow velocities, for instance *NoLay & all* v_w (five scenarios for each geometrical set-up).

Due to the excessive runtime of the simulations, their number has been restricted and an application of comprehensive statistical analysis is limited. The range and the variance of the different scenario set-ups is illustrated by applying standard statistics as median, 25th quartile and 75th quartile, minimum and maximum values via box-whisker-plots calculated with Grapher 7.0 (Golden Software Inc., 2007). Since the data density is sparse, whiskers and quartiles are often the same value as well as median and quartiles (figure 4.8).

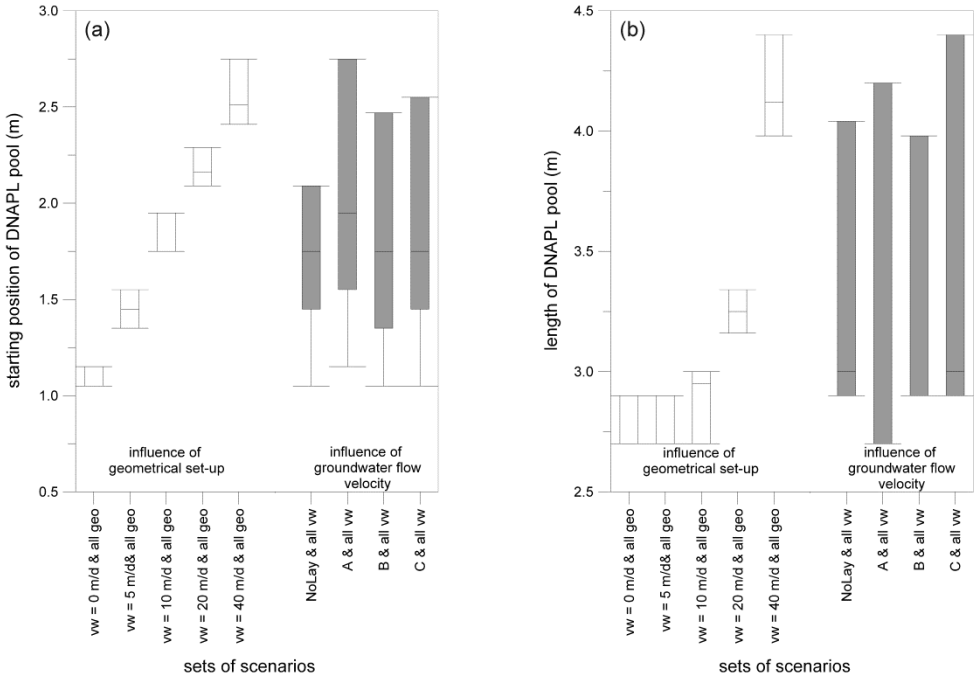

Figure 4.8 Box-whisker-plots of a) start position of DNAPL pool, b) pool length, showing minimum & maximum (whiskers), 25th quartile & 75th quartile (length of box), and median

The range of differences in the start position of the DNAPL pool due to varying applied geometrical set-ups comprises 0.18 m – 0.42 m, while the IQR covered due to influences of applied v_w varies between 1.08 m and 1.50 m. This illustrates that the DNAPL pool is stronger influenced in its position by the streaming groundwater than by the lenses of the scenarios.
Investigating the overall pool length of the different scenarios, the influence of the geometrical set-up causes variances of the range of 0.18 m – 0.42 m, while the groundwater leads to a span of the range of 1.08 m – 1.50 m.
Comparing the differences in the IQR of the pool position due to the layering of the subsoil (max ± 0.42 m) with the differences due to enhanced groundwater flow (max. ± 1.50 m), it becomes prominent, that the DNAPL pool reacts more sensitive to changes in groundwater flow velocity than to changes in the here applied layering of the subsoil. The same trend is observed for the pool length.

Nevertheless, it has to be emphasized that this sensitivity analysis is strictly restrained to the here applied geometrical set-ups and flow velocities. By the conducted scenario modeling it is not yet possible to give a universally valid classification. Moreover, it will have to be investigated for each case separately, due to the huge variances in natural soils and in occurring groundwater flow velocities, including any spatio-temporal variances on small and large scale.

4.4 Conclusions

4.4.1 Homogenous scenario

In the applied model set-up, the DNAPL body is even affected by groundwater flow velocities of $v_w = 0.05$ m/d in its position, its size and its geometrical structure.
Although the displacement of the DNAPL pool is in the range of some centimetres in the small scale 2D models for $v_w < 1.0$ m/d, it seems not to be significant. This would be coherent with the investigations performed by Dekker and Abriola (2000), which conducted their investigation on a 2D scale of 10 m length and 5 m depth. But transferring the results to field scale problem, it should be investigated more closely. Assuming the same geological setting as in the simulations, the inclined percolation path could lead for $1.0 \text{ m/d} < v_w < 40.0$ m/d to a first occurrence of the DNAPL pool on the bottom of the aquifer of 0.4 m - 16.0 m in downstream direction. Combining this with the displacing and conveying effects of the streaming water, which affect the latter pooling DNAPL body, a TCE pool could theoretically be transported approx. 5.4 km in downstream direction at $v_w = 1.0$ m/d. Of course, this range will be diminished in a natural setting significantly, via pooling effects in small depressions, inclined impermeable layers, dissolution processes, entrapment in residual saturation, sorption processes, irregular flow fields, and small scale heterogeneities, as observed in the laboratory experiments. But the theoretical magnitude of these extrapolated values exhibits, that the process has also to be expected on a large scale even at low groundwater flow velocities and should be investigated further, being coherent with the recommendations of Gerhard et al. (2007).
Increasing the groundwater flow velocity to values typically encountered in aquifers influenced by artificial activities, e.g. Pump & Treat and drinking water production, or in narrowing alluvial aquifers in the foothill of mountains ($v_w > 1.0$ m/d), the impact of groundwater flow velocities significantly affects the DNAPL behaviour during and after the infiltration. The effects are an inclined percolation path, and a thinned and displaced DNAPL pool. Possible consequences for field sites with high groundwater flow velocities will be a shifted position within the aquifer, possible new flow paths, a changed geometry of the DNAPL source zone and as a result a changed dissolution behaviour and thus a modified longevity of the DNAPL source zone.

4.4.2 Layered scenarios

In the chosen highly permeable medium, the position and length of the DNAPL pool is more sensitive to the applied flow velocities of 5.0 m/d to 40.0 m/d than to the spatial positions of the impermeable lenses. Generally, the pool migrates at high groundwater flow velocities ($v_w \geq 5.0$ m/d) less in upstream direction but predominantly in downstream direction. Flow

velocities of 10.0 m/d and higher can elongate a DNAPL pool by approximately 30 % regardless of the applied geometry of these set-ups and transport it in the downstream direction of the original contamination source zone. The applied geometries enhance the displacement of the DNAPL pool by 10 % - 29 % compared to the respective homogeneous scenarios. But different realizations regarding flow velocity and geometrical set-up can cause the same results regarding length and position of the DNAPL pool, complicating the determination of sensitive parameters. However, the length of the impermeable layers (0.18 m) of the chosen set-up is small compared to the overall length of 10.00 m of the model domain. Introducing longer capillary barriers would lead to a stronger influence of the layered subsoil regarding the position of the TCE pool on bottom of the aquifer. Moreover, the studies revealed that the amount of fingering is significantly reduced at high groundwater flow velocities, since the higher the groundwater flow velocity the lower the probability for DNAPL passing a lens on the upstream site. This would be important for sites characterized by hydraulic connections between several aquifers, e.g. in upstream direction of the industrial area, and for estimating the contaminated soil volume.

Additionally, a higher amount of the TCE is stored in the pool on the bottom of the model domain instead of remaining on impermeable layers on the percolation path. This will strongly influence the mass transfer and dissolution rates of the DNAPL body. Two intermingled aspects are the reason for these geometrical effects on the DNAPL architecture: Firstly, the transportation effects of the streaming water, pushing the DNAPL in downstream direction, and secondly the higher mass transfer rate due to the higher groundwater flow velocities, which dissolves the percolation paths faster than the DNAPL pools (Sale and McWhorter, 2001; Parker and Park, 2004).

Transferring the results of the small scale simulations to a field scale problem and assuming the same material properties as in the models, it should be expected that the main body of a DNAPL contamination will not be in close proximity to the original infiltration point at flow velocities of $v_w \geq 5.00$ m/d, but rather in the downstream area of the surface source zone depending on the elapsed time since the spilling accident. Assuming a 50 m deep aquifer with groundwater flow velocities of 5 m/d – 10 m/d the main DNAPL body would reach the bottom of the aquifer not directly below the aboveground contamination source zone. Instead it would reach the bottom approx. 5 m in downstream direction due to the inclined percolation path induced by the high flow velocities. The first occurrence on the bottom of the aquifer in 50 m depth would only slightly be influenced by the geometrical setting of the lenses on the site scale, if the relative length and position of the lenses are similar to the relation of the experimental set-up. From this starting position the DNAPL then migrates with the groundwater as described for the homogenous settings.

Encountering multiple aquifer formations at a field site, any position of hydraulic connections in the downstream area have to be taken into account for site investigation. Even at considerable distances to the surface contamination point, the DNAPL could reach the hydraulic window due to high groundwater flow velocities and be displaced through the interconnection to a deeper aquifer. In forming a secondary, deeper source zone, it may hardly or not be accessible for existing remediation facilities at a site. This may be of vital importance when designing site remediation and containment facilities in order to prevent displacement and spreading of the contaminant to a larger area or to a deeper aquifer. On the other hand, hydraulic connections in the upstream area of the contamination source will be of minor im-

portance the higher the groundwater flow velocity in the aquifer is as long as the aquitard are planar and horizontal. The existence of tilted impermeable layers could though dominate the DNAPL flow behaviour even at high flow velocities.

4.4.3 Summary conclusions

The homogenous and layered scenarios revealed that a DNAPL body can be transported spatio-temporally within a homogenous or layered stratum even at groundwater flow velocity of 0.05 m/d. High groundwater flow velocities will change the geometry, the architecture and mainly the position of a TCE source zone significantly. This leads to a direct impact on the dissolution behaviour, the mass transfer rates and thus the longevity of a DNAPL contamination. Especially in areas with high natural groundwater flow velocities, the impacts will be numerous. Altered positions of the source zone, changed flow paths, percolation to deeper aquifers could all be consequences of high groundwater flow velocities, complicating site investigation and remediation. Possible influences of artificially enhanced groundwater flow velocities, either by Pump & Treat or by drinking water facilities, on a stationary DNAPL source zone still has to be investigated.

4.5 Further prospects

As next step, a dual approach of scenario and field site modeling of Rho, Italy, will be conducted. The scenario modeling will include large scale simulations of real site materials with simplified geometrical set-up, adapted from the real field site. Different scenarios with variations in contamination mass, spill time period, groundwater flow velocities and heterogeneous material distribution will be performed.

Acknowledgments

We would like to thank our colleagues from La Sapienza University Rome (A. Luciano, P. Viotti and M. Petrangeli Papini), who conducted the laboratory experiments and generously provided the primary data set to calibrate the multiphase model. This research is financially supported by the European Union under the 7th European Framework, Project ModelPROBE (n° 213161).

References

3M (2005): 3M Novec TM 7100 - Engineered Fluid. Product Information. 3M Electronics. St. Paul, MN, USA. pp. 8.

Bao, W.M.J., Vogler, E.T. and Chrysikopoulos, C.V. (2004): Nonaqueous liquid pool dissolution in three-dimensional heterogeneous subsurface formations. Environmental Geology 43: 968-978.

Bradford, S.A., Rathfelder, K.M., Lang, J. and Abriola, L.M. (2003): Entrapment and dissolution of DNAPLs in heterogeneous porous media. Journal of Contaminant Hydrology 67: 133-157.

Broholm, K., Feenstra, S. and Cherry, J.A. (2005): Solvent Release into a Sandy Aquifer. 2. Estimation of DNAPL Mass Based on a Multiple-Component Dissolution Model. Environ. Sci. Technol. 39(1): 317-324.

Chang, L.-C., Chen, H.-H., Shan, H.-Y. and Tsai, J.-P. (2009): Effect of connectivity and wettability on the relative permeability of NAPLs. Environmental Geology 56(7): 1437-1447.

Christ, J.A., Lemke, L.D. and Abriola, L.M. (2009): The influence of dimensionality on simulations of mass recovery from nonuniform dense non-aqueous phase liquid (DNAPL) source zones. Advances in Water Resources 32(3): 401-412.

Dekker, T.J. and Abriola, L.M. (2000): The influence of field-scale heterogeneity on the infiltration and entrapment of dense nonaqueous phase liquids in saturated formations. Journal of Contaminant Hydrology 42(2-4): 187-218.

Erning, K., Schäfer, D., Dahmke, A., Luciano, A., Viotti, P. and Petrangeli Papini, M. (2010): Simulation of DNAPL distribution depending on groundwater flow velocities using TMVOC. In: M. Schirmer, E. Hoehn and T. Vogt (Editors). IAHS Publication: Groundwater Quality Management in a Rapidly Changing World. Proceedings of the 7th International Groundwater Quality Conference held in Zurich, Switzerland, 13-18 June 2010. Red Books. IAHS. Oxfordshire. pp. 128-131.

Fagerlund, F.F., Niemi, A. and Illangasekare, T.H. (2006a): Modeling NAPL Source Zone Formation in Stochastically Heterogeneous Layered Media - a Comparison with Experimental Results. TOUGH Symposium 2006. Lawrence Berkeley National Laboratory, Berkeley, California.

Fagerlund, F.F., Niemi, A. and Odén, M. (2006b): Comparison of relative permeability-fluid saturation-capillary pressure relations in the modelling of non-aqueous phase liquid infiltration in variably saturated, layered media. Advances in Water Resources 29(11): 1705-1730.

Falta, R.W., Pruess, K., Finsterle, S. and Battistelli, A. (1995): T2VOC User´s Guide. LBL-36400. U.S. Department of Energy.158 pp.

Falta, R.W. (2003): Simulation of subgridblock scale DNAPL pool dissolution using a dual domain approach. TOUGH Symposium 2003. Lawrence Berkeley National Laboratory, Berkeley, California.

Falta, R.W., Basu, N. and Rao, P.S. (2005): Assessing impacts of partial mass depletion in DNAPL source zones: II. Coupling source strength functions to plume evolution. Journal of Contaminant Hydrology 79(1-2): 45-66.

Gerhard, J.I., Pang, T. and Kueper, B.H. (2007): Time Scales of DNAPL Migration in Sandy Aquifers Examined via Numerical Simulation. GROUND WATER 45(2): 147-157.

Golden Software Inc. (2007): Grapher 7.0. Golden.

Greifenhagen, G. (2000): Untersuchungen zur Hydrogeologie des Stadtgebietes Darmstadt mit Hilfe eines Grundwasserinformationssystems - unter Verwendung von einer Datenbank, Datenmodellierung und ausgewählten statistischen Methoden. Diss. FB Material- und Geowissenschaften. Darmstadt.221 pp.

Herfort, M., Ptak, T., Hümmer, O., Teutsch, G. and Dahmke, A. (1998): Testfeld Süd: Einrichtung der Testfeldinfrastruktur und Erkundung hydraulisch-hydrogeochemischer Parameter des Grundwasserleiters. Grundwasser 3(4): 159-166.

Herfort, M. and Ptak, T. (2002): Multitracer-Versuch im kontaminierten Grundwasser des Testfeldes Süd. Grundwasser 1: 31-40.

Hoehn, E. and Santschi, P.H. (1987): Interpretation of tracer displacement during infiltration of river water to groundwater. Water Resources Research 23(4): 366-340.

Hoehn, E. and Von Gunten, H.R. (1989): Radon in groundwater: A tool to assess infiltration from surface waters to aquifers. Water Resources Research 25(8): 1795-1803.

Illangasekare, T.H., Ramsey, J.L., Jensen, K.H. and Butts, M.B. (1995): Experimental study of movement and distribution of dense organic contaminants in heterogeneous aquifers. Journal of Contaminant Hydrology 20(1-2): 1-25.

Illangasekare, T.H., Munakata Marr, J., Siegrist, R.L., Soga, K., Glover, K.C., Moreno-Barbero, E., Heiderscheidt, J.L., Saenton, S., Matthew, M., Kaplan, A.R., Kim, Y., Dai, D. and Page, J.W.E. (2006): Mass Transfer from Entrapped DNAPL Sources Undergoing Remediation: Characterization Methods and Prediction Tools. SERD Project No. CU-1294. Colorado School of Mines.410 pp.

Jawitz, J.W., Fure, A.D., Demmy, G.G., Berglund, S. and Rao, P.S.C. (2005): Groundwater contaminant flux reduction resulting from nonaqueous phase liquid mass reduction. Water Resources Research 41: 15.

Jellali, S., Benremita, H., Muntzer, P., Razakarisoa, O. and Schäfer, G. (2003): A large-scale experiment on mass transfer of trichloroethylene from the unsaturated zone of a sandy aquifer to its interfaces. Journal of Contaminant Hydrology 60(1-2): 31-53.

Kueper, B.H. and Frind, E.O. (1988): An overview of immiscible fingering in porous media. Journal of Contaminant Hydrology 2(2): 95-110.

Lee, K.Y., Lee, J.-Y. and Mellett, J.J. (2004): Transport of dissolved methoxy-nonafluorobutane through a saturated column. Environmental Geology 46(6): 883-889.

Li, H., Chen, J. and Yang, J. (2011): Pore-scale removal mechanisms of residual light non-aqueous phase liquids in porous media. Environmental Earth Sciences 64(8): 2223-2228.

Luciano, A., Viotti, P. and Petrangeli Papini, M. (2010): Laboratory investigation of DNAPL migration in porous media. Journal of Hazardous Materials 176(1-3): 1006-1017.

Miles, B., Maji, R., Sudicky, E.A., Teutsch, G. and Peter, A. (2008): A pragmatic approach for estimation of source-zone emissions at LNAPL contaminated sites. Journal of Contaminant Hydrology 96(1-4): 83-96.

Page, J.W.E., Soga, K. and Illangasekare, T. (2007): The significance of heterogeneity on mass flux from DNAPL source zones: An experimental investigation. Journal of Contaminant Hydrology 94(3-4): 215-234.

Pankow, J.F. and Cherry, J.A. (1996): Dense Chlorinated Solvents and Other DNAPLs in Groundwater. Waterloo Press. Waterloo. 522 pp.

Parker, J.C. and Lenhard, R.J. (1987): A Model for Hysteretic Constitutive Relations Governing Multiphase Flow in Porous Media. 1. Saturation-Pressure Relations. Water Resources Research 23(12): 2187-2196.

Parker, J.C. and Park, E. (2004): Modeling field-scale dense nonaqueous phase liquid dissolution kinetics in heterogeneous aquifers. Water Resources Research 40: 12 PP.

Pruess, K. and Battistelli, A. (2002): TMVOC, A Numerical Simulator for Three-Phase Non-isothermal Flows of Multicomponent Hydrocarbon Mixtures in Saturated-Unsaturated Heterogeneous Media. Report LBNL-49375. Berkeley.192 pp.

Rivett, M.O. and Feenstra, S. (2005): Dissolution of an Emplaced Source of DNAPL in a Natural Aquifer Setting. Environmental Science & Technology 39(2): 447-455.

Saenton, S., Illangasekare, T.H., Soga, K. and Saba, T.A. (2002): Effects of source zone heterogeneity on surfactant-enhanced NAPL dissolution and resulting remediation end-points. Journal of Contaminant Hydrology 59(1-2): 27-44.

Sale, T.C., Zimbron, J.A. and Dandy, D.S. (2008): Effects of reduced contaminant loading on downgradient water quality in an idealized two-layer granular porous media. Journal of Contaminant Hydrology 102(1-2): 72-85.

Soga, K., Page, J.W.E. and Illangasekare, T.H. (2004): A review of NAPL source zone remediation efficiency and the mass flux approach. Journal of Hazardous Materials 110(1-3): 13-27.

Thunderhead Engineering (2011): PetraSim - Interactive Model Creation for Advanced Flow, Transport and Heat Transfer Models. In: T.E.C. Inc. (Editor). Manhattan, USA.

Von Gunten, H.R., Karametaxas, G., Krähenbühl, U., Kuslys, M., Giovanoli, R., Hoehn, E. and Keil, R. (1991): Seasonal biogeochemical cycles in riverborne groundwater. Geochimica et Cosmochimica Acta 55(12): 3597-3609.

Zhu, J. and Sykes, J.F. (2004): Simple screening models of NAPL dissolution in the subsurface. Journal of Contaminant Hydrology 72(1-4): 245-258.

5 Multiphase model driven site assessment of the area of the former industrial facility Chimica di Bianchi in Rho / Italy

Published as

Erning, K. and Schäfer, D. (2011): Multiphase model driven site assessement of the former industrial facility Chimica di Bianchi in Rho / Italy. In: M. Kästner (Editor). ModelPROBE report second period (12/2009-05/2011): Workpackage 9.2: Field Demonstration and Cross Validation. pp. 187-197.

5.1 Introduction

The area of the former industrial facility Chimica di Bianchi in Rho, Italy is characterized by high concentrations of dissolved chlorinated solvents in the subsurface. Below the facility two aquifers of interest are separated by a several meter thick aquitard. High concentrations of the dissolved DNAPLs Tetrachloroethylen (PCE) and Trichloroethylen (TCE) were found in the uppermost aquifer *Superficiale* as well as in the deeper aquifer *Prima Falda*.

Two complementing containment and remediation measures are conducted up to date. Firstly the assumed location of the DNAPL source zone in the uppermost aquifer *Superficiale* is encapsulated from the surface down till the aquitard. Secondly a Pump & Treat facility is installed as hydraulic containment for both aquifers. Since the concentrations of the dissolved PCE and TCE in both aquifers remained high even after the installation and operation of these facilities, there is the possibility that the original DNAPL source zone migrated within this multi-aquifer formation in lateral and / or vertical direction even to the deeper aquifer *Prima Falda*.

One possible pathway could be that the DNAPL was transported by the streaming groundwater prior to the installation of the containment in downstream direction and possibly migrated through a hydraulic connection to the deeper aquifer *Prima Falda*(figure 4.10)Another pathway could be leakage through the aquitard, if the aquitard turns out to be not completely impermeable for NAPLs. Both possibilities depend on the material parameters of the geological stratum, the physico-chemical properties of the DNAPLs and on the groundwater flow velocities at the site. Another possibility would include the passage along the steel walls of the encapsulation, if they penetrate the *Aquitard* and reach into the *Prima Falda*.

Since the already installed facilities for containment and remediation are neither efficient with respect to the remediation aims nor with respect to the operational costs, it is planned to install a Permeable Reactive Barrier (PRB) downstream of the contaminant source zone. For an effective operation of the PRB, the positioning of the barrier with respect to the location of the contaminants is essential and therefore the knowledge of the position of the contaminants in the aquifers.

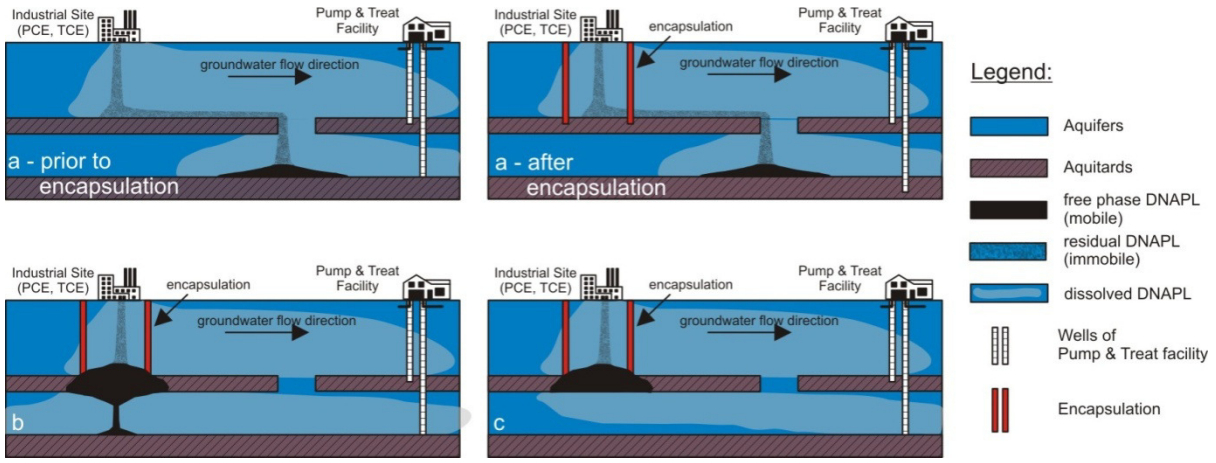

Figure 5.1 Potential pathways for DNAPLs at the Rho site: a) potential transport of DNAPL by streaming groundwater prior to / after installation of encapsulation including potential passage to deeper aquifer through a hydraulic connection b) migration through aquitard prior to / after installation of encapsulation, passage as free phase into deeper aquifer c) migration into aquitard, storage as free phase in aquitard, dissolution into deeper aquifer

There are two different ways to locate a potential migrated DNAPL source zone in the subsoil:

a) Additional site investigation using drilling, Direct Push and geophysical measurement in order to directly detect the occurrence of free phase in the subsoil. These techniques are time and cost consuming. Moreover, drilling and Direct Push will only deliver spatial point data, while geophysics can cover a wider area but with varying accuracy regarding resolution in depth.

b) Multiphase model driven site assessment, which is used in this investigation: Based on the already available datasets of previous investigations of the site, varying scenario models of the geology, the hydrogeology and of the multiphase transport of occurring DNAPLs are conducted:

- Modeling the geology from borehole datasets in order to locate preferential flow paths and potential hydraulic connections between the two aquifers.
- Modeling the multiphase transport of the DNAPLs with respect to the groundwater flow velocities of the aquifers in order to reconstruct the pathways of the DNAPL in the past and to locate the present day DNAPL source zone.

The accuracy of the modeling primarily depends on the quality and data density of the primary datasets, on the applied modeling software and its limitations, on the performance of the computers at hand and of the necessary simplifications which have to be applied.

Modeldriven site assessment is not a single tool at hand, but moreover a cost effective and time efficient instrument to supplement field site investigation and the decision making process regarding potential site investigation and site remediation.

5.2 Methodology of multiphase model driven site assessment

Multiphase model driven site assessment combines varying pre-existing datasets to create a three-dimensional model of the subsurface of the subsoil (figure 4.11). Depending on the primary task, different point of interests can be investigated. Incorporated informations are ob-

tained by historical site investigation, literature studies and data from classical site investigation campaigns.

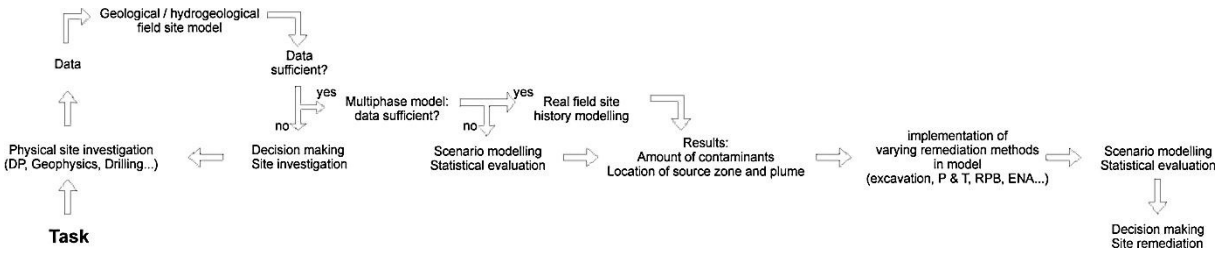

Figure 5.2 Sketch of principle methodology of model driven site assessment

In the first step, all available information of pre-existent sources is collected and analyzed. Historical site investigation provides informations on the variety of contaminants, approximated contaminant mass, contamination history and location of potential source zone, e.g. buildings and facilities. Data of physical site investigations, provided e.g. by Direct Push, drilling or geophysics, supply informations about the geological stratum, its stratigraphic-hydraulic units and their spatial extends.
Based on the data of the physical site investigation, a geological – hydrogeological field site model is constructed, visualizing distributions and / or significant data gaps. If the quality of the geological site model is sufficient, the multiphase model regarding the contamination history is included. If the quality is not sufficient to answer the main point of interest, a new field campaign or scenario modeling of the unknown parameters should be conducted. The same sufficiency loop has to be followed regarding the data quality of the multiphase model, until the data quality is acceptable, or the scenarios can statistically be evaluated.

5.2.1 Historical site investigation and literature studies

During an operational time of at least 50 - 75 years, the facility Chimica di Bianchi mainly produced chlorinated solvents, like PCE and TCE (Leccese et al., 2007). The primary leakage point seemed to be a former disposal basin of 10 m × 10 m (figure 4.12) leading to a maximum contamination of 180 mg/l TCE and 50 mg/l 1,1,2,2-tetrachlorethane in dissolved form in the underlying aquifers (Werban et al., 2007). Several sampling campaigns over the last years (Leccese et al., 2007) indicated the presence of a DNAPL pool as long-term source zone, which probably migrated to the underlying aquifer *Prima Falda* (Bozzano et al., 2007).
In the 1980s the former disposal basin was encapsulated by placing impermeable steel walls through the whole thickness of the aquifer *Superficiale*, using the aquitard as a bottom seal. Furthermore, a Pump & Treat hydraulic containment was installed in approx. 2005 in both aquifers downstream of the former industrial site.In full operation, the overall 19 wells could increase the groundwater flow velocity in the *Superficiale* up to ca. 1.8 – 2.0 m/d. Due to the high operational costs of the Pump & Treat facility it is right now not running with its full capacity (personal communication M. Petrangeli Papini).

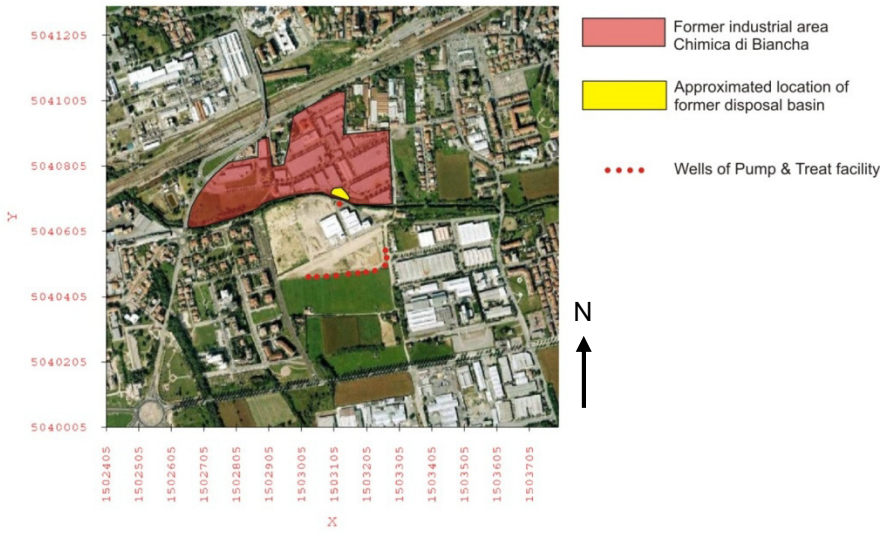

Figure 5.3 Position of industrial site and Pump & Treat facility (Coordinates in GAUSS-BOAGA; source: GOOGLE EARTH, 2010, edited)

5.2.2 Geological site modeling based on pre-existing data

The following description of the geological and hydrogeological characterisation is the combination of three different sources, which were analyzed and interpreted for the investigations: Literature studies of previous scientific investigations, existing MODFLOW models provided by La Sapienza University Rome, Italy and by geological modeling (using GMS 6.5, performed at CAU Kiel, Germany) based on the same dataset as the MODFLOW models.
The site is quite well investigated on a regional scale regarding the geological composition of the subsurface with a total of over 260 boreholes on an area of 16 km² in the surroundings of the industrial site. But 50 % of the boreholes are with an incomplete geological description and additional 10 % are only 1 m deep. Furthermore, the boreholes are not evenly distributed over the area of interest, but clustered at specific location, resulting in a decreased precision of the modeling. The resulting usable borehole dataset consists of 165 drillings, which reflects 9 boreholes per square kilometer.
The dataset of these drillings includes the original geological description of the materials as well as an already existing definition of the materials as *Aquifer Superficiale*, *Aquitard* and *Aquifer Prima Falda*. Based on this pre-processing of the data, two different types of site models were developed:

- Geological-geostructural model using the original dataset and grouping the materials due to their geological descriptions into aquifers (gravel and sand) and aquitards (silt and clay)
- Geohydraulic modeling of the predefined hydraulic units *Superficiale*, *Aquitard* and *Prima Falda*.

Due to the differing approaches, the results of the model vary, especially in the spatial distributions of the hydraulic relevant units.

Hydrogeological set-up of the area Rho

The Rho region is geologically characterized by alluvial and glacial-fluviatile quarternary sediments (Bozzano et al., 2007) of widely varying grain size. The area is hydrogeologically characterized by a multi aquifer formation of an unconfined aquifer, called *Superficiale*, separated by a several meter thick *Aquitard* from a second confined aquifer, called *Prima Falda*.

Unsaturated zone and Superficiale

The first ten meters below ground surface (bgs) consist of gravel-sandy material with a low content of silty and clayey material. The uppermost 4 – 6 meters are unsaturated, followed by the phreatic uppermost aquifer *Superficiale*. The literature studies denotate a porosity of 20 % and a hydraulic conductivity ranging from 1×10^{-6} m/s to 1×10^{-2} m/s (table 4.8). General groundwater flow direction is from NNE to SSE with a natural groundwater flow velocity of approximately 1 m/d.

Aquitard

At about 10 m bgs a discontinous clay layer (*Aquitard*) of thickness ≤ 5 m separates the *Superficiale* from the semi-confined aquifer *Prima Falda*. The *Aquitard* consists mainly of clay, but is according to literature studies and geological modeling of the sites interrupted in irregular intervals. In general the *Aquitard* is characterized by a max. thickness of five meters and a hydraulic conductivity of 1×10^{-9} to 1×10^{-7} m/s.

Table 5.1 Hydrogeological parameters at the Rho Site supplied by different literature studies of previous investigations

Name	Material	Hydraulic gradient [%]	Transmissivity [m²/s]	Hydraulic conductivity [m/s]	Porosity [%]
Superficiale	gravel, sand	-	$0{,}26\times10^{-2}$ - $1{,}5\times10^{-2}$ (a)	1×10^{-4} - $3{,}3\times10^{-4}$ (a) 3×10^{-4} - 3×10^{-2}(b) 10^{-6}(c)	20 (a)
Aquitard	clay	-	-	7.0×10^{-8} (vertical) (a) 10^{-9} - 10^{-7} (vertical) (b)	-
Prima falda	gravel, sand, silty-clay lenses	0.6 (a)	$0{,}26\times10^{-2}$ - $1{,}5\times10^{-2}$ (a)	1×10^{-4} - $3{,}3\times10^{-4}$ (a) 2×10^{-4} - 8×10^{-4}(b) 10^{-6}(c)	20 (a) – 45 (c)

\- noinformation in literature
(a) Beretta et al. (2005)
(b) Bozzano et al. (2007)
(c) Leccesse et al. (2007)

For the structural geological modeling of the area, the spatial density of primary data points was not sufficient to verify a general distribution or to define the accurate location of gaps in *Aquitard* in the model. Especially in the downstream area of the industrial site, the geostructural model exhibits no occurrence of the *Aquitard* at all, possibly due to the missing borehole data (figure 4.13).

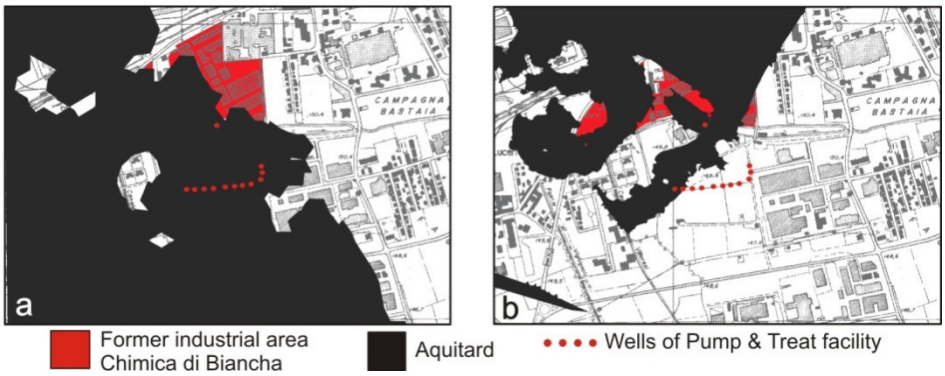

Figure 5.4 Example of varying models based on different classification of primary dataset: a) distribution of hydraulic defined *Aquitard*. b) Distribution of geological defined aquitard, consisting of silt and clay layers. Detail of model domain.

For modeling groundwater flow and DNAPL distribution, a continuous distribution of all the layers had to be assumed. Potential gaps in the *Aquitard* have to be constructed manually by assigning respective material parameters to the specific areas. Both ways, calculating with an ubiquitous *Aquitard* and / or including the gaps manually will lead to uncertainties in the modeling, but represent two acceptable scenarios based on the available primary dataset.
Applying this boundary condition, the top of the assumed ubiquitous *Aquitard* is inclined from north to south by 0.7 % and is characterized by indentations and ridges of maximum three meters difference in height, creating preferential flow paths and potential geometrical sinks for the DNAPLs (figure 4.14).

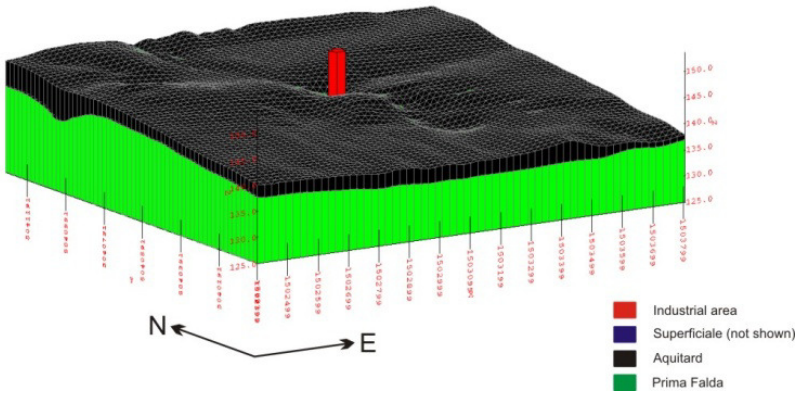

Figure 5.5 Topography and thickness of assumed ubiquitous *Aquitard* on top of the *Prima Falda* (cut off at depth = 125 m), *Superficiale* not shown, height super-elevated by factor 15

Prima Falda

The second aquifer *Prima Falda*, below the *Aquitard,* has an average thickness of ca. 35 m. It consists mainly of coarse grained sandy and gravely material with isolated silty-clayey lenses of limited extension. Porosity ranges between 20 % and 45 % and hydraulic conductivity between 1×10^{-6} m/s to 1×10^{-4} m/s, corresponding to the values of the *Superficiale* (Bozzano et al., 2007; Leccese et al., 2007). Due to the interrupted clay layer of the *Aquitard* between the *Superficiale* and the *Prima Falda*, there are phreatic conditions as well as confined conditions at a regional scale for the *Prima Falda* (Bozzano et al., 2007). The general groundwater flow direction is from NW to SE, with a general hydraulic gradient of 0.6 % and a median groundwater flow velocity of approximately 1.8 m/d.

The *Prima Falda* is confined in further depth by a ca. 5 - 10 m thick silty-clay layer, which is inclined by 0.7 % towards south (Beretta et al., 2005).

5.2.3 Multiphase modeling of potential DNAPL pathways

Possible transport of DNAPLs due to groundwater flow within the aquifer

As a first step, small scale multiphase modeling was used to qualify and quantify the influence of thirteen different groundwater flow velocities in a homogenous permeable medium to verify or falsify a possible transport of the DNAPLs by the streaming water in downstream direction. TCE was chosen as representative DNAPL.

The models were calibrated by means of small scale laboratory experiments and covered the whole range from 0 m/d up until 40 m/d of groundwater pore velocity (v_w). The reader is referred to Luciano et al. (2010) for details of the set-up and the results of the laboratory experiments, and to Erning et al. (2010a) for details of the multiphase modeling.

As evidenced in the laboratory experiments, there is a clear impact of the applied pore velocity on the percolation path and the position of the pooling DNAPL (Luciano et al., 2010).

Applying the multiphase software TMVOC, it could be proven that the DNAPL TCE is even influenced at $v_w \geq 0.05$ m/d in its spatial distribution, its extent and its maximum saturation. These are also important factors for the dissolution kinetics of NAPLs and the longevity of a DNAPL source zone, respectively. Moreover, even at this low groundwater flow velocities, the DNAPL is transported by the streaming water in downstream direction (Erning et al., 2010a).

However, the impacts of groundwater flow velocities of $v_w < 1$ m/d seemed not to be of great significance on the investigated spatio-temporal scale of five hours simulation time in a small 2D model of 0.6 m depth and 10 m length.

Furthermore, the impact of a layered stratum was investigated, as for instance represented by silty and clayey lenses in a sandy aquifer. In the range of $v_w = 0 - 5$ m/d, the effects of the applied layered stratum superimposes the effects of an enhanced groundwater flow velocity (figur 4.15). At groundwater flow velocities higher than 5 m/d, the effects of the streaming water are the dominant process in defining the position and the extent of a DNAPL source zone.

This small scale multiphase modeling investigations elucidated that a transport of the DNAPLs in the uppermost aquifer *Superficiale* due to the natural groundwater flow velocity could have been possible with respect to material parameters and groundwater flow velocities at the Rho site.

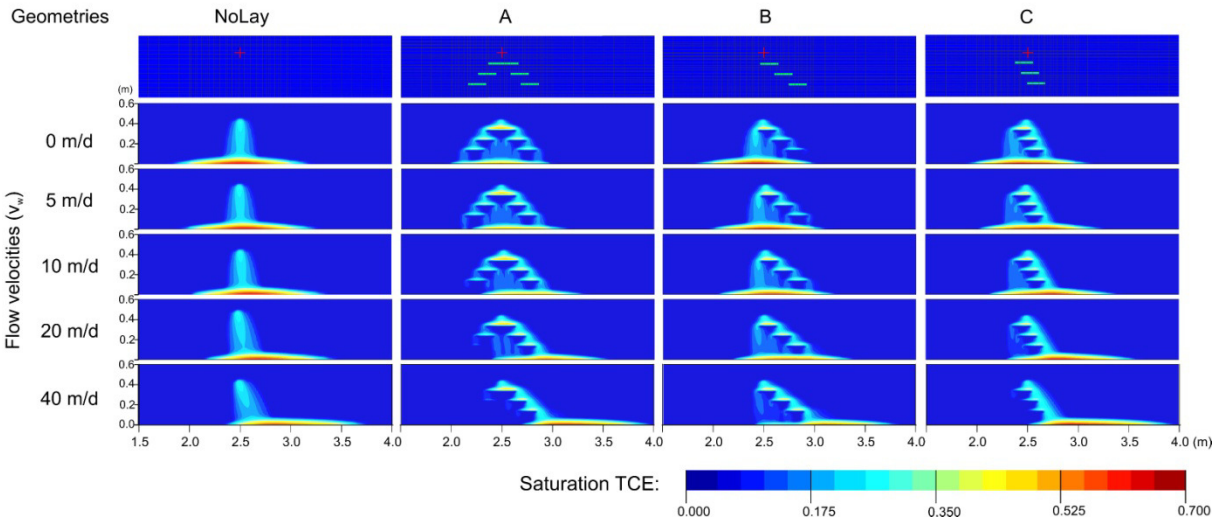

Figure 5.6 Spatial position of TCE at t = 6 000 s (end of infiltration period) for increasing groundwater flow velocities and subsurface geometries, cross marks infiltration point, detail of model domain (1.5 m < X < 4 m), groundwater flow from left to right

Possible migration of the DNAPL through the aquitard between the two aquifers

Conceptual model

To reveal the principles of DNAPL migration through potential aquitards, the spreading behaviour of TCE in an enhanced 2D model with the dimensions 500 m × 1 m × 11 m in the directions X, Y and Z was investigated. The X-direction is parallel to the groundwater flow in the uppermost aquifer *Superficiale*. The material parameters of the uppermost six meters of the model represent the *Superficiale*, the following five meters in depth represent different aquitard materials, ranging from silty-clayey sand to dense clay (cf. table 4.8 & 4.9). By decreasing the vertical permeability of all layers by a factor of ten in comparison to the horizontal permeability for the simulations on this natural field site scale, it was possible to rebuild effects of a stratified medium, like it is encountered in reality, in a simple and roughly approximated way. The whole model domain is fully water saturated.

The top of the aquitards are assumed in first approximation to be horizontal and planar. The second aquifer *Prima Falda* was not included into the model in order to save runtime. But if the DNAPL passes through the aquitard material and pools on the bottom of the model domain, it would imply for a passage of the DNAPL into the deeper aquifer *Prima Falda*.
The spill area is located in the model at the top with a distance of 125 m to the left side / inflow of the model. The distance from the spill point to the right side of the model / outflow sums up to 375 m and is the same as the distance at the field site between the former industrial facility and the Pump & Treat installation. Therefore, it implies that if the DNAPL leaves the model domain in the downstream direction (right side of the model), it would pass the present day position of the Pump & Treat facility, either prior to or after the installation of the wells, since they never operated with full capacity.
The model was discretized with a resolution of 1 m in all three directions, resulting in an overall cell number of 5 500 cells and keeping the runtime in an acceptable range of 1 – 2 days.

Table 5.2 Material parameters of the different applied aquitards

Name	AQUIT A	AQUIT B	AQUIT C	AQUIT D
Geology	Silt, sandy silt, clayey sand, till	Clay	Silty sand, fine grained sand	Clay
Effective porosity	0.02	0.02	0.02	0.02
Horizontal Intrinsic permeability (m^2)	1.0×10^{-15}	1.0×10^{-19}	1.0×10^{-13}	1.0×10^{-17}
Vertical Intrinsic permeability (m^2)	1.0×10^{-16}	1.0×10^{-20}	1.0×10^{-14}	1.0×10^{-18}
Horizontal hydraulic conductivity (m/s)	1.0×10^{-8}	1.0×10^{-12}	1.0×10^{-6}	1.0×10^{-10}
Vertical hydraulic conductivity (m/s)	1.0×10^{-9}	1.0×10^{-13}	1.0×10^{-7}	1.0×10^{-11}

Boundary Conditions of multiphase model

Two different flow velocities were applied to the model by first order boundary conditions regarding the hydraulic head at the inflow and outflow of the model:

- As a base case, every scenario was calculated without groundwater flow.
- As a next step, a groundwater flow velocity of 1 m/d was applied, which represents the natural flow field in the *Superficiale* without the operating Pump & Treat facility.

Thus the two different scenarios regarding the groundwater flow velocity cover as minimum and maximum scenario the whole range of the expected natural groundwater flow velocity at the Rho site.Since there is no information on the spill rate, a total spill of 50 t from the disposal basin to the aquifers was assumed, comparable to similar contaminations in Germany (Grandel and Dahmke, 2008). The spill rate was simulated in two different scenarios: Firstly we assumed that the total mass was spilled in a relatively short time frame of 25 years, resulting in a spill rate of 2 tons per year. Secondly, a leakage time of 50 years was applied, resulting in an input of 1 ton TCE per year into the scenario. After each simulated spill time period, the infiltration was deactivated and the further distribution process of TCE in the subsoil was analyzed for additional 50 and 25 years, respectively. The resulting 75 years in overall simulation time for both spill scenarios correspond hereby to the operational time of the industrial facility from approx. 1910 up until the installation of the impermeable barrier around the former contaminant spill area.The variations in the input parameters for the simulations resulted in a total of sixteen differing scenarios in 2D.

5.2.4 Results and Discussion

Since the main point of interest is the present position of a potential undetected DNAPL source zone, the focus is put on the presentation of the results on the position and length of the DNAPL pool in the model domain at the end of the simulated time period at $t = 75$ years.

The DNAPL pool is defined as the area with a saturation of the DNAPL TCE higher than the residual saturation and thus of the still mobile part of the DNAPL. The residual saturation for the applied geological media is defined for the simulation as $S_r = 0.05$, corresponding to an occupation of 5 % of the available pore space of the stratum and consistent with literature studies of corresponding materials (Falta et al., 1995; Pruess and Battistelli, 2003). If the saturation of the DNAPL declines to values $S_r \leq 0.05$, the DNAPL would be trapped in the porous medium and could only be influenced by subsequent dissolution processes.

As it can be seen in the figure 4.16, the location of the DNAPL source zone after 75 years of industrial operation depends primarily on two parameters:

- Geological properties of the aquitard
- Groundwater flow velocity in the aquifer *Superficiale*.

The influence of the mass spill rate is in relation to the other aspects not significant and will not be discussed in detail here.

Depending on the material parameters, the *Aquitard* between the uppermost aquifer *Superficiale* and the deeper aquifer *Prima Falda* would only be an effective aquitard for the DNAPL, if it consisted of pure clay. The realisations B and D both represent such a scenario. In the base case scenario without groundwater flow the DNAPL migrates vertically through the *Superficiale* and accumulates on top of the aquitards B and D in proximity to the spill point. The pools stretch over ca 200 – 310 m on top of aquitard B and over 222 – 301 m on top of aquitard D, with the main mass center directly below the former industrial area.

Applying the documented groundwater flow velocity of Rho of $v_w = 1$ m/d to the model domain, the pool is transported downstream and the DNAPL body is significantly diminished in its volume and mass due to enhanced dissolution processes as a consequence of the streaming water. The pools are either positioned at $v_w = 1$ m/d at approx. 275 m $< X <$ 500 m or reduced to values below residual saturations, due to enhanced dissolution processes, when infiltrating 50 tons TCE over 50 years instead of 25 years.

In the realisations A and C of the aquitard, the material is only a slight barrier for the passing DNAPL. The mass centre is positioned within the aquitard after 75 years of simulation, the position depending on the applied groundwater flow velocities.

In both cases A and C, the DNAPL migrates through the whole thickness of the aquitards, implying a passage to the deeper Aquifer *Prima Falda* and a continued transport in downstream direction with the general groundwater flow direction of the *Prima Falda*. Since the realisations A and C are quite permeable, the DNAPL is additionally transported within the aquitards with the streaming groundwater.

As aquitard C is represented by a higher permeability, the DNAPL is distributed over a wider area than in realisation A and the downstream transport is enhanced. Defining the position of the pools is not sensible for the field site application, because any pooling on the bottom of the aquitard would not

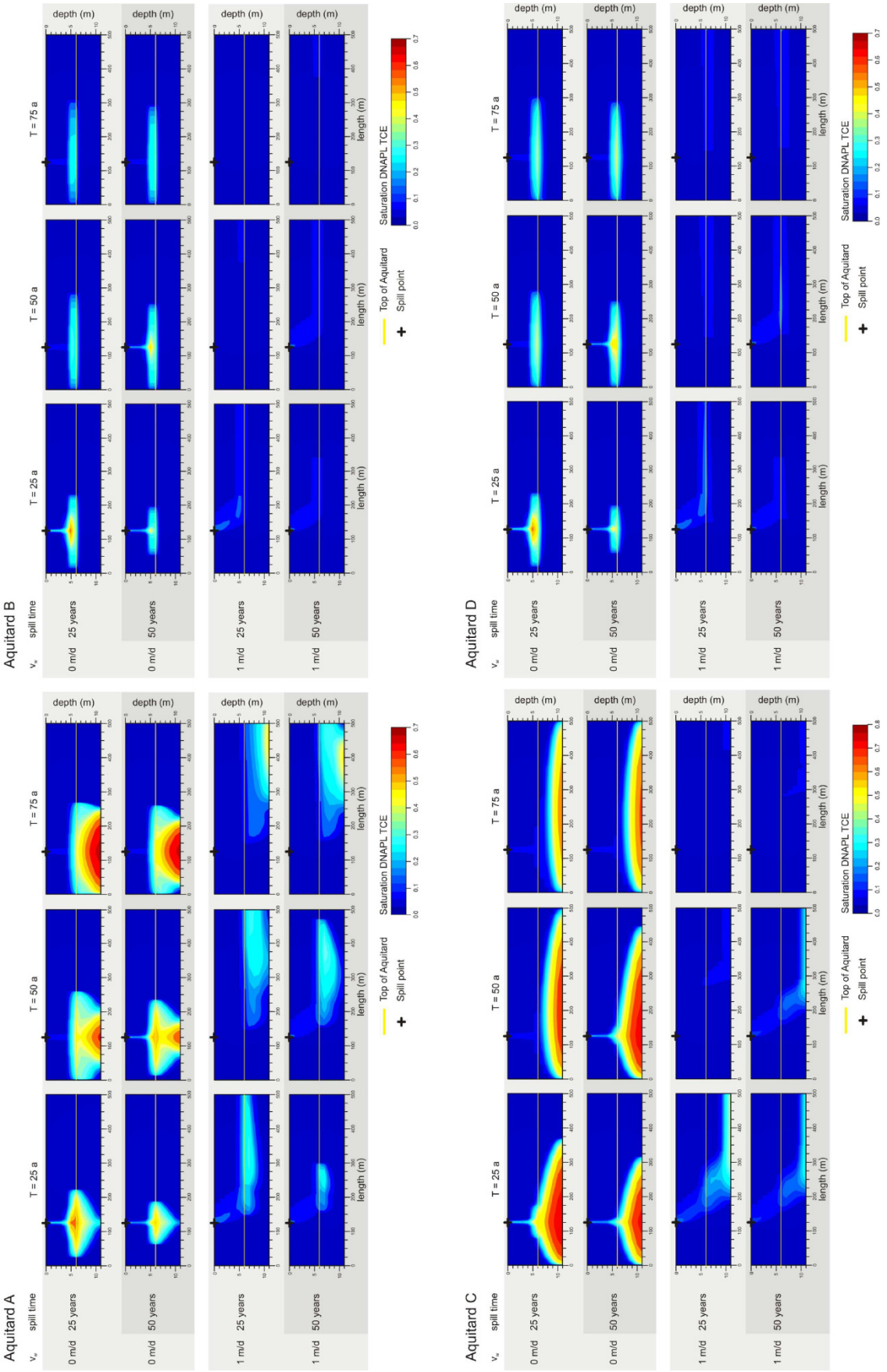

Figure 5.7 Lateral distribution of TCE in scenarios aquitard A - D at the time steps 25 yrs, 50 yrs and 75 yrs, at $v_w = 0$ m/d and $v_w = 1$ m/d and with seepage periods (spill times) of 25 years and 50 years.

develop in such an extent at the real field site, since the DNAPL would migrate to the deeper aquifer *Prima Falda*.

5.3 Conclusion

In the simplified 2D multiphase model of the Rho site two aspects are prominent: The vertical distribution of the DNAPL depends on the permeability of the *Aquitard*. The lateral distribution depends on the groundwater flow velocities in the aquifers.
Since information on the geological parameters of the *Aquitard* at the site vary widely between and within literature studies and borehole datasets, a definite modeling is not yet possible. Instead four different realisations of the documented aquitard material were modelled, two of them representing typical clays, two representing silty-clayey sand and silty sand. In the later two of the four scenarios the DNAPL passes through the aquitard. Transferring these results to the field site, it implies a migration of the main DNAPL source zone to the deeper aquifer *Prima Falda*.
However, if the *Aquitard* at Rho consists mainly of clay, the DNAPL could have pooled on top of it in the last 75 years and would have been transported with the natural groundwater flow in downstream direction. As a consequence it is possible that only a part of the original source zone was encapsulated in the 1980s, while the main mass remained undetected in the downstream area. These undetected pools could furthermore sink through a hydraulic connection in the downstream area to the deeper aquifer *Prima Falda*.
A combination of several aspects, irregular distribution of the permeability of the *Aquitard* parameters and a possible hydraulic connection for instance, could have been intermingled at the site as well.
The next step in the *multiphase model driven site assessment* would be an additional field investigation via Direct Push or geophysics, since the multiphase model exhibited that a main point of interest needs to be on a better definition on the *Aquitard* material. Direct Push and borehole geophysics could deliver valuable informations about the material parameters of the *Aquitard*, while the spatial distribution of the *Aquitard* and potentially even the distribution of the DNAPL could be mapped by ground surface geophysics.
For the positioning of the new field investigations, the geostructural model of the region functions as a guideline, by exhibiting the most prominent geological data gaps at the site.
The multiphase model provides a first approximation of the potential location of the DNAPL source zone. Although definite locations can not be provided at this early state of *multiphase model driven site assessment*, it elucidates that one should be prepared to investigate even in longer distances in lateral and vertical direction to the original spill area.
However, multiphase modeling requires detailed and extensive data input as well as time-intensive computer performances. In order to model one specific field site exactly, informations on all materials, their spatial distribution, the exact time period of the leakage of the contaminants as well as the primary amount of contaminant mass is necessary. Investigations to obtain all these information are neither cost-efficient nor time-effective, nor would the runtime of the simulations be. Therefore simplifications and approximations have to be applied to the multiphase models. Nevertheless, even this simplified models can be of substantial support for the decision making process at a brownfield site and a sensible complementation to different methods of physical site investigation.

Literature

Beretta, G.P., Bozzano, F., Del Bon, A., Majone, M., Nardoni, F. and Eva Pacioni, M.P. (2005): Importanza delle indagini per la caratterizzazione geologica ed idrogeologica di un sito inquinato nel comune di Rho (Milano). Giornale di Geologia Applicata 2: 106-112.

Bozzano, F., Petitta, M., Del Bon, A., Nardoni, F. and Pacioni, E. (2007): Conceptual model and flow numerical simulation of aquifer contaminated by chlorinated solvents in Rho (MI). Italian Journal of Engineering Geology and Environment(Special Issue 2007): 97-105.

Erning, K., Schäfer, D., Dahmke, A., Luciano, A., Viotti, P. and Petrangeli Papini, M. (2010): Simulation of DNAPL distribution depending on groundwater flow velocities using TMVOC. In: M. Schirmer, E. Hoehn and T. Vogt (Editors). IAHS Publication: Groundwater Quality Management in a Rapidly Changing World. Proceedings of the 7th International Groundwater Quality Conference held in Zurich, Switzerland, 13-18 June 2010. Red Books. IAHS. Oxfordshire. pp. 128-131.

Falta, R.W., Pruess, K., Finsterle, S. and Battistelli, A. (1995): T2VOC User´s Guide. LBL-36400. U.S. Department of Energy.158 pp.

Grandel, S. and Dahmke, A. (2008): Leitfaden Natürliche Schadstoffminderung bei LCKW-kontaminierten Standorten: Methoden, Empfehlungen und Hinweise zur Untersuchung und Beurteilung; BMBF-Förderschwerpunkt "Kontrollierter natürlicher Rückhalt und Abbau von Schadstoffen bei der Sanierung kontaminierter Grundwässer und Böden" (KORA), KORA - Themenverbund 3 - Chemische Industrie, Metallverarbeitung. Institut für Geowissenschaften, Abt. Angewandte Geologie. Kiel.364 pp.

Leccese, M., Aulenta, F., Petrangeli Papini, M., Viotti, P., Rossetti, S. and Majone, M. (2007): Anaerobic bioremedation of chlorinated solvents contaminated aquifers in the presence of DNAPL: The Rho test site project. Italian Journal of Engineering Geology and Environment Special Issue 2007: 107-114.

Pruess, K. and Battistelli, A. (2002): TMVOC, A Numerical Simulator for Three-Phase Non-isothermal Flows of Multicomponent Hydrocarbon Mixtures in Saturated-Unsaturated Heterogeneous Media. Report LBNL-49375. Berkeley.192 pp.

Werban, U., Leven, C., Reboulet, E., Leccese, M., Viotti, P. and Dietrich, P. (2007): Technologies for a fast characterization of subsurface structures - an example from the Milano-Rho site. Italian Journal of Engineering Geology and Environment(Special Issue 2007): 8.

6 Multiphase modeling of the impact of groundwater pore velocities on DNAPL migration in the multi-aquifer formation of Rho, Italy

Work in progress

Erning, K., Dahmke, A. and Schäfer, D. (2013 (submitted)): Multiphase modeling of the impact of groundwater flow velocities on DNAPL migration in the multi-aquifer formation of Rho, Italy. Italian Journal of Engineering Geology and Environment.

Abstract

2D multiphase modeling of DNAPL behavior in realistic subsurface morphology of the former industrial site Chimica di Bianchi provided evidence, that moderate groundwater pore velocities are sufficient to transport a TCE phase body over large distances in the downstream direction. In the investigated model set-up, the DNAPL was found to be able to counteract the morphological effects of a slope of 2.5 ° and leave depressions and trenches. The displacement depends directly on the encountered hydraulic pressure regime. Moreover, only materials with a hydraulic conductivity lower than 1×10^{-9} m/s were impermeable to the DNAPL over a time period of 75 years.

The modeling approach presented in this study provides an explanation for the inaccurate, or often even unknown, position of DNAPL source zones at many industrial sites. Furthermore, by narrowing down possible locations, the simulations proved to be a valuable tool for both investigation and remediation activities of DNAPL contaminated sites.

Keywords: Multiphase modeling, DNAPL, TCE, groundwater velocity, morphology, aquitard

6.1 Introduction

Many industrial sites worldwide suffer from industrial contaminations. The most common organic contaminants are chlorinated solvents (Hassanizadeh et al., 2004; Moran et al., 2006; Grandel and Dahmke, 2008; Umweltbundesamt, 2011). Based on estimations of Hassanizadeh et al. (2004), more than 6 800 tons of chlorinated solvents were spilled in the U.S.A. between the years 1998 and 2001 due to accidents or improper handling. In Germany, they are the main contaminants at more than 9 000 sites (Grandel and Dahmke, 2008; Umweltbundesamt, 2011).

Chlorinated solvents pose a significant challenge to site investigation and remediation, because most of them are Dense Non-Aqueous Phase Liquids (DNAPLs) due to their physicochemical properties. When DNAPLs are released to the environment, they infiltrate into the subsurface and move predominantly downwards within the subsoil. DNAPLs will move in the subsoil as long as sufficient mass is available or until they are stopped by an impermeable barrier. Often they accumulate in morphological sinks within low and impermeable materials,

e.g. depressions and trenches of an aquitard. Based on various investigations of the last decades (Mackay et al., 1985; Kueper and Frind, 1988; Schwille, 1988; Kueper et al., 1989; Mercer and Cohen, 1990; Powers et al., 1994b; Illangasekare et al., 1995; Pankow and Cherry, 1996; Helmig, 1997; Bradford et al., 1998; Dekker and Abriola, 2000; Abriola and Lemke, 2002; Bradford et al., 2003; Gerhard and Kueper, 2003b; Jawitz et al., 2005) it is assumed that the DNAPL movement is solely influenced by its physico-chemical behavior and by the material of the subsoil. Considering these information when creating a conceptual model for site investigation and remediation, it is often not possible to explain or define the distribution of DNAPLs and their dissolved components at industrial sites. A typical example for this problematic case of site investigation is the former industrial site Chimica di Bianchi in Rho, Italy. Based on current knowledge about DNAPL behavior in the subsoil, it is not possible to explain the distribution of dissolved contaminant measured at monitoring wells.

The Rho site is characterized by decades of production of dyes, which caused mainly contaminations with perchloroethylene (PCE) and trichloroethylene (TCE). The factory was located on a multi-aquifer formation with an assumed impermeable aquitard at approx. 5 - 10 m below ground surface. Spent DNAPLs were disposed in an open basin, assuming harmless volatilization. In the 1980s the assumed hot spot of DNAPL contamination in the upper aquifer was encapsulated. The encapsulation system was rooted in the aquitard below the former disposal basin and concentrations of dissolved contaminants in the upper aquifer decreased over the next years as expected. But concentrations of dissolved PCE and TCE in the deeper aquifer remained unchanged high. Based on the conceptual model there are several explanations:

The encapsulation system may be permeable in vertical direction, due to penetration of the bottom sealing aquitard during installation. The bottom sealing aquitard may be not continuously present below the assumed hot spot. Both aspects would explain reduced concentrations in the upper aquifer and still enhanced concentrations in the deeper aquifer. But based on our previous investigations (Luciano et al., 2010; Erning et al., 2012), there may be another explanation: The DNAPL was not present at the assumed hot spot, when it was encapsulated in the 1980s, but was transported downstream by natural groundwater pore velocity of approx. 1 – 2 m/d.

Previously conducted small scale laboratory (Luciano et al., 2010) and multiphase modeling investigations (Erning et al., 2012) have shown that high groundwater pore velocities can significantly influence the movement and distribution of the DNAPLs TCE and HFE-7100 (3M, 2005) in water saturated porous medium. The DNAPL was transported in downstream direction in each scenario as direct consequence of the enhanced pore velocity. Considering the implications of the conducted small scale investigation for real field sites, several issues of real field site geology are still unaddressed: potential large amount of spilled contaminants, unknown spill mass and spill time, morphologic effects of impermeable layers (depression, trenches, ridges), natural groundwater flow velocities.

Considering a real field site, estimated amounts of contamination spills range between a few hundreds of kilograms and more than 250 tons (Grandel and Dahmke, 2008). The time scale of contaminant spill is generally estimated to be at least decades for most chlorinated solvents. We assume that there will be a significant impact on the position of the DNAPL due to the groundwater pore velocity at large scale.

Moreover, it is generally assumed, that DNAPLs accumulate in depression forming pools, which remain immobile independently of the groundwater flow velocity. Based on the previous laboratory and model investigations we assume that high hydraulic pressure as enhanced groundwater pore velocities can hinder pooling effects of DNAPLs and may even "push" them upwards against the inclination of impermeable barriers. It could also be possible, that the documented aquitard is not impermeable for DNAPLs, but exhibits a slight long-term permeability.
These three hypotheses are tested in a realistic 2D cross section of the subsurface of the former industrial site Rho. Twenty-six scenarios with varying material parameters are modeled with the multiphase modeling software TMVOC (Pruess and Battistelli, 2002). Influences of varying groundwater pore velocity on position, mass and volume of the DNAPL TCE are quantified and statistically analyzed.
The overall aim of he conducted study is to advance our understanding of DNAPL behavior in the saturated zone at real field sites and to improve site investigation and remediation processes. It may even illuminate one of the most important questions of site investigation and remediation: Where is the long time source zone of DNAPLs?

6.2 Methods

6.2.1 Field site

The reference site is located in Rho, Italy close to the north west of Milano and contains the former industrial area of Chimica di Bianchi. The industrial site comprises approx. 0.16 km² with a surrounding investigation area of 1.8 km² (figure 1).

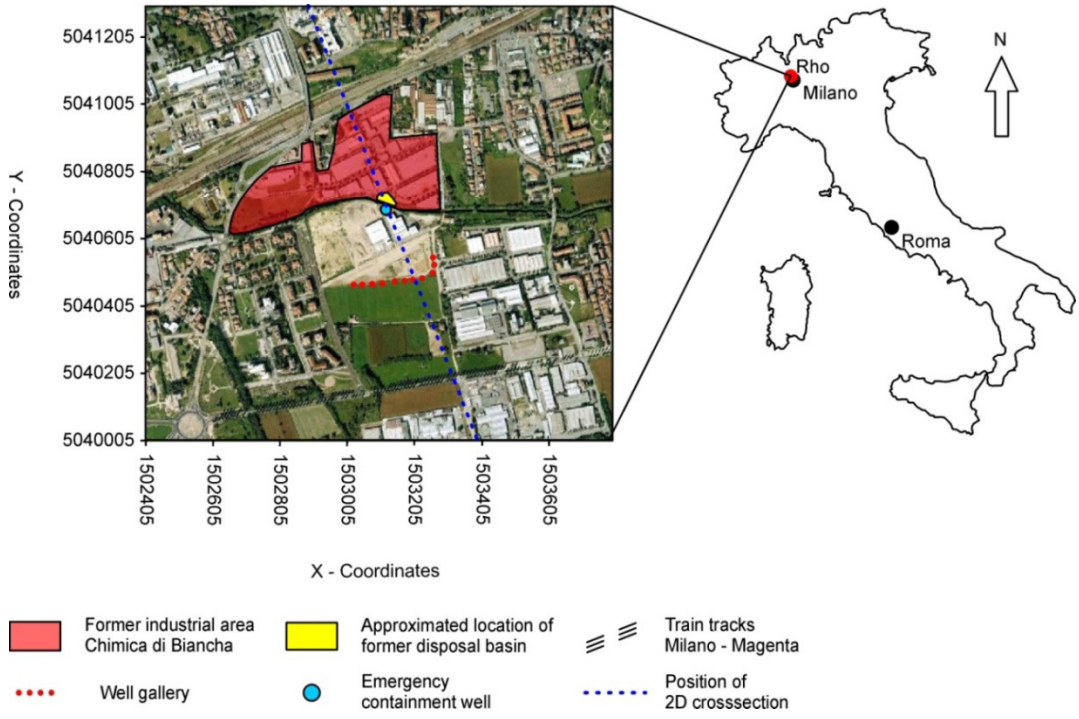

Figure 6.1 Area of interest, overlaid by aerial picture (adapted from Google Earth, 2010), coordinates in Gauss-Boaga

The Rho region is characterized by alluvial and fluvio-glacial quaternary sediments (Bozzano et al., 2007) of widely varying grain size (table 1). At the site, there are two interconnected aquifers of interest (*Superficiale* and *Prima Falda*), which are separated by an interrupted thin clay layer (*Aquitard*) at approx. 5 – 10 m depth. In further depth, the deeper aquifer *Prima Falda* is confined by an impermeable silty-clay layer approx. 55 – 65 m below ground surface level (bgsl). Due to the interrupted clay layer of the *Aquitard* at the regional scale, there are both phreatic and confined conditions for the *Prima Falda*. According to Beretta et al. (2005) and Bozzano et al. (2007), a vertical discharge of ca. 40 m^3/a has to be expected from *Superficiale* to *Prima Falda*. It is still unknown, whether the aquifers are also interconnected at a local scale or even directly within the area of interest.

Table 6.1 Range of hydrogeological parameters at the Rho Site from, provided by literature studies (Beretta et al., 2005; Bozzano et al., 2007; Leccese et al., 2007)

Name hydraulic unit	material	thickness [m]	range of hydraulic conductivity [m/s]	porosity [%]	hydraulic gradient [%]
Superficiale (upper unconfined aquifer)	silty sand sand gravel	10 5 – 12	1E-06 1E-02	20.0	0.4
Aquitard	silty clay clay	1 – 4	1E-09 1E-07	na	na
Prima Falda (lower confined aquifer)	silty-clayey layers sand gravel	20 – 45 15 – 40	1E-06 1E-03	20.0 45.0	0.4 0.6

During an operational time of at least 50 years, the facility Chimica di Bianchi mainly produced chlorinated solvents, like PCE and TCE (Leccese et al., 2007). The most probable leakage point seems to be a former disposal basin of 10 m × 10 m, leading to an aqueous contamination of up to 180 mg/l TCE as dissolved phase in the deeper aquifer *Prima Falda* (Werban et al., 2007), whereas concentration range at values $< 100\mu g/l$ in the shallower aquifer *Superficiale* (Leccese et al., 2007).
However, both the timeframe and the probable amount of spilled DNAPLs are unknown.
In 1982 the hotspot of the former disposal basin was encapsulated (Leccese et al., 2007) and the containment system was embedded in the assumed *Aquitard*. Additionally, one emergency well and a well gallery with 19 wells were installed downstream of the hotspot in order to capture the plume. The emergency well is installed approximately 50 m downstream of the former disposal basin and the well gallery ca. 375 m in downstream direction, i.e. to the South-East (figure 4). As far as the authors know, the well gallery never operated at full capacity, while the emergency well operates continuously.
Several sampling campaigns over the last years (Leccese et al., 2007) indicate the presence of a DNAPL pool acting as long-term source zone, which probably migrated to the underlying aquifer *Prima Falda* (Bozzano et al., 2007).

6.2.2 Primary data

The primary data for the multiphase modeling is a borehole dataset of varying sources (universities, municipal and federal government) including more than 250 boreholes of the Rho region. The data set contains soil classification, characterization of the hydraulic units *Superficiale*, *Aquitard* and *Prima Falda* and water table elevation. Each classified hydraulic unit comprises several classes of permeabilities (cp. table 1), which act overall either as aquifer or aquitard, but are not homogenous within. Hydraulic heads were obtained via groundwater monitoring from 1996 until 2006, indicating a general groundwater flow in *Superficiale* from NNW to SSE. Based on the classification of the hydraulic units, a 3D structural-geological model of the area (figure 2) was constructed in *GMS – Groundwater modeling software* (Aquaveo, 2012).

The three units *Superficiale*, *Aquitard* and *Prima Falda* dip from north to south by approx. 0.4 %. Average thicknesses are ca. 7 – 9 m for *Superficiale*, 1 – 8 m for *Aquitard* and ca. 45 m for the deeper aquifer *Prima Falda*. While the top of *Superficiale* (figure 2) shows only minimal morphology, the top of the aquitard is characterized by trenches and depressions (figure 3). The first trench elongates from NW to SE through the former industrial site. A second trench with E – W orientation interconnects below the industrial site with the first one and forms a depression directly below the former disposal basin. The depression is separated from the first trench in south-eastern direction by a small ridge of 4 m height. The northern half of the aquitard forms a slight plateau, caused by the east-west trench. The morphology of the top of the deeper aquifer *Prima Falda* follows partly the topography of the aquitard, showing inversely the main features of trenches and depressions.

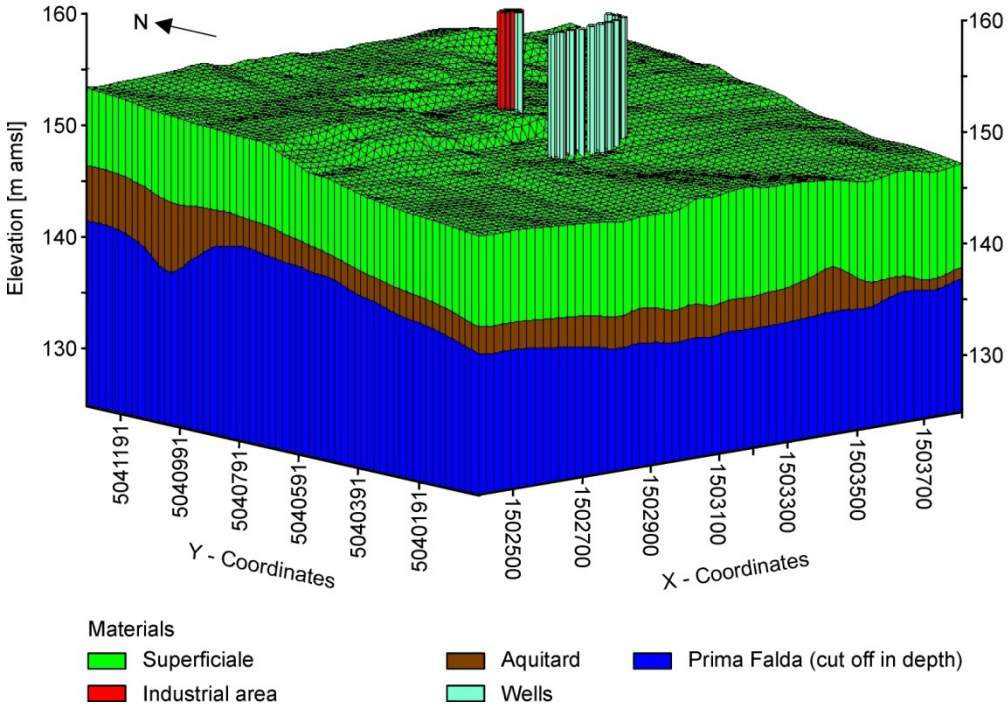

Figure 6.2 Perspective view of Modflow model, all hydraulic units, z-magnification 1 : 25

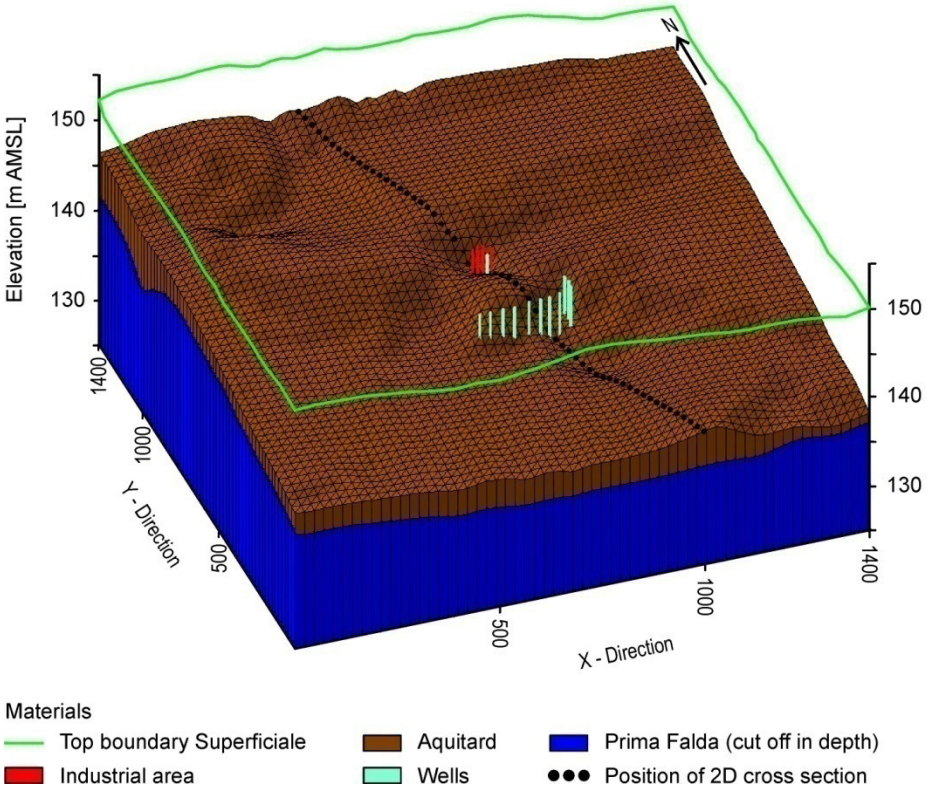

Figure 6.3 Perspective view of *Aquitard* and *Prima Falda* (*Superficiale* not shown), z-magnification 1 : 25

6.2.3 Geometry of multiphase model

A 2D cross section parallel to groundwater flow was cut through the hydraulic 3D model and the geometries and properties of the respective layers transformed for upload into the multiphase modeling software TMVOC. Before data import, the layers were recalculated in their geospatial system, setting the beginning of the 2D cross section to the values x = 0 and y = 0, resulting in sets of x - normalized plains with the original heights of the morphology of the subsoil hydraulic units (figure 4) in meter above mean sea level (m amsl). The layers were uploaded into TMVOC and defined by varying sets of material parameters (cf. table 2), creating a 2D cross section for multiphase modeling. The 2D cross section starts 605 m upstream of the disposal basin and has an overall length of 1400 m. The maximum height is 51 m.

The 2D cross section was discretized into 560 cells in x – direction (cell length = 2.5 m) and 1 cell in y – direction (cell length = 1 m). The discretization in z – direction (depth) has no uniform spacing, but was defined as five rows per hydraulic unit. Thus the thickness of the cells varies between decimeters for the *Aquitard* and several decimeters to meters for the aquifers *Superficiale* and *Prima Falda*.

The unsaturated zone was not included in the modeling process because a) the extent of retardation and degradation processes within the zone are unknown, and b) the modeling of unconfined aquifer and vadose zone is at least by a factor 50 more runtime consuming. The upper aquifer *Superficiale* was therefore cut off at the water table elevation.

The average cell number is a minimum of 5 600 up to the maximum of 21 600, requiring a runtime of hours to several days on an Intel quad core PC (3.00 GHz, 3.25 GB RAM).

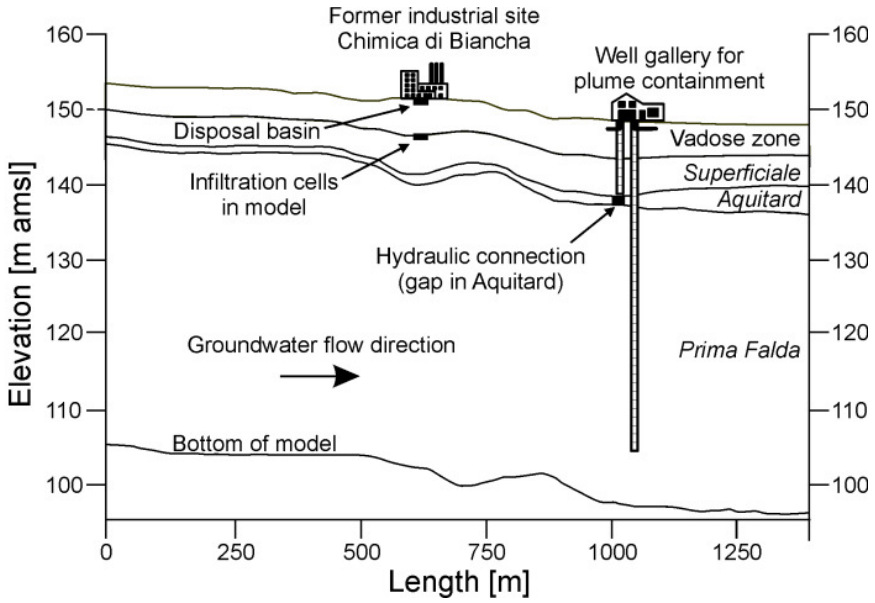

Figure 6.4 2D cross section converted for multiphase modeling

6.2.4 Hydraulic conditions and material parameters

The groundwater flows from left to right in all scenarios and is controlled by fixed pressure conditions and water head elevations, respectively, in the boundary cells.
Three consecutive steps were performed for setting up the scenarios:
In order to investigate the influence of hydraulic conditions, the initial material parameters for the upper aquifer *Superficiale* were at first set to the median of documented material parameters and a mean groundwater flow velocity of 1 m/d (*Superficiale* # 3, table 2). Then, the water table was fixed at the documented hydraulic heads of the reference site and the material parameters of *Superficiale* were adapted to obtain, with the given hydraulic head, a mean groundwater pore velocity of 1 m/d (*Superficiale* # 4). In order to investigate the influence of the material parameters, the hydraulic conductivity of the *Superficiale* was then varied by four orders of magnitude (*Superficiale* # 1, # 2, # 5 and # 6) by adapting values of porosity and intrinsic permeability.
Overall six varying materials were thus tested as aquifer *Superficiale*. By this, the range of documented materials for the aquifer should be represented and possible influences of the geological description as well as of the hydraulic pressure system determined.
The documented geological description of the borehole data set for the so-called *Aquitard* ranges over several classes of hydraulic conductivity. Since the spatial distribution of the materials is not known in detail for the *Aquitard*, five possible materials from silty sand (*Aquitard* # a) to pure clay (*Aquitard* # e) were modeled (table 2).
Because the movement of DNAPLs is defined by capillary pressure (p_c) and relative permeability (k_r) in dependency of the saturation (S) of the respective fluids, each material requires its own formulation of p_c - S and k_r - S dependencies. Well-documented formulations (Falta et al., 1995; Pruess and Battistelli, 2002; Pruess et al., 2002) for the p_c – S and k_r – S functions were chosen according to Parker and Lenhard (1987) and Stone (1970) and adapted to the applied materials according to (Falta et al., 1995) and Pruess and Battistelli (2002).

Table 6.2 Material parameters of scenario modeling

Name of Material	Geological material	Porosity	Hydraulic conductivity [m/s]	Resulting maximum pore velocities [m/d]
Superficiale # 1	Fine grained sand	0.300	5.90E-04	0.01
Superficiale # 2	Medium to coarse grained sand	0.200	1.00E-03	1.00
Superficiale # 3	Coarse grained sand	0.300	5.90E-03	0.07
Superficiale # 4	Medium grained gravel / coarse grained sand	0.200	5.90E-02	1.00
Superficiale # 5	Medium gravel	0.325	5.90E-02	0.62
Superficiale # 6	Medium to coarse grained gravel	0.350	5.90E-01	5.72
Aquitard # a	Silty sand	0.020	1.00E-06	0.00
Aquitard # b	Silty sand	0.020	1.00E-07	0.00
Aquitard # c	Clayey silt	0.020	1.00E-08	0.00
Aquitard # d	Silty clay	0.020	1.00E-09	0.00
Aquitard # e	Clay	0.020	1.00E-10	0.00
Prima Falda # 7	Fine grained gravel	0.200	1.00E-02	0.14

6.2.5 Scenario combinations

Overall twenty-six scenarios (table 4) were calculated to mirror the range of the main features at the Rho site. Thereby the most sensitive parameter for the DNAPL movement at the site Rho and similar sites shall be assessed.

The highest and lowest permeable *Aquitard* material (*Aquitard* # a and # e) were combined with all materials of the *Superficiale*. The *Aquitard*s # b, # c and # e were only combined with *Superficiale* # 5. *Superficiale* # 5 represents a typical gravelly aquifer with good hydraulic conductivity and a general mean groundwater pore velocity of 0.62 m/d, which is typical for many aquifers used for drinking water supply.

The material parameters for *Prima Falda* # 7 were kept constant, because main points of interest are the possible pathways from the *Superficiale* through the *Aquitard*.

In the scenarios simulating a perfectly impermeable *Aquitard* # e, the deeper confined aquifer *Prima Falda* was deactivated in order to save runtime, since the DNAPL cannot pass the *Aquitard* #e.

Additionally, three scenarios consisting of *Superficiale* # 2, *Aquitard* # e, *Prima Falda* # 7 and a mean pore velocity $v_w = 1$ m/d were created, which include a hydraulic connection between the two aquifers (cf. figure 6.4). By this, the behavior of the DNAPL after passing through a hydraulic connection to the deeper aquifer was investigated. The discretization of the deeper aquifer *Prima Falda* was refined in order to extinct effects of discretization on the DNAPL distribution.

Table 6.3 Combination of parameters for scenario modeling

Scenario name	Upper Aquifer #	*Aquitard* #	Lower Aquifer #	Pore velocity in upper Aquifer (m/d)
1a_0.01	1	a	7	0.01
2a_0	2	a	7	0.00
2a_1	2	a	7	1.00
2e_0	2	e	-	0.00
2e_1	2	e	-	1.00
2e_1_gap1	2	e	7	1.00
2e_1_gap2	2	e	7	1.00
2e_1_gap3	2	e	7	1.00
3a_0.07	3	a	7	0.07
3e_0.07	3	e	-	0.07
4a_0	4	a	7	0.00
4a_1	4	a	7	1.00
4e_0	4	e	-	0.00
4e_1	4	e	-	1.00
5a_0	5	a	7	0.00
5a_0.62	5	a	7	0.62
5b_0	5	b	7	0.00
5b_0.87	5	b	7	0.87
5c_0	5	c	7	0.00
5c_0.61	5	c	7	0.61
5d_0	5	d	7	0.00
5d_0.62	5	d	7	0.62
5e_0	5	e	-	0.00
5e_0.62	5	e	-	0.62
6a_5.72	6	a	7	5.72
6b_5.72	6	b	-	5.72

6.2.6 DNAPL infiltration

Since no information on the mass of contaminants was available for the Rho site, the amount of spilled DNAPL is assumed to be 50 tons over a time period of 50 years, based on literature studies of similar sites in Germany (Grandel and Dahmke, 2008).
The DNAPL infiltration started after obtaining steady state conditions with regard to hydraulic pressure, i.e. steady groundwater flow. For practical reasons (i.e., model complexity and runtime), only TCE infiltration was modeled, although a mixture of TCE and PCE exists at the former industrial site Rho. The DNAPL was infiltrated at the position of the former disposal basin in eleven equally sized cells (area of 27.5 m^2) over a time period of 50 years, resulting in an infiltration rate of 0.25 kg/d $\times$ cell. Additional 25 years without further DNAPL leakage were modeled in order to observe the behavior of TCE after the removal of industrial buildings above ground in the 1980s.

6.2.7 Data interpretation

In order to quantify the influence of groundwater flow and material parameters on the DNAPL position, the center of mass (CoM) of the phaseous TCE was calculated for each scenario. The mass of TCE_{NAPL} (M_{TCE}) per cell was calculated using density of TCE as

NAPL (ρ_{TCE}), saturation of TCE (S_{TCE}), volume per cell (V_{cell}) and the respective porosity of the cell φ:

$$M_{TCE} = S_{TCE} \times \rho_{TCE} \times \phi \times V_{cell} \tag{6.1}$$

The varying influences on the position of the centre of mass in lateral and vertical direction are summarized by Box-Whisker-Plots. Because of the skewness of the data, the Kruskal-Wallace- and the U-Test were applied for statistical analysis of influencing factors.
Summarizing the variances in position, amount and volume of TCE as free phase, the changes are exemplarily described for the end of the simulation time (t = 75 a). The simulations are grouped into three categories:
Vel1 = Scenarios without groundwater flow ($v_w = 0$ m/d),
Vel2 = Scenarios with groundwater flow slower than 1 m/d (0 m/d $< v_w <$ 1 m/d) and
Vel3 = Scenarios with $v_w \geq 1$ m/d.
The analysis of the most sensitive and dominating factors for position, mass and volume of DNAPL are conducted for all 26 scenarios, including the three scenarios with a hydraulic connection and adapted discretization in depth (2e_1_gap1, 2e_1_gap2, 2e_1_gap3).

6.3 Results

6.3.1 Spatial distribution of the DNAPL

The applied groundwater flow velocities significantly influence the position of the DNAPL TCE during and after infiltration. The material definition of *Aquitard* defines the vertical passage of the DNAPL by either being completely impermeable of by exhibiting slight to good long-term permeability.
The spatio-temporal behavior of the simulated DNAPL after 50 years and 75 years is exemplarily shown for eight of the 26 conducted scenarios (figure 6.5). The simulation after 50 years represents the conditions which could have been encountered, when site investigation and remediation started in the 1980s, while the results after 75 years represent possible current locations of the DNAPL, assuming no containment of the source zone.
Two varying aquifer materials (*Superficiale* # 2 and *Superficiale* # 4) in combination with two aquitards (*Aquitard* # a and *Aquitard* # e) and two different groundwater flow velocities ($v_w = 0$ m/d and $v_w = 1$ m/d) are represented by the chosen scenarios 2a_0, 2a_1, 2e_0, 2e_1, 4a_0, 4a_1, 4e_0 and 4e_1.
Aquitard # a and *Aquitard* # e are the minimal and maximal permeable materials, which were investigated as *Aquitard* material. The aquifers *Superficiale* # 2 and *Superficiale* # 4 both represent typical sandy aquifers, with *Superficiale* # 2 slightly being the less permeable aquifer. Since groundwater pore velocity is set to $v_w = 1$ m/d in both scenarios, the hydraulic pressure in *Superficiale* # 2 is higher than in *Superficiale* # 4.
Figure 6.5a illustrates the DNAPL distribution by its saturation in the scenarios without groundwater flow at t = 50 a. In **scenario 4a_0** the DNAPL perpendicularly infiltrates the aquifer, fills up the depression and forms a primary pool on top of the aquitard while penetrating it and continuing infiltration of the deeper aquifer. It occupies a volume of 32.9 m^3 with a total mass of 48.5 t. In the following 25 a (figure 6.5c) it continues its gravity driven

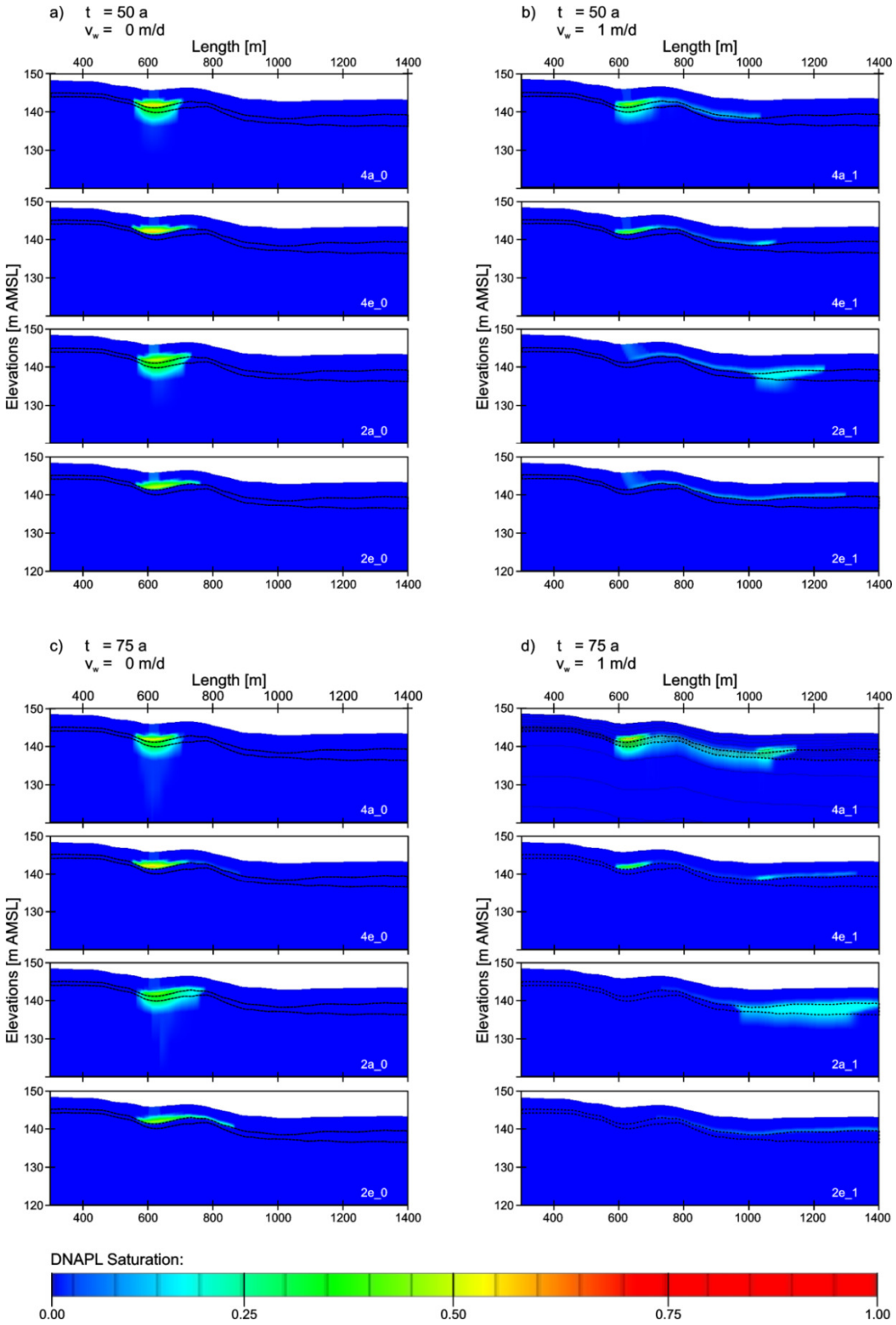

Figure 6.5 Spatial distribution and saturation of DNAPL at varying material compositions and groundwater flow velocities for eight varying scenarios (2a_0, 2e_0, 2a_1, 2e_1, 4a_0, 4e_0, 4a_1and 4e_1) after 50 years and 75 years
a) at t = 50 a & v_w = 0 m/d, b) at t = 50 a & v_w = 1 m/d, c) at t = 75 a & v_w = 1 m/d and d) at t = 75 a & v_w = 1 m/d

downward movement and reaches a depth of 125 m amsl, thus travelling approximately 21 m in depth, through both aquifers, which are separated by an aquitard with reduced permeability. Its overall volume at t = 75 a is reduced to 32.6 m^3 with a mass of phaseous TCE of 48.2 t, exhibiting only slightest dissolution in the stagnant groundwater.

When TCE encounters the impermeable aquitard in **scenario 4e_0**, it pools completely within the depression of the aquitard at t = 50 a. It occupies a volume of 33.7 m^3 with a total mass of 49.8 t. Since it occupies a smaller volume than in scenario 4a_0, the saturation of the available pore space is enhanced, improving the relative permeability of the porous medium for TCE and improving its mobility. Within 25 years after removal of the spill zone, the DNAPL distributes evenly within the depression of the aquitard and flows over the ridge to the right of the infiltration area (figure 6.5c). It continues its movement in the upper aquifer and reaches the position x = 900 m as free phase. This movement is only influenced by the subsurface topography of the aquitard, since there is no groundwater flow in scenario 4e_0. Its final volume at t = 75 a is still 33.7 m^3 with a mass of 49.8 t. Within twenty-five years, it lost only 54 kg or 0.1 % of its mass due to dissolution processes.

In the scenarios 4a_1 and 4e_1 the groundwater flow velocity is increased to v_w = 1 m/d and the position of the DNAPL is significantly influenced by the streaming water (figure 6.5b, d). Due to the vector of hydraulic pressure, TCE infiltrates the subsoil not perpendicularly any more, but with an inclined percolation path to the downstream direction. It pools not symmetrically in the depression but prone to the downstream area, being pushed over the ridge of the depression and continuing its downstream distribution in the upper aquifer. TCE penetrates the aquitard and infiltrates the second aquifer in **scenario 4a_1** (figure 6.5b) with lesser amount of TCE than in the stagnant scenario 4a_0. Its total mass of 34.4 t is distributed over a volume of 23.2 m^3, being 29 % less mass than in scenario 4a_0, illustrating the enhanced dissolution due to the streaming water. Twenty-five years later at t = 75 a it has formed a secondary pool in the upper aquifer *Superficiale* approximately at x - position 1050 – 1180 m. Additionally, it is stored in nearly all compartments of the *Aquitard* between x = 590 m and x = 1180 m, but it only occupies the upper two meters of the underlying aquifer *Prima Falda*.

In **scenario 4e_1**, the DNAPL moves over the ridge of the depression during the fifty years of infiltration and spreads out as continuous pool from x = 585 m to x = 1084 m. At the end of the simulated time (t = 75 a), the TCE free phase pool ranges from x = 588 m to x = 1331 m with a total mass of 33.3 t TCE with a volume of 22.5 m^3.

The DNAPL distribution pattern is significantly impacted by a change of material for the upper aquifer. In the **scenario 2a_0** (less permeable aquifer *Superficiale*) a slightly smaller volume of subsoil is occupied by the DNAPL after 50 years of infiltration (figure 6.5a). It occupies a volume of 31.3 m^3 with a total of 46.2 t TCE. It penetrates the aquifer and the aquitard slower than in scenario 4a_0 and infiltrates the second aquifer to a depth of 132 m amsl. At t = 75 a (figure 6.5c) it spreads over a volume of 32.6 m^3 with 48.2 t phaseous TCE, distributed between x = 564 m and x = 776 m, already starting to pass the highest point of the ridge. In the second aquifer *Prima Falda* it is present down to a depth of 125 m amsl as free phase.

Encountering the impermeable aquitard in the **scenario 2e_0** (figure 6.5a) the DNAPL pools on top of the aquitard as in scenarios 4e_0, covering a volume of 33.7 m^3 with a mass of 49.7 t and a reduced saturation of the subsoil. After the removal of the spill zone, the

DNAPL is redistributed in the subsoil due to gravitation. At t = 75 a it transgresses the ridge of the depression and continues its downhill movement to the right of the model domain (figure 6.5c). It covers a length of 305 m on top of the aquitard, reaching from x = 561 m to x = 866 m with 49.6 t of phaseous TCE in a volume of 33.6 m^3.
Enhancing the pore velocity in the upper aquifer to 1 m/d (scenarios 2a_1 and 2e_1), similar trends as in scenarios 4a_1 and 4e_1 can be observed. In **scenario 2a_1** (figure 6.5b) the DNAPL infiltrates the upper aquifer *Superficiale* # 2 inclined to the downstream direction and does not pool in the depression of the aquitard, but is pushed downstream over the ridge by the groundwater. It does not infiltrate *Aquitard* # a in the surroundings of the spill area, but starts infiltrating at x = 987 m, i.e. 382 m downstream of the industrial site. Its mass of 34.9 t occupies a volume of 23.6 m^3. Within the first 25 years after source removal, the DNAPL moved out of the area of the original contamination zone (figure 6.5d) and forms a long-term source zone on top, within and below the aquitard at x = 955 – 1400 m (minimum). Since the DNAPL reached the end of the model domain at t = 70 a, this can only be regarded as a minimum length of the DNAPL pool.
Comparing **scenario 2e_1** to scenario 4e_1 a faster movement of the DNAPL is predominantly visible (figure 6.5b). After 50 years of infiltration it is evenly distributed with a maximum saturation of $S_{NAPL} = 0.125$ over a length of 672 m, reaching from x = 626 m - 1298 m on top of the impermeable aquitard, without any significant pooling effects in the depression below the infiltration area. After the removal of the spill zone, the DNAPL is dissolved below the infiltration area and it stretches as thin pool (figure 6.5d) with maximum saturation of $S_{DNAPL} = 0.08$ from x = 716 m to the end of the model domain. It covers a volume of 13.1 m^3 with a total mass of phaseous TCE of 19.5 t.

6.3.2 Position of DNAPL and Center of mass

The 26 scenarios exhibit a huge variety in the position of TCE_{NAPL}, depending on the combinations of material parameters and applied groundwater pore velocities. Figure 6.6 depicts the distribution of mobile DNAPL of all conducted scenarios after 75 years of simulation time.
In 20 scenarios TCE has passed the ridge at the downstream side of the depression after 75 years. Only in six scenarios the DNAPL accumulates solemnly in the depression. These six scenarios are characterized by aquifer materials ranging from medium grained gravel with coarse grained sand to medium grained gravel, and $v_w = 0$m/d to $v_w = 0.01$ m/d.
If the groundwater pore velocity exceeds $v_w < 0.07$ m/d, the DNAPL passes the ridge of the downstream side of the depression independently of the hydraulic conductivity of the aquifer material. Even in less permeable material, the DNAPL is transported out of the depression by the streaming groundwater, i.e. if the hydrodynamic pressure is sufficient.
The vertical travel distance of TCE is steered by the permeability of the applied aquitard material. TCE infiltrates all aquitards, except aquitard # e (pure clay). In the scenarios with aquitards # a, # b and # c, TCE percolates into the upper most meters of the second aquifer Prima Falda. But infiltration into aquitard #d occurs only in the uppermost centimeters of the aquitard layer, where the DNAPL is stored as longterm source zone.

The three scenarios with hydraulic connection between the upper and the lower aquifer (identified by black box in figure 6.6) exhibit that prognoses of the infiltration depths into the deeper aquifer depend strongly on the discretization of the aquifer: All three scenarios are composed of the same materials and groundwater flow velocities, but with refined discretization of the second aquifer. In the scenario 2e_1_gap1, discretization in depth of the deeper aquifer Prima Falda is ca. 7.8 m per row (5 rows). TCE is present as free phase in the gap and in the uppermost meters of Prima Falda. Refined discretization in scenario 2e_1_gap2 to 2.4 m cell height (16 rows) results in a percolation depth of ca. 20 m into the second aquifer. Further refinement to a vertical discretization of 50 rows à 0.75 m height of the deeper aquifer Prima Falda results in no percolation into the deeper aquifer at all, but the DNAPL remains within the gap between the aquifers and is only dissolved into the deeper aquifer Prima Falda, leading to an extended contamination plume (not shown). Because the main point of interest of this study is the distribution within the upper aquifer and potential passage into the deeper aquifer, but not the distribution pattern within the deeper aquifer, we did not investigate questions of discretization further.

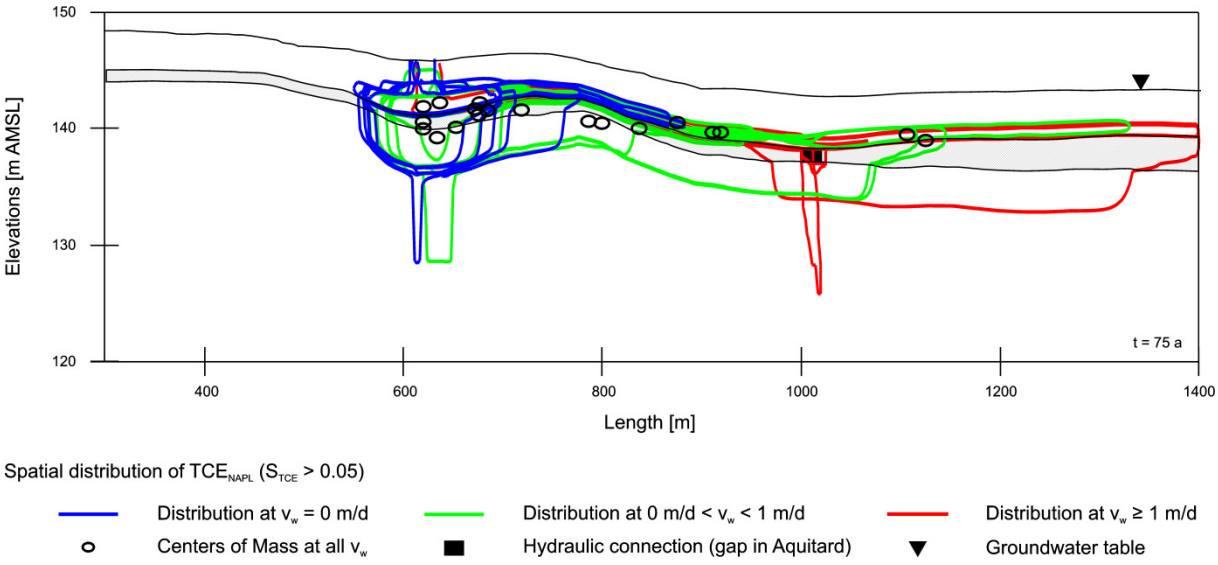

Figure 6.6 Spatial distribution of mobile TCE_{NAPL} ($S_{TCE} > 0.05$) as isolines and Center of Mass as dots of all conducted scenarios (z-magnification 1 : 25)

By analyzing the distribution of the center of mass of mobile DNAPL of all 26 conducted scenarios, general trends can be recognized: The variance in the position of the centre of mass (figure 6.7) shows large interquartile ranges (IQR) regarding the lateral position and slighter variances regarding the position in depth. The IQR for the lateral position ranges at 622 – 679 m for the no flow scenarios (Vel1, $v_w = 0$ m/d) with median at 623 m, at 636 – 791 m for Vel2 (0 m/d $< v_w <$ 1 m/d) with median at 682 m and at 800 - 1128 m for Vel3 ($v_w \geq 1$ m/d) with median at 913 m. The highest applied groundwater pore velocity of 5.72 m/d causes a complete dissolution of the DNAPL at t = 54 a (6e_5.72) and t = 63 a (6a_5.72), respectively, and the plume of dissolved TCE leaves the model domain completely. The remaining seven scenarios of the category of $v_w \geq 1$ m/d (Vel3) all have a groundwater pore velocity of 1 m/d, due to the initialization of the systems.
The centre of mass of the vertical position varies at 139 – 142 m amsl.

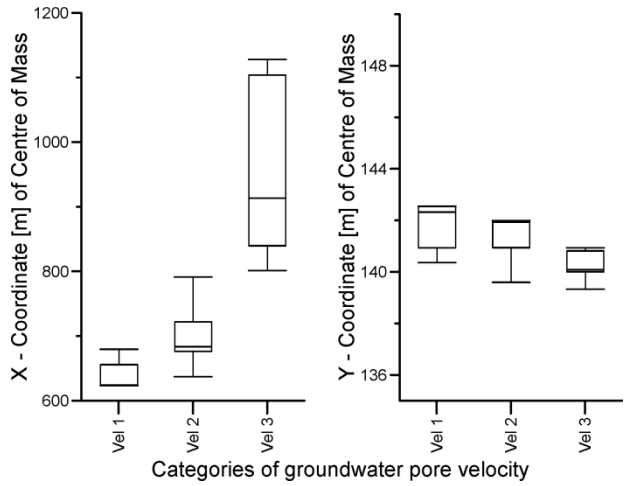

Figure 6.7 Variance in position of centre of mass at t = 75 a for $v_w < 0$m/d (Vel1), 0 m/d $< v_w <$ 1 m/d (Vel2) and $v_w \geq 1$ m/d (Vel3)

6.3.3 Mass of the DNAPL

In the scenarios without groundwater flow (Vel1), the amount of phaseous TCE varies between 30.6 t (5e_0) and 49.8 t (4e_0) in the model domain at the end of simulation time (t = 75 a), depending on the materials of the hydraulic units. Interquartile range (IQR) spans from 46.6 t to 49.7 t, with median at 49.4 t (figure 6.8).

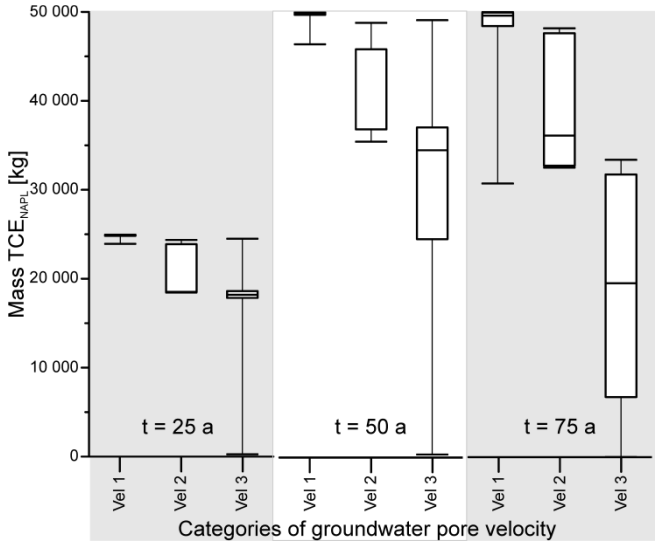

Figure 6.8 Boxplots of effects of groundwater flow velocity on mass of TCE at time steps 25 a, 50 a and 75 a for $v_w < 0$m/d (Vel1), 0 m/d $< v_w <$ 1 m/d (Vel2) and $v_w \geq 1$ m/d (Vel3

Enhancing the groundwater flow to 0 $< v_w <$ 1 m/d (Vel2), the total mass of phaseous TCE in the model domain differs between 32.4 t and 50.0 t. The IQR comprises 32.6 t – 45.0 t with the median at 36.0 t TCE phase being present.
At groundwater flow velocities of 1 m/d or higher (max $v_w = 5.72$ m/d), the mass of phaseous TCE is reduced to values between 0.0 t (scenarios 6a_5.72 and 6b_5.72) and 33.3 t

of the original infiltrated amount of 50.0 t. IQR is between 5.1 t and 29.4 t with the median at 19.5 t.

6.3.4 Volume of the DNAPL

In close relation to the mass of TCE phase, the amount of the volume of TCE phase (figure 6.9) shows the same trends.
At stagnant conditions without groundwater flow (Vel1), the volume of TCE phase ranges from 20.7 m^3 to 33.7 m^3 with the median at 33.4 m^3. The interquartile range comprises 31.5 m^3 to 33.6 m^3 with the median being at 33.4 m^3. The second category with groundwater flow velocities $0 < v_w < 1$ m/d (Vel2), shows minimum and maximum values of 21.9 m^3 and 32.5 m^3, respectively. IQR is from 22.1 m^3 to 30.4 m^3 and the median at 24.6 m^3. In the third category (Vel3, $v_w \geq 1$ m/d), minimum NAPL volume is 0.0 m^3, since the dissolution process at $v_w = 5.72$ m/d are predominant. Maximum present DNAPL volume is 22.5 m^3, significantly less than in category Vel1 or Vel2. The median is at 13.1 m^3 with IQR ranging from 3.5 m^3 to 19.9 m^3.

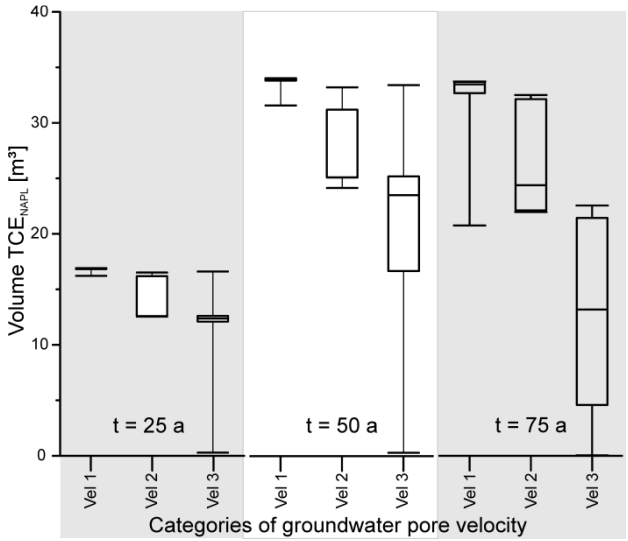

Figure 6.9 Boxplots of effects of groundwater flow velocity on volume of TCE at time steps 25 a, 50 a and 75 a for $v_w < 0$m/d (Vel1), 0 m/d $< v_w <$ 1 m/d (Vel2) and $v_w \geq 1$ m/d (Vel3)

6.4 Discussion

6.4.1 Spatial distribution and position of centre of mass

In the 2D cross section of the former industrial site Chimica di Bianchi in Italy, the groundwater pore velocity causes a significant downstream displacement of the DNAPL TCE and influences mass and volume of the mobile DNAPL by enhancing dissolution processes.
The statistical Kruskal Wallis-Test shows a clear significance for the influence of the groundwater flow on the position of the centre of mass.
Although the significant influence of the groundwater pore velocity seems to contradict modeling and experimental results by Dekker and Abriola (2000); Kamon et al. (2004); Putzlocher et al. (2006), it is a direct result of the set-ups of the conducted experiments and models. Previously conducted investigations cover groundwater velocities of 0.002 – 0.12 m/d (Putzlocher et al., 2006), 0.007 – 1.33 m/d (Gerhard et al., 2007), 0.0008 – 0.008 m/d (Dekker and Abriola, 2000) and max. $v_w = 0.4$ m/d (Kamon et al., 2004). The natural groundwater flow at the field site Rho ranges between 1 – 2 m/d, which possibly has been further increased by operation of the capturing wells. In gravelly aquifers in mountain valleys, groundwater flow velocities can easily exceed 1 – 2 m/d. Natural groundwater flow velocities in those regions are documented with 3.5 – 5.0 m/d (Hoehn and Santschi, 1987; Hoehn and Von Gunten, 1989; Von Gunten et al., 1991), 5.0 m/d (Herfort and Ptak, 2002) and maximum values at local scale of 10 m/d (Herfort et al., 1998). Comparing these regions with the area of Rho, the investigated groundwater pore velocities are a low, but good approximation of general gorundwater flow velocities encountered in Europe.
Enhanced groundwater flow velocities can counteract effects of subsurface morphology as trenches and depressions, in which the DNAPL would pool at stagnant or very low groundwater flow velocities. In the investigated model set-up, TCE is transported uphill out of a depression with an inclination of 2.5° of the slopes event at $v_w \geq 0.01$ m/d.
The distribution of the DNAPL is not only influenced during the infiltration of the contaminant, but also after stopping the injection of further DNAPL. It redistributes in the subsoil depending on the local pressure regime. The distances of DNAPL movement within the scenarios conducted for these investigations is within the range, which Imhoff et al. (2003) predicted for real field sites, when applying inspectional analysis as upscaling tool to results of laboratory experiments.
But according to Putzlocher et al. (2006), significant reductions in the transport distances of DNAPLs and in the pool length are caused by heterogeneous composition of the subsurface. Therefore, distribution patterns at the real field site will be shortened by a maximum of factor 50 and more compact than in the investigated scenarios.
The influence of the applied aquifer material is only significant for the lateral position, while the aquitard material has no statistical significant influence on the centre of mass at all. Although the variance caused by the aquitard material is mathematically not significant, the aquitard at the site below the disposal basin is at the vertical position ca. 140 – 142 m, i.e. the variance of the vertical position shows penetration of the aquitard. Moreover, figure 6.7 illustrates that the lower the groundwater flow velocity, the shallower is the transportation in depth after 75 years of simulation time. The reasons are on the one hand that the DNAPL infiltrates the downstream slope of the depression at $v_w \geq 0$ m/d, when encountering slight

permeable aquitard materials. On the other hand, a simultaneous downstream displacement takes place at enhanced groundwater flow velocities. This leads to a downstream transportation of the DNAPL to an area of the model domain, where the aquitard is located deeper and the consequent pooling of the DNAPL on top of the aquitard or within the aquitard at that position.
The position of the DNAPL body is furthermore not solely dependent on the measured groundwater pore velocity, but on the hydraulic pressure encountered in the aquifer, i.e. the combination of intrinsic material parameters and hydraulic pressure gradient: high hydraulic pressure can be caused either by reduction of material´s permeability or by increasing the hydraulic gradient. The same v_w can exist at complete different pressure regimes and governs the phase flux by:

$$F_\beta = v_w \rho_\beta n = -k \frac{k_{r\beta}\rho_\beta}{\mu_\beta} (\nabla P_\beta - \rho_\beta G) \tag{6.2}$$

Where

F_β	Darcy flux of phase β [m/s]
ρ_β	Density of phase β [kg/m³]
n	porosity [-]
k	Intrinsic permeability of the material [m²]
$k_{r\beta}$	Relative permeability of phase β [m²]
μ_β	Dynamic viscosity of phase β [Pa s]
P_β	Fluid pressure in phase β [Pa] with $P_\beta = P + P_{c\beta}$
P	Pressure in reference phase (here: water) [Pa]
$P_{c\beta}$	Capillary pressure between the involved fluids [Pa]
G	Gravitational acceleration [m/s²]

The aquifer composition has furthermore no significant impact on the spatial position of the center of mass of the mobile DNAPL body. On contrast, the investigated aquitard materials exhibit a more complex impact on the DNAPL. Pure clays and silty clays (*Aquitard* # d and # e) are impermeable for DNAPL penetration as expected and prove to be a reliable barrier. Whereas aquitards comprised of silt, clayey silt or any kind of low permeable fine sand (*Aquitard* # a, # b and # c) are no long-term barrier for the vertical DNAPL movement. In our model set-up, the DNAPL TCE was able to infiltrate and even penetrate all materials, which were characterized by a hydraulic conductivity higher than 1 x 10^{-9} m/s.

6.4.2 Mass of DNAPL

The U-Test exhibited a clear influence of the groundwater pore velocity on the mass of the DNAPL (p-values < 0.016). There was no statistical significance due to the general material composition of the aquifers and the aquitard, unless comparing the median of DNAPL mass in the scenarios in *Superficiale* # 2 vs. *Superficiale* # 6 and *Superficiale* # 5 vs. *Superficiale* # 6 directly to each other.
The correlation between mass of DNAPL and groundwater velocity is consistent with findings by Saba et al. (2001); Parker and Park (2004); Grant and Gerhard (2007), but the rate of dissolution is probably overestimated due to the dimensionality of the model. Although

(Christ et al., 2005) exhibited a good approximtation to 3D problems by representative 2D models, the water flux may be forced through contaminated regions of the source zone, that might be by-passed in 3D and thus increasing dissolution processes (Christ et al., 2009). Moreover, TMVOC assumes instantaneous dissolution, although dissolution processes are kinetically sterred and dependant on the surface area of the NAPL body (Sale and McWhorter, 2001). This would imply a reduced dissolution at the field scale in comparison to the model predictions.

6.4.3 Volume of DNAPL

Analyzing the development of volume with regard to the applied groundwater pore velocities, significant differences in the medians of all three applied groups are exhibited (p-values < 0.016). Analyzing the values of volume with respect to the material parameters, there is only a statistical significant difference between the aquifer materials *Superficiale* # 2 vs. *Superficiale* # 6 and *Superficiale* # 5 vs. *Superficiale* # 6, when comparing directly to each other with the Whitney-Wilcoxon-Mann-U-Test. Otherwise, there is no significant influence of the aquifer material on the development of the volume of phaseous TCE. The varying applied aquitard materials exhibit no significant influence at all.

6.4.4 Implication for former industrial site Chimica di Bianchi, Rho

Extrapolating the results of the 2D modeling to the field site Rho, the following conclusions can be drawn:
The geological description of the assumed *Aquitard* is not sufficient to define the material as an impermeable layer for DNAPL movement. The documented material classes, which comprise the so-called *Aquitard*, range over several grain classes, from silty sand to pure clay. But only the aquitard materials with $k_f < 10^{-9}$ m/s (clays, *Aquitard* # d and # e) are impermeable for TCE. If only minor amounts of silt or sand (*Aquitard* # b and # c) or a mixture of sandy silt or silty sand (*Aquitard* # a) is present, the DNAPL passes through these materials in the model predictions. This would imply a potential percolation of the assumed bottom sealing aquitard of the encapsulating system at the field site Rho assuming no groundwater flow at the site. Additional investigation of the *Aquitard* material and its hydraulic conductivity at the site with groundpenetration and borehole geophysics (georadar, electric conductivity DP, DP injection logging e.g.) could clarify the unsolved question of distribution of material classes within the Aquitard, its distribution and its resulting permeability.
Since the natural groundwater flow velocity at the Rho site is documented with approximately 1 – 2 m/d in average, it is more probable, that a major amount of the DNAPL moved out of the depression below the industrial site and was not encapsulated in the 1980s at all. The DNAPL may even have passed the position of the well gallery prior to their installation.
We assume that the DNAPL passed the so-called *Aquitard* between the hotspot and the emergency well and probably also further downstream, since the ongoing monitoring campaigns at the site still measure high concentration of dissolved TCE in the deeper aquifer, in which the emergency well and part of the well gallery are installed. Whether TCE passed directly through the assumed *Aquitard* or through a hydraulic connection can not be verified

based only on numerical simulation of the multiphase flow, because the primary information of the distribution of the *Aquitard* material is too sparse.
Moreover, the real subsurface morphology of the *Aquitard* is not only a 2D depression below the former industrial site Chimica di Bianchi, but a complex three-dimensional morphology of hydraulic units. As the 3D model exhibited (figure 6.3), there are two trenches crossing below Chimica di Bianchi. The first trench is nearly oriented northwest to southeast, while the second trench stretches from east to west. The crossing of these two trenches creates the depression below the industrial site. In our model, the 2D cross section cuts through the highest slope of the depression, i.e. the slope to the sout-east of the hot spot. The DNAPL is able to transgress this slope of 2.5° at groundwater pore velocities of less than a meter per day. But the slope to the southwest of the depression, belonging to the east – west elongated trench, is lower than the slope of the 2D cross section. It has to be assumed that the DNAPL probably followed this trench and it could currently easily be located to the west of the well gallery. This assumption is consistent with geophysical investigations conducted by Cardarelli and Di Filippo (2009) at the Rho site, which found by applying electrical resistivity and induced polarization tomography measurements in 2D and 3D anomilies, which indicate a potential DNAPL body south-west of the former industrial site.

6.5 Conclusion

The DNAPL distribution in the conducted scenarios is significantly influenced by the encountered groundwater pore velocities. Contrary to previous assumptions, the DNAPL can move out of depressions, even at slowest groundwater pore velocities. The depression in the conducted scenarios exhibits a rising slope of 2.5° in downstream direction (height of the ridge ca. 4m). Groundwater flow velocities of $v_w = 0.01$ m/d are sufficient to transport the DNAPL over the ridge. The transport is not dependent on the size of the depression or the amount of spilled DNAPL, as long as it is not trapped in residual saturation. Furthermore, the groundwater pore velocity enhances the downstream displacement of the DNAPL TCE. Downstream displacement at $v_w \leq 1$ m/d can be increased by a factor of more than ten compared to scenarios without groundwater flow, e.g. occurrence of free phase TCE further than 775 m downstream of the source zone instead of 75 m downstream. But the magnitude of the downstream displacement depends not only on the groundwater pore velocity, but actually on the hydrodynamic pressure gradient in the system, i.e. the combination of hydraulic gradient and intrinsic material parameters. High hydrodynamic pressure gradients increase the downstream displacement even in units with reduced permeability. This means that neglection of either hydraulic gradient or permeability will create a distorted distribution pattern, because the groundwater flow velocity in low permeable material will be slow, meanwhile the hydrodynamic pressure gradient will be huge.
In the investigated scenarios, there is a statistically significant influence of the groundwater pore velocity while the material composition of the upper aquifer only shows a significant impact on the DNAPL distribution pattern in its extreme material composition (maximum and minimum permeability as pure well sorted gravel and fine sand).
The scenario modeling furthermore revealed that aquitards that hinder vertical groundwater movement are possibly permeable for infiltrating DNAPLs, because of the higher density and lower viscosity of the DNAPLs. In the multiphase flow simulations, only materials with

$k_f < 10^{-9}$ m/s (pure clays) were efficient long term barriers for vertical DNAPL movement. Any kind of clayey material with slightest amounts of silt or sand is permeable for DNAPLs within the investigated time frame of 75 years. Layers of sandy silt and silty sand (10^{-7} m/s $< k_f <$ 10^{-8} m/s) will not stop the vertical DNAPL movement, but only slow it down. At the same time, these materials will act as long term storage units for the DNAPLs, creating subsequent secondary source zones.

Three scenarios were calculated with varying discretization in depth of the deeper aquifer. These simulations exhibited that the vertical penetration depth strongly depends on the cell size of the model. As we calculated the deeper aquifer with the same resolution as the upper aquifer (2.5 × 1 × 0.75 m, runtime ca. 50 hours), TCE did not infiltrate into the deeper aquifer as free phase, but only dissolved in water. Coarser discretization (2.5 × 1 × 2.4 m, runtime ca. 6.5 hours) leads to an infiltration depth of ca. 20 m into the deeper aquifer or to no infiltration at all at cell sizes of 2.5 × 1 × 7.8 m (runtime ca. 7 hours). Aspects of descretization of the deeper aquifer were not further investigated, since research focus was set on possible transport mechanisms out of the area of interest (upper aquifer Superficiale) in lateral or in vertical direction. But a sensible discretization of the multiphase model would be essential, if penetration depth in the deeper aquifer is the main focus of interest.

The results of the scenario modeling depend furthermore on the boundary conditions of the model. Because the DNAPL infiltration is modeled in 2D, transport and dissolution of the free phase are enhanced compared to reality. In the 2D model the DNAPL is forced through the NAPL contaminated area, but it would bypass the source zone in a 3D scenario, following the path of least resistance, i.e. the path with highest permeability, which is the area with no NAPL present. Transportation lengths as well as dissolution rates are therefore overestimated in our model. But up until now it is not possible with the applied software to simulate realistic 3D multiphase models with cell numbers of several tens of thousands cell.

The simulations depend furthermore on the chosen set of scaling parameters for the entry pressure in the capillary pressure function. Because no measurements of the material of the field site were available, literature values were applied and bear a specific uncertainty. Measurements of the capillary pressure of the materials at the site would reduce this level of uncertainty.

In order to reduce the level of uncertainties, a multiphase modeler would need detailed information about the spatial distribution of material classes, their exact classification due to permeability, water table elevations of the area of interest and laboratory measurements of the capillary entry pressure for the investigated fluid-material combination. But investigation on such a detailled level is time- and cost consuming. Therefor site investigation should concentrate on efficient characterization of the hydraulic units and their distribution as well as on local and regional water table elevation. This would deliver the needed information for correct implementation of the hydraulic pressure gradient in the multiphase model and to increase the accuracy of the model prediction. Meanwhile, scenario modeling is a good approximation and a helpful tool for the planning of site investigation and site remediation actions.

Acknowledgments

We would like to thank our colleagues from La Sapienza University Rome (A. Bozzano, A. Luciano, M. Leccese, M. Petrangeli Papini and P. Viotti and their teams) for the field investigations at the Rho site and the generous provision of the data. This research was in parts financially supported by the European Union under the 7th European Framework, Project ModelPROBE (no 213161).

References

3M (2005): 3M Novec TM 7100 - Engineered Fluid. Product Information. 3M Electronics. St. Paul, MN, USA. pp. 8.

Abriola, L.M. and Lemke, L.D. (2002): The influence of hydraulic property correlation on predictions of DNAPL entrapment and recovery. Calibration and Reliability in Groundwater Modelling: A Few Steps Closer to Reality (Proceedings of ModelCARE 2002, Prague, Czech Republic, 17-20.June 2002). IAHS Publ. 277: 3-9.

Aquaveo (2012): Groundwater Modeling System - GMS. Provo.

Beretta, G.P., Bozzano, F., Del Bon, A., Majone, M., Nardoni, F. and Eva Pacioni, M.P. (2005): Importanza delle indagini per la caratterizzazione geologica ed idrogeologica di un sito inquinato nel comune di Rho (Milano). Giornale di Geologia Applicata 2: 106-112.

Bozzano, F., Petitta, M., Del Bon, A., Nardoni, F. and Pacioni, E. (2007): Conceptual model and flow numerical simulation of aquifer contaminated by chlorinated solvents in Rho (MI). Italian Journal of Engineering Geology and Environment(Special Issue 2007): 97-105.

Bradford, S.A., Abriola, L.M. and Rathfelder, K.M. (1998): Flow and entrapment of dense nonaqueous phase liquids in physically and chemically heterogeneous aquifer formations. Advances in Water Resources 22(2): 117-132.

Bradford, S.A., Rathfelder, K.M., Lang, J. and Abriola, L.M. (2003): Entrapment and dissolution of DNAPLs in heterogeneous porous media. Journal of Contaminant Hydrology 67: 133-157.

Cardarelli, E. and Di Filippo, G. (2009): Electrical resistivity and induced polarization tomography in identifying the plume of chlorinated hydrocarbons in sedimentary formation: a case study in Rho (Milan – Italy). Waste Managment and Research 27(Sep 2009): 595-602.

Christ, J.A., Lemke, L.D. and Abriola, L.M. (2005): Comparison of two-dimensional and three-dimensional simulations of dense nonaqueous phase liquids (DNAPLs): Migration and entrapment in a nonuniform permeability field. Water Resources Research 41(W01007): 1-12.

Christ, J.A., Lemke, L.D. and Abriola, L.M. (2009): The influence of dimensionality on simulations of mass recovery from nonuniform dense non-aqueous phase liquid (DNAPL) source zones. Advances in Water Resources 32(3): 401-412.

Dekker, T.J. and Abriola, L.M. (2000): The influence of field-scale heterogeneity on the infiltration and entrapment of dense nonaqueous phase liquids in saturated formations. Journal of Contaminant Hydrology 42(2-4): 187-218.

Erning, K., Grandel, S., Dahmke, A. and Schäfer, D. (2012): Simulation of DNAPL infiltration and spreading behaviour in the saturated zone at varying flow velocities and alternating subsurface geometries. Environmental Earth Sciences 65(4): 1119-1131.

Falta, R.W., Pruess, K., Finsterle, S. and Battistelli, A. (1995): T2VOC User´s Guide. LBL-36400. U.S. Department of Energy.158 pp.

Gerhard, J.I. and Kueper, B.H. (2003): Capillary pressure characterisitcs necessary for simulating DNAPL infiltration, redistribution, and immobilization in saturated porous media. Water Resources Research 39(8): 17 PP.

Gerhard, J.I., Pang, T. and Kueper, B.H. (2007): Time Scales of DNAPL Migration in Sandy Aquifers Examined via Numerical Simulation. GROUND WATER 45(2): 147-157.

Grandel, S. and Dahmke, A. (2008): Leitfaden Natürliche Schadstoffminderung bei LCKW-kontaminierten Standorten: Methoden, Empfehlungen und Hinweise zur Untersuchung und Beurteilung; BMBF-Förderschwerpunkt "Kontrollierter natürlicher Rückhalt und Abbau von Schadstoffen bei der Sanierung kontaminierter Grundwässer und Böden" (KORA), KORA - Themenverbund 3 - Chemische Industrie, Metallverarbeitung. Institut für Geowissenschaften, Abt. Angewandte Geologie. Kiel.364 pp.

Grant, G.P. and Gerhard, J.I. (2007): Simulating the dissolution of a complex dense nonaqueous phase liquid source zone: 2. Experimental validation of an interfacial area - based mass transfer model. Water Resources Research 43(12): W12409.

Hassanizadeh, S.M., Schotting, R.J., Gray, W.G. and Pinder, G.F. (2004): Solid Waste and Emergency Response. Washington, DC.

Helmig, R. (1997): Multiphase flow and transport processes in the subsurface. A contribution to the modeling of hydrosystems. Environmental Engineering. Springer. Berlin; Heidelberg; New York; Barcelona; Budapest; Hong Kong; London; Milan; Paris; Santa Clara; Tokyo. 367 pp.

Herfort, M., Ptak, T., Hümmer, O., Teutsch, G. and Dahmke, A. (1998): Testfeld Süd: Einrichtung der Testfeldinfrastruktur und Erkundung hydraulisch-hydrogeochemischer Parameter des Grundwasserleiters. Grundwasser 3(4): 159-166.

Herfort, M. and Ptak, T. (2002): Multitracer-Versuch im kontaminierten Grundwasser des Testfeldes Süd. Grundwasser 1: 31-40.

Hoehn, E. and Santschi, P.H. (1987): Interpretation of tracer displacement during infiltration of river water to groundwater. Water Resources Research 23(4): 366-340.

Hoehn, E. and Von Gunten, H.R. (1989): Radon in groundwater: A tool to assess infiltration from surface waters to aquifers. Water Resources Research 25(8): 1795-1803.

Illangasekare, T.H., Ramsey, J.L., Jensen, K.H. and Butts, M.B. (1995): Experimental study of movement and distribution of dense organic contaminants in heterogeneous aquifers. Journal of Contaminant Hydrology 20(1-2): 1-25.

Imhoff, P.T., Mann, A.S., Mercer, M. and Fitzpatrick, M. (2003): Scaling DNAPL migration from the laboratory to the field. Journal of Contaminant Hydrology 64(1-2): 73-92.

Jawitz, J.W., Fure, A.D., Demmy, G.G., Berglund, S. and Rao, P.S.C. (2005): Groundwater contaminant flux reduction resulting from nonaqueous phase liquid mass reduction. Water Resources Research 41: 15.

Kamon, M., Endo, K., Kawabata, J., Inui, T. and Katsumi, T. (2004): Two-dimensional DNAPL migration affected by groundwater flow in unconfined aquifer. Journal of Hazardous Materials 110(1-3): 1-12.

Kueper, B.H. and Frind, E.O. (1988): An overview of immiscible fingering in porous media. Journal of Contaminant Hydrology 2(2): 95-110.

Kueper, B.H., Abbott, W. and Farquhar, G. (1989): Experimental observations of multiphase flow in heterogeneous porous media. Journal of Contaminant Hydrology 5(1): 83-95.

Leccese, M., Aulenta, F., Petrangeli Papini, M., Viotti, P., Rossetti, S. and Majone, M. (2007): Anaerobic bioremedation of chlorinated solvents contaminated aquifers in the presence of DNAPL: The Rho test site project. Italian Journal of Engineering Geology and Environment Special Issue 2007: 107-114.

Luciano, A., Viotti, P. and Petrangeli Papini, M. (2010): Laboratory investigation of DNAPL migration in porous media. Journal of Hazardous Materials 176: 1006-1017.

Mackay, D.M., Roberts, P.V. and Cherry, J.A. (1985): Transport of organic contaminants in groundwater. Environmental Science & Technology 19(5): 384-392.

Mercer, J.W. and Cohen, R.M. (1990): A review of immiscible fluids in the subsurface: Properties, models, characterization and remediation. Journal of Contaminant Hydrology 6(2): 107-163.

Moran, M.J., Zogorski, J.S. and Squillace, P.J. (2006): Chlorinated Solvents in Groundwater of the United States. Environmental Science & Technology 41(1): 74-81.

Pankow, J.F. and Cherry, J.A. (1996): Dense Chlorinated Solvents and Other DNAPLs in Groundwater. Waterloo Press. Waterloo. 522 pp.

Parker, J.C. and Lenhard, R.J. (1987): A Model for Hysteretic Constitutive Relations Governing Multiphase Flow in Porous Media. 1. Saturation-Pressure Relations. Water Resources Research 23(12): 2187-2196.

Parker, J.C. and Park, E. (2004): Modeling field-scale dense nonaqueous phase liquid dissolution kinetics in heterogeneous aquifers. Water Resources Research 40: 12 PP.

Powers, S.E., Abriola, L.M. and Weber, W.J., Jr. (1994): An experimental investigation of nonaqueous phase liquid dissolution in saturated subsurface systems: Transient mass transfer rates. Water Resources Research 30(2): 321-332.

Pruess, K. and Battistelli, A. (2002): TMVOC, A Numerical Simulator for Three-Phase Non-isothermal Flows of Multicomponent Hydrocarbon Mixtures in Saturated-Unsaturated Heterogeneous Media. Report LBNL-49375. Berkeley.192 pp.

Pruess, K., Oldenburg, C. and Moridis, G. (2002): TOUGH2 User´s Guide, Version 2.0. LNNL-43134. Berkeley.210 pp.

Putzlocher, R., Kueper, B.H. and Reynolds, D.A. (2006): Relative velocities of DNAPL and aqueous phase plume migration. Journal of Contaminant Hydrology 88(3-4): 321-336.

Saba, T., Illangasekare, T.H. and Ewing, J. (2001): Investigation of surfactant-enhanced dissolution of entrapped nonaqueous phase liquid chemicals in a two-dimensional groundwater flow field. Journal of Contaminant Hydrology 51(1-2): 63-82.

Sale, T.C. and McWhorter, D.B. (2001): Steady State Mass Transfer from Single-Component Dense Nonaqueous Phase Liquids in Uniform Flow Fields. Water Resources Research 37: 393-404.

Schwille, F. (1988): Dense chlorinated solvents in porous and fractured media. Translation of: Leichtfüchtige Chlorkohlenwasserstoffe in porösen und klüftigen Medien. Lewis Publishers, Inc. Chelsea.

Stone, H.L. (1970): Probability Model for Estimating Three-Phase Relative Permeability. Trans. SPE of AIME 249: 214-218.

Umweltbundesamt (2011): Bundesweite Übersicht zur Altlastenstatistik (Stand 7/2011). http://www.umweltbundesamt.de/boden-und-altlasten/altlast/web1/deutsch/1_3.htm [2012,30.10.].

Von Gunten, H.R., Karametaxas, G., Krähenbühl, U., Kuslys, M., Giovanoli, R., Hoehn, E. and Keil, R. (1991): Seasonal biogeochemical cycles in riverborne groundwater. Geochimica et Cosmochimica Acta 55(12): 3597-3609.

Werban, U., Leven, C., Reboulet, E., Leccese, M., Viotti, P. and Dietrich, P. (2007): Technologies for a fast characterization of subsurface structures - an example from the Milano-Rho site. Italian Journal of Engineering Geology and Environment(Special Issue 2007): 8.

7 Conclusion

The incentive for the investigation of multiphase modeling as site investigation tool is the still unknown position of long-term DNAPL source zones in the subsoil at many industrial sites worldwide, although most sites are regarded as thoroughly investigated by classical methods.

The modeling approach presented in this study provides an explanation for the inaccurate or often even unknown position of DNAPL source zones at many industrial sites. Effective site remediation depends on the level of accuracy concerning the position and the probable amount of phaseous contaminants acting as long-term source zone. Dissolution behavior and thus longevity of the source zone strongly depends on the source zone geometry, i.e. its distribution in the subsoil. Misjudgment of position and mass of the source zone can lead to increased time and cost demands or, as worst case, to complete failure concerning remediation according to health safety standards.

Planning of remediation actions depends directly on the available information provided by site investigation campaigns. Lines of evidence are not existent in most cases and have to be supplemented by lines of indications for the occurrence and position of the source zone. Because traditional and well-established physical site investigation (e.g. drilling and monitoring wells) is costly, time consuming, delivers only sparse spatial data and bears the potential of unwillingly spreading of the contaminants. Therefore most campaigns are restricted in the number of investigations performed at the site, the data density and thus the level of accuracy actually needed in most cases for a thorough risk assessment.

New methods of non- and low-invasive site investigation techniques are required to breach the gap between “affordable” and “necessary”. Enhanced geophysics for faster and better characterization of the subsoil, tree-core monitoring for fast characterization of possible hotspots, new statistical analysis of sparse data and new approaches in modeling of contaminants are possible non- and low-invasive methods, as investigated by the EU-ModelPROBE project.

The multiphase modeling of the DNAPL seepage history, based on existing data of previous historical and physical site investigation bears the potential to investigate sparse data sets and enhance our understanding of possible pathways of DNAPLs in the subsoil in dependency of the geological composition of the subsoil and hydrogeological settings. It can contribute to the decision making process regarding additional site investigation campaigns or site remediation actions by exhibiting prominent data gaps, addressing unsolved questions regarding material parameters and indicating consequently possible positions of DNAPL source zones.

The test site for the multiphase modeling is the ModelPROBE reference site Chimica di Bianchi in Rho, Italy. This former industrial site of glue and dye production represents typical challenges encountered at numerous brownfield sites. Nearly 80 years of industrial usage lead to high concentrations of dissolved chlorinated solvents in the two underlying aquifers. Several site investigation campaigns and site remediation actions were performed in the last 30 years. The site is regarded as well investigated by conventional methods and containment actions were performed between 1980 and 2010. Concentrations of dissolved contaminants

still exceed safety regulation, although the assumed source zone was encapsulated and several wells currently capture the plume of dissolved contaminants.
Data of previous site investigation is existent, but delivers no sufficient explanation for the unchanged high concentrations of dissolved contaminants in the subsoil. Information about probable spill location, spill amount and spill time are sparse. Detailled information about the technical consummation of containment actions performed is sparse to non-existent.
The subsurface is assumed to consist of two highly permeable quaternary, alluvial aquifers, which are separated by an impermeable aquitard of silty - clayey composition. Distribution of the assumed aquitard has to be interpolated from moderate spatial point data and is neither accurate nor complete. The potential subsurface morphology of the aquitard can generate potential preferential flow paths for DNAPLs, as within trenches or depressions. Naturally occuring groundwater flow velocities in both aquifers are in the range of 1 – 2 m/d, which are typical values for Europe.
It is assumed that a secondary DNAPL hot spot in the subsoil acts as long-term source zone of dissolved contaminants, but its position cannot be approximated by conventional site investigation methods.
The multiphase modeling combines all available information about contamination history, geological composition of the subsoil and hydrogeological parameters in order to narrow down possible locations of DNAPL hot spots in the saturated zone. By investigating several site specific, potentially sensitive parameters concerning the DNAPL behavior in the subsoil, an additional line of indication can be concluded. The information obtained by multiphase modeling help to improve further decision making processes regarding site investigation and site remediation plans.
But the quality of the multiphase model is restricted by the quantity and quality of primary data, which either has to be delivered by site investigation campaigns, by laboratory experiments or by literature studies. The level of accuracy and the density of the primary data determine the level of accuracy of the multiphase model, although inaccurate or missing information can partly be dealed with by enhanced interpolation methods and partly by modeling of varying scenarios.
The investigation aims comprises four issues and resulting questions in order to localize the unknown position of a DNAPL source zone:

Issue 1 – Documented natural groundwater flow velocities at many industrial sites are much higher than typical groundwater flow velocities investigated in already conducted laboratory experiments and scenario models. Groundwater flow can furthermore be increased, when Pump & Treat facilities operate at the sites. At the former industrial site Chimica di Bianchi natural groundwater flow velocities are approximately 1 – 2 m/d and several wells are capturing the plume of dissolved contaminants.

Could increased groundwater flow velocities have affected the position of the DNAPL source zone?

Small scale laboratory experiments with high groundwater flow velocities (max. vw = 40m/d) were used to calibrate small scale homogenous multiphase models. Thirteen varying groundwater flow velocities were investigated by scenario modeling concerning their impact on the position of a DNAPL TCE body in the saturated zone. Based on the

results, phaseous TCE in homogenous media is already affected by groundwater flow velocities of 0.05 m/d. Distribution pattern, dissolution rate and consequently the size of the DNAPL body are directly affected by the encountered flow velocities. Extrapolating the small scale scenarios to a homogeneous field scale problem, the main DNAPL body could theoretically be transported over 5.4 km within 50 years at groundwater flow velocity of $v_w = 1$ m/d

Transferring the results of the calibrated small scale multiphase models to the site Chimica di Biachi indicates a possbile transport of the main DNAPL phase body over significant distances prior to the encapsulation of the assumed source zone. However, small scale heterogeneities in the material parameters can superimpose the influcence of the groundwater flow velocity by creating preferential flow path, as it was observed in the laboratory experiments.

Issue 2 – Geological descriptions of hydraulic units as aquifers and aquitards vary generally by several orders of magnitude in reality. At the site Chimica di Bianchi, the geological description of the present aquitard includes mixtures of silty sand, sandy silt, silty clay and pure clay, and acting as overall impermeable layer for groundwater. In general groundwater aquitards are assumed to be effective barriers for vertical DNAPL movement.

Are the assumed aquitard materials also impermeable for DNAPLs?

The layer, which is assumed as aquitard and in which the encapsulation of the assumed source zone was rooted, is neither generally distributed at the site, nor can it be regarded as impermeable for phaseous TCE. The available description of bore logs at the site as well as provided by literature characterizes the aquitard as a mixture of clay, silty clay, clayey silt and silty sand. Multiphase modeling of respective scenarios exhibited that only pure clays with a hydraulic conductivity lower than 10^{-9} m/s are long-term barriers for vertical DNAPL movement. But it has to be stated that it is not sufficient to regard the hydraulic permeability or the intrinsic permeability of the material. The entry pressure according to the capillary pressure regime has to be taken into account, since it steers the entrance of NAPLs into the pore space. As long as there are no specific measurements of the entry pressure of the specific material – fluid combination of the site, values for the capillary pressure - saturation function have to be adapted from literature. Due to the non-specific data, variances are possible. Nevertheless, hydraulic conductivity of 10^{-9}m/s (i.e. pure clays) can be considered effective DNAPL barrier as a rule of thumb.

Issue 3 – Spatial information about the distribution of hydraulic units is generally sparse, because traditional site investigation is mostly drilling and only in single cases supported by geophysical areal investigations. The distribution of geological units has to be interpolated from point data (bore-logs, borehole informations) in most cases. At Chimica di Bianchi in Rho it is assumed that the impermeable material of the aquitard is omnipresent at the site, but geological modeling conducted in this study indicate that the aquitard may have several missing areas.

Is it possible that the DNAPL migrated through a gap in the aquitard to the deeper aquifer?

Although the site Chimica di Bianchi is regarded as thoroughly investigated with more than 250 bore logs in the area, the primary information of the subsoil is not sufficient to define the aquitard material as being omnipresent at the site. It is known from literature that the aquitard is missing at regional scale. The 3D structural models which were conducted based on the original bore logs of the site do not support the hypothesis of an omnipresent aquitard at the site. It is more likely, that there are several lenses of clayey and silty material, which can be overlapping and continuously distributed over distances of several meters, but which are not ubiquitous at the area of Chimica di Biancha.
Performed multiphase model scenarios exhibited that migration of DNAPLs within an aquifer due to streaming groundwater and subsequent passing through a gap in the aquitard is possible. The exact location of such a hydraulic connection between the two aquifers could not be concluded from the models, due to the sparse primary data.
Within the second aquifer, the DNAPL TCE percolated only to a depth of tens of meters. It is concluded, that it is unlikely, that the DNAPL pools on the bottom of the second aquifer at the site. The scenario modeling indicates an entrapment in residual saturation in the uppermost meters of the deeper aquifer and resulting dissolution over long time periods.

Issue 4 – Aquitards and low permeable units are in reality charcterized by complex morphological features, as depressions, trenches, ridges and eroded areas. Assuming an omnipresent, impermeable aquitard at the site Chimica di Bianchi, the surface of this aquitard shows typical subsurface mor-phology with trenches, depressions and ridges.

What are the influences of subsurface morphologies on the DNAPL movement and its final position?

Twenty-six scenarios with constant subsurface morphology of the aquitard, but with varying material compositions and varying groundwater flow velocities were conducted to address Issue 4. If groundwater flow is stagnant, the morphology defines the DNAPL distribution. It will follow gravity driven solely the inclination of the impermeable layers and accumulate at the deepest location. But the results of the scenarios with groundwater flow indicate, that even moderate groundwater flow velocities of $v_w = 0.07$ m/d are sufficient to transport the DNAPL TCE out of a depression with sloped walls of 2.5° (ca. 4 m relative height difference on 200 m).
The exact length of the pathway of the DNAPL TCE is overestimated in the scenarios, since all materials are assumed to be homogenous – anisotropic. It is well known from literature, that implementing small scale heterogeneities into the model or experiments results in shortened pathways of NAPLs. Generally the reduction is in the range of 50 % compared to distances in homogenous scenarios (Putzlocher et al., 2006). Unfortunately, the applied multiphase simulator TMVOC is not (yet) able to handle heterogeneous permeability fields in realistic site scenarios. But even if all values of pathways delivered by multiphase modeling are reduced by 50 %, it still implicates a significantly changed position for the DNAPL at the site Chimica di Bianchi and thus an inefficient positioning of the containment barriers and wells.

The multiphase modeling of the DNAPL seepage history provided valuable information for the former industrial site Chimica di Bianchi. Most importantly it came to attention that the

site investigation already conducted is not sufficient to define the position of the DNAPL. In order to improve the quality of prediction, geophysical investigation would be a helpful add-on. By mapping the spatial distribution of soil classes with georadar, geoelectricity or even seismic, it could be possible to define the position and extend of impermeable layers more accurately. Including this information into the multiphase model would increase the level of accuracy. More detailled historical investigations regarding spill mass and spill time frame would also improve accuracy

But up until now, the 3D modeling of contaminant spill provides huge challenges. Due to excessive runtime when modeling with cell numbers larger than 10 000 and the complex initialization of groundwater flow conditions, I do not recommend multiphase modeling with TMVOC as advisable tool for field investigations.

It is a valuable tool for investigating specific questions arising at sites and for investigating fundamental principles governing multiphase flow behavior of DNAPLs. But conduction of realistic 3D models with accurate resolution is not yet possible within an acceptable time frame. I hope that future improvements concerning stability and performance might enable standard applications of 3D multiphase models in an iterative site investigation process, but currently it is only possible to conduct simplified 2D scenarios in order to answer most principles questions.

8 Acknowledgements

First and of all, I would like to thank Prof. Dr. A. Dahmke and PD Dr. Dirk Schäfer of the Department of Applied Geology of the University of Kiel for giving me the possibility of the conducted research. Additionally I would especially like to thank them for the inspiring discussions, critical but constructive feedback und never ending positive support.
Special thanks have to be given to Prof. M. Petrangeli Papini, Prof. P. Viotti and Dr. A. Luciano for the intensive collaboration, their generous providing of the primary data and for answering all my question concerning the laboratory set-up. Moreover I would like to thank them for the intensive discussion during the excellent evening dinners in Rome.
My heartfelt thanks to Dr. S. Grandel and Dr. F. Dethlefsen for helping me improving my scientific writing skills and for great patience in correcting and discussion my papers.
Furthermore I would like to say a big thank you to everyone of the departments Applied Geology and Geohydromodeling for encouragement, inspiring working conditions and positive feedback.
Special thanks go to all my fellow PhD students for constructive proof-reading, critical analysis of the information level of figures and graphics and for steady supply of coffee, chocolate and hope.
Thanks to all my friends and relatives for enduring bursts of excitements as well as extremely high stress-levels, including the typical stressfull anti-social behavior.
And of course, the most special thanks to you, my Smeckhead!

9 References

3M (2005): 3M Novec TM 7100 - Engineered Fluid. Product Information. 3M Electronics. St. Paul, MN, USA. pp. 8.

3M (2008): Material Safety Data Sheet HFE-7100 3M(TM) Novec(TM) Engineered Fluid. http://multimedia.3m.com/mws/mediawebserver?66666UtN&ZUxL99XLxMaMxME5Vu9KcuZgVU_LXT1u666666-- [2008,September 16].

Abriola, L.M. and Lemke, L.D. (2002): The influence of hydraulic property correlation on predictions of DNAPL entrapment and recovery. Calibration and Reliability in Groundwater Modelling: A Few Steps Closer to Reality (Proceedings of ModelCARE 2002, Prague, Czech Republic, 17-20.June 2002). IAHS Publ. 277: 3-9.

Abriola, L.M. (2003): Effectiveness of DNAPL source zone treatment in heterogeneous media: The role of interphase mass transfer. ACS Division of Environmental Chemistry, Preprints 43.

Aquaveo (2012): Groundwater Modeling System - GMS. Provo.

ASTM (2011): Standard Practice for Classification of Soils for Engineering Purposes (Unified Soil Classification System). ASTM D2487 - 11. ASTM. pp. 11.

Bao, W.M.J., Vogler, E.T. and Chrysikopoulos, C.V. (2004): Nonaqueous liquid pool dissolution in three-dimensional heterogeneous subsurface formations. Environmental Geology 43: 968-978.

Basu, N.B., Fure, A.D. and Jawitz, J.W. (2008a): Predicting dense nonaqueous phase liquid dissolution using a simplified source depletion model parameterized with partitioning tracers. Water Resources Research 44.

Basu, N.B., Fure, A.D. and Jawitz, J.W. (2008b): Simplified contaminant source depletion models as analogs of multiphase simulators. Journal of Contaminant Hydrology 97(3-4): 87-99.

Beretta, G.P., Bozzano, F., Del Bon, A., Majone, M., Nardoni, F. and Eva Pacioni, M.P. (2005): Importanza delle indagini per la caratterizzazione geologica ed idrogeologica di un sito inquinato nel comune di Rho (Milano). Giornale di Geologia Applicata 2: 106-112.

Bozzano, F., Petitta, M., Del Bon, A., Nardoni, F. and Pacioni, E. (2007): Conceptual model and flow numerical simulation of aquifer contaminated by chlorinated solvents in Rho (MI). Italian Journal of Engineering Geology and Environment(Special Issue 2007): 97-105.

Bradford, S.A., Abriola, L.M. and Rathfelder, K.M. (1998): Flow and entrapment of dense nonaqueous phase liquids in physically and chemically heterogeneous aquifer formations. Advances in Water Resources 22(2): 117-132.

Bradford, S.A., Vendlinski, R.A. and Abriola, L.M. (1999): The entrapment and long-term dissolution of tetrachloroethylene in fractional wettability porous media. Water Resour. Res. 35: 2955-2964.

Bradford, S.A., Rathfelder, K.M., Lang, J. and Abriola, L.M. (2003): Entrapment and dissolution of DNAPLs in heterogeneous porous media. Journal of Contaminant Hydrology 67: 133-157.

Broholm, K., Feenstra, S. and Cherry, J.A. (1999): Solvent Release into a Sandy Aquifer. 1. Overview of Source Distribution and Dissolution Behavior. Environmental Science & Technology 33(5): 681-690.

Broholm, K., Feenstra, S. and Cherry, J.A. (2005): Solvent Release into a Sandy Aquifer. 2. Estimation of DNAPL Mass Based on a Multiple-Component Dissolution Model. Environ. Sci. Technol. 39(1): 317-324.

Brooks, R.H. and Corey, A.T. (1964): Hydraulic Properties of Porous Media. Hydrol. Pap. 3. Fort Collins.

Brusseau, M.L., Nelson, N.T., Oostrom, M., Zhang, Z., Johnson, G.R. and Wietsma, T.W. (2000): Influence of Heterogeneity and Sampling Method on Aqueous Concentrations Associated with NAPL Dissolution. Environmental Science & Technology 34(17): 3657-3664.

Burdine, N.T. (1953): Relative permeability calculations from pore-size distribution data. Journal of Petroleum Technology 5(3): 71-78.

Cardarelli, E. and Di Filippo, G. (2009): Electrical resistivity and induced polarization tomography in identifying the plume of chlorinated hydrocarbons in sedimentary formation: a case study in Rho (Milan – Italy). Waste Managment and Research 27(Sep 2009): 595-602.

Chang, L.-C., Chen, H.-H., Shan, H.-Y. and Tsai, J.-P. (2009): Effect of connectivity and wettability on the relative permeability of NAPLs. Environmental Geology 56(7): 1437-1447.

Christ, J.A., Lemke, L.D. and Abriola, L.M. (2005): Comparison of two-dimensional and three-dimensional simulations of dense nonaqueous phase liquids (DNAPLs): Migration and entrapment in a nonuniform permeability field. Water Resources Research 41(W01007): 1-12.

Christ, J.A., Lemke, L.D. and Abriola, L.M. (2009): The influence of dimensionality on simulations of mass recovery from nonuniform dense non-aqueous phase liquid (DNAPL) source zones. Advances in Water Resources 32(3): 401-412.

Christ, J.A., Ramsburg, C.A., Pennell, K.D. and Abriola, L.M. (2010): Predicting DNAPL mass discharge from pool-dominated source zones. Journal of Contaminant Hydrology 114(1-4): 18-34.

Cohen, R.M. and Mercer, J.W. (1993): DNAPL Site Evaluation, (Epa Project Officer: J. Matthews). C. K. Smoley/CRC Press. Boca Raton, Florida.

Darcy, H. (1856): Les fontaines publique de la ville de Dijon. Victor Dalmont. Paris. 647 pp.

Dekker, T.J. and Abriola, L.M. (2000): The influence of field-scale heterogeneity on the infiltration and entrapment of dense nonaqueous phase liquids in saturated formations. Journal of Contaminant Hydrology 42(2-4): 187-218.

Enfield, C.G., Wood, A.L., Espinoza, F.P., Brooks, M.C., Annable, M. and Rao, P.S.C. (2005): Design of aquifer remediation systems: (1) Describing hydraulic structure and NAPL architecture using tracers. Journal of Contaminant Hydrology 81(1-4): 125-147.

Erning, K., Schäfer, D., Dahmke, A., Luciano, A., Viotti, P. and Petrangeli Papini, M. (2009): Simulation of DNAPL infiltration into groundwater with differing flow velocities using TMVOC combined with PetraSim. TOUGH Symposium 2009. Proceedings TOUGH Symposium. LBNL. Berkeley, CA, USA.

Erning, K., Schäfer, D., Dahmke, A., Luciano, A., Viotti, P. and Petrangeli Papini, M. (2010a): Simulation of DNAPL distribution depending on groundwater flow velocities using TMVOC. In: M. Schirmer, E. Hoehn and T. Vogt (Editors). IAHS Publication: Groundwater Quality Management in a Rapidly Changing World. Proceedings of the 7th International Groundwater Quality Conference held in Zurich, Switzerland, 13-18 June 2010. Red Books. IAHS. Oxfordshire. pp. 128-131.

Erning, K., Schäfer, D., Dahmke, A., Luciano, A., Viotti, P. and Petrangeli Papini, M. (2010b): Simulation of DNAPL distribution depending on groundwater flow velocities

using TMVOC. International Groundwater Quality Conference 2010. Zurich, Switzerland.

Erning, K., Schäfer, D., Grandel, S., Dahmke, A., Luciano, A., Viotti, P. and Petrangeli Papini, M. (2010c): Model investigation of DNAPL distribution in the saturated zone for varying groundwater flow velocities and subsurface geometry. ConSoil 2010. Salzburg, Austria.

Erning, K. and Schäfer, D. (2011): Multiphase model driven site assessement of the former industrial facility Chimica di Bianchi in Rho / Italy. In: M. Kästner (Editor). ModelPROBE report second period (12/2009-05/2011): Workpackage 9.2: Field Demonstration and Cross Validation. pp. 187-197.

Erning, K., Grandel, S., Dahmke, A. and Schäfer, D. (2012): Simulation of DNAPL infiltration and spreading behaviour in the saturated zone at varying flow velocities and alternating subsurface geometries. Environmental Earth Sciences 65(4): 1119-1131.

Fagerlund, F. (2006): Experimental and Modelling Studies on the Spreading of Non-Aqueous Phase Liquids in Heterogeneous Media. Uppsala Universitet. Uppsala. 70 pp.

Fagerlund, F.F., Niemi, A. and Illangasekare, T.H. (2006a): Modeling NAPL Source Zone Formation in Stochastically Heterogeneous Layered Media - a Comparison with Experimental Results. TOUGH Symposium 2006. Lawrence Berkeley National Laboratory, Berkeley, California.

Fagerlund, F.F., Niemi, A. and Odén, M. (2006b): Comparison of relative permeability-fluid saturation-capillary pressure relations in the modelling of non-aqueous phase liquid infiltration in variably saturated, layered media. Advances in Water Resources 29(11): 1705-1730.

Falta, R.W., Pruess, K., Finsterle, S. and Battistelli, A. (1995): T2VOC User´s Guide. LBL-36400. U.S. Department of Energy.158 pp.

Falta, R.W. (2003): Simulation of subgridblock scale DNAPL pool dissolution using a dual domain approach. TOUGH Symposium 2003. Lawrence Berkeley National Laboratory, Berkeley, California.

Falta, R.W., Basu, N. and Rao, P.S. (2005a): Assessing impacts of partial mass depletion in DNAPL source zones: II. Coupling source strength functions to plume evolution. Journal of Contaminant Hydrology 79(1-2): 45-66.

Falta, R.W., Suresh Rao, P. and Basu, N. (2005b): Assessing the impacts of partial mass depletion in DNAPL source zones: I. Analytical modeling of source strength functions and plume response. Journal of Contaminant Hydrology 78(4): 259-280.

Feenstra, S., Cherry, J.A. and Parker, B.L. (1996): Conceptual Models for the Behavior of Dense Non-Aqueous Phase Liquids (DNAPLs) in the Subsurface. In: J.F. Pankow and J.A. Cherry (Editors). Dense Chlorinated Solvents and other DNAPLs in Groundwater. Waterloo Press. Portland, Oregon. pp. 522.

Fure, A.D., Jawitz, J.W. and Annable, M.D. (2006): DNAPL source depletion: Linking architecture and flux response. Journal of Contaminant Hydrology 85(3-4): 118-140.

Gerhard, J.I. and Kueper, B.H. (2003a): Influence of constitutive model parameters on the predicted migration of DNAPL in heterogeneous media. Water Resources Research 39(10): 13 PP.

Gerhard, J.I. and Kueper, B.H. (2003b): Capillary pressure characterisitcs necessary for simulating DNAPL infiltration, redistribution, and immobilization in saturated porous media. Water Resources Research 39(8): 17 PP.

Gerhard, J.I. and Kueper, B.H. (2003c): Relative permeability characteristics necessary for simulating DNAPL infiltration, redistribution, and immobilization in saturated porous media. Water Resources Research 39(1213): 16 PP.

Gerhard, J.I., Pang, T. and Kueper, B.H. (2007): Time Scales of DNAPL Migration in Sandy Aquifers Examined via Numerical Simulation. GROUND WATER 45(2): 147-157.

Gilliom, R.J., Alley, W.M. and Gurtz, M.E. (1995): Design of the National Water-Quality Assessment Program - Occurence and Distribtuion of Water-Quality Condition. Reston, VA.

Golden Software Inc. (2007): Grapher 7.0. Golden.

Grandel, S. and Dahmke, A. (2008): Leitfaden Natürliche Schadstoffminderung bei LCKW-kontaminierten Standorten: Methoden, Empfehlungen und Hinweise zur Untersuchung und Beurteilung; BMBF-Förderschwerpunkt "Kontrollierter natürlicher Rückhalt und Abbau von Schadstoffen bei der Sanierung kontaminierter Grundwässer und Böden" (KORA), KORA - Themenverbund 3 - Chemische Industrie, Metallverarbeitung. Institut für Geowissenschaften, Abt. Angewandte Geologie. Kiel.364 pp.

Grant, G.P. and Gerhard, J.I. (2004): Sensitivity of Predicted DNAPL Source Zone Longevity to Mass Transfer Correlation Model. In: R.N. Young and H.R. Thomas (Editors). Geoenvironmental Engineering: Integrated management of groundwater and contaminated land. Telford Publishing. London. pp. 59-67.

Grant, G.P. and Gerhard, J.I. (2007): Simulating the dissolution of a complex dense nonaqueous phase liquid source zone: 2. Experimental validation of an interfacial area - based mass transfer model. Water Resources Research 43(12): W12409.

Grant, G.P., Gerhard, J.I. and Kueper, B.H. (2007): Multidimensional validation of a numerical model for simulating a DNAPL release in heterogeneous porous media. Journal of Contaminant Hydrology 92(1-2): 109-128.

Grathwohl, P. (2006): Langzeitverhalten organischer Schadstoffe in Boden und Grundwasser. Grundwasser 11(3): 157-163.

Greifenhagen, G. (2000): Untersuchungen zur Hydrogeologie des Stadtgebietes Darmstadt mit Hilfe eines Grundwasserinformationssystems - unter Verwendung von einer Datenbank, Datenmodellierung und ausgewählten statistischen Methoden. Diss. FB Material- und Geowissenschaften. Darmstadt.221 pp.

Hassanizadeh, S.M., Schotting, R.J., Gray, W.G. and Pinder, G.F. (2004): Solid Waste and Emergency Response. Washington, DC.

Helmig, R. (1997): Multiphase flow and transport processes in the subsurface. A contribution to the modeling of hydrosystems. Environmental Engineering. Springer. Berlin; Heidelberg; New York; Barcelona; Budapest; Hong Kong; London; Milan; Paris; Santa Clara; Tokyo. 367 pp.

Herfort, M., Ptak, T., Hümmer, O., Teutsch, G. and Dahmke, A. (1998): Testfeld Süd: Einrichtung der Testfeldinfrastruktur und Erkundung hydraulisch-hydrogeochemischer Parameter des Grundwasserleiters. Grundwasser 3(4): 159-166.

Herfort, M. and Ptak, T. (2002): Multitracer-Versuch im kontaminierten Grundwasser des Testfeldes Süd. Grundwasser 1: 31-40.

Hoehn, E. and Santschi, P.H. (1987): Interpretation of tracer displacement during infiltration of river water to groundwater. Water Resources Research 23(4): 366-340.

Hoehn, E. and Von Gunten, H.R. (1989): Radon in groundwater: A tool to assess infiltration from surface waters to aquifers. Water Resources Research 25(8): 1795-1803.

Illangasekare, T.H., Ramsey, J.L., Jensen, K.H. and Butts, M.B. (1995): Experimental study of movement and distribution of dense organic contaminants in heterogeneous aquifers. Journal of Contaminant Hydrology 20(1-2): 1-25.

Illangasekare, T.H., Saenton, S., Dai, D., Moore, Q. and S. Majid Hassanizadeh, R.J.S.W.G.G.a.G.F.P. (2002): Modeling for determination of pre- and post remediation prediction of dissolved contaminant concentration downstream of NAPL source zones. Developments in Water Science. Elsevier. pp. 843-850.

Illangasekare, T.H., Munakata Marr, J., Siegrist, R.L., Soga, K., Glover, K.C., Moreno-Barbero, E., Heiderscheidt, J.L., Saenton, S., Matthew, M., Kaplan, A.R., Kim, Y., Dai, D. and Page, J.W.E. (2006): Mass Transfer from Entrapped DNAPL Sources Undergoing Remediation: Characterization Methods and Prediction Tools. SERD Project No. CU-1294. Colorado School of Mines.410 pp.

Imhoff, P.T., Mann, A.S., Mercer, M. and Fitzpatrick, M. (2003): Scaling DNAPL migration from the laboratory to the field. Journal of Contaminant Hydrology 64(1-2): 73-92.

Institut für Arbeitsschutz der Deutschen Gesetzlichen Unfallversicherung (IFA) (2012): Gefahrstoffdatenbanken (GESTIS). Deutsche Gesetzliche Unfallversicherung e.V. (DGUV),.

Jawitz, J.W., Fure, A.D., Demmy, G.G., Berglund, S. and Rao, P.S.C. (2005): Groundwater contaminant flux reduction resulting from nonaqueous phase liquid mass reduction. Water Resources Research 41: 15.

Jellali, S., Benremita, H., Muntzer, P., Razakarisoa, O. and Schäfer, G. (2003): A large-scale experiment on mass transfer of trichloroethylene from the unsaturated zone of a sandy aquifer to its interfaces. Journal of Contaminant Hydrology 60(1-2): 31-53.

Johnson, R.L. and Pankow, J.F. (1992): Dissolution of dense chlorinated solvents into groundwater. 2. Source functions for pools of solvent. Environ. Sci. Technol. 26(5): 896-901.

Kamon, M., Endo, K., Kawabata, J., Inui, T. and Katsumi, T. (2004): Two-dimensional DNAPL migration affected by groundwater flow in unconfined aquifer. Journal of Hazardous Materials 110(1-3): 1-12.

Kästner, M., Braeckevelt, M., Döberl, G., Cassiani, G., Petrangeli Papini, M., Leven-Pfister, C. and Van Ree, D. (2012): Model-Driven Soil Probing, Site Assessment and Evaluation - Guidance on Technologies. Sapienza Università Editrice. Rome, Italy. 307 pp.

Kavanaugh, M.C., Rao, P.S., Abriola, L., Cherry, J.A., Destouni, G., Falta, R.W., Major, D., Mercer, J.W., Newell, C.J., Sale, T., Shoemaker, S., Teutsch, G. and Udell, K. (2003): The DNAPL Remediation Challenge: Is There a Case for Source Depletion? EPA/600/R-03/143. US EPA. Cincinatti.129 pp.

Kueper, B.H. and Frind, E.O. (1988): An overview of immiscible fingering in porous media. Journal of Contaminant Hydrology 2(2): 95-110.

Kueper, B.H., Abbott, W. and Farquhar, G. (1989): Experimental observations of multiphase flow in heterogeneous porous media. Journal of Contaminant Hydrology 5(1): 83-95.

Kueper, B.H. and Frind, E.O. (1991): Two-Phase Flow in Heterogeneous Porous Media: 2. Model Application. Water Resour. Res. 6: 1057-1070.

Kueper, B.H., Redman, D., Starr, R.C., Reitsma, S. and Mah, M. (1993a): A Field Experiment to Study the Behaviour of Tetrachloroethylene Below the Water Table: Spatial Distribution of Residual and Pooled DNAPL. GROUND WATER 31(5): 756-766.

Kueper, B.H., Redman, D., Starr, R.C., Reitsma, S. and Mah, M. (1993b): A Field Experiment to Study the Behavior of Tetrachloroethylene Below the Water Table: Spatial Distribution of Residual and Pooled DNAPL. GROUND WATER 31(5): 756-766.

Lawrence Berkeley National Laboratory (2012): TMVOC Software. http://esd.lbl.gov/research/projects/tough/software/ [2012,November 04].

Lawrence National Berkeley Laboratory (2012): TOUGH History - Historical Overview of TOUGH Simulators http://esd.lbl.gov/research/projects/tough/history.html [2012,13.11.].

Leccese, M., Aulenta, F., Petrangeli Papini, M., Viotti, P., Rossetti, S. and Majone, M. (2007): Anaerobic bioremedation of chlorinated solvents contaminated aquifers in the

presence of DNAPL: The Rho test site project. Italian Journal of Engineering Geology and Environment Special Issue 2007: 107-114.

Lee, K.Y., Lee, J.-Y. and Mellett, J.J. (2004): Transport of dissolved methoxy-nonafluorobutane through a saturated column. Environmental Geology 46(6): 883-889.

Lemke, L.D. and Abriola, L.M. (2003): Predicting DNAPL entrapment and recovery: the influence of hydraulic property correlation. Stochastic Environmental Research and Risk Assessment 17: 408-418.

Li, H., Chen, J. and Yang, J. (2011): Pore-scale removal mechanisms of residual light non-aqueous phase liquids in porous media. Environmental Earth Sciences 64(8): 2223-2228.

Liang, H. and Falta, R.W. (2008): Modeling field-scale cosolvent flooding for DNAPL source zone remediation. Journal of Contaminant Hydrology 96(1-4): 1-16.

Luciano, A., Viotti, P. and Petrangeli Papini, M. (2010): Laboratory investigation of DNAPL migration in porous media. Journal of Hazardous Materials 176: 1006-1017.

Mackay, D.M., Roberts, P.V. and Cherry, J.A. (1985): Transport of organic contaminants in groundwater. Environmental Science & Technology 19(5): 384-392.

Mackay, D.M. and Cherry, J.A. (1989): Groundwater contamination: pump-and-treat remediation. Environmental Science & Technology 23(6): 630-636.

Manzello, S.L. and Yang, J.C. (2002): An experimental study of high Weber number impact of methoxy-nonafluorobutane C4F9OCH3 (HFE-7100) and n-heptane droplets on a heated solid surface. International Journal of Heat and Mass Transfer 45(19): 3961-3971.

Mayer, A.S. and Miller, C.T. (1996): The influence of mass transfer characteristics and porous media heterogeneity on nonaqueous phase dissolution. Water Resources Research 32(6): 1551-1567.

McCarthy, K.A. and Johnson, R.L. (1992): Transort of volatile organic compounds across the capillary fringe. Water Resour. Res. 29: 1675-1683.

Mercer, J.W. and Cohen, R.M. (1990): A review of immiscible fluids in the subsurface: Properties, models, characterization and remediation. Journal of Contaminant Hydrology 6(2): 107-163.

Miles, B., Maji, R., Sudicky, E.A., Teutsch, G. and Peter, A. (2008a): A pragmatic approach for estimation of source-zone emissions at LNAPL contaminated sites. Journal of Contaminant Hydrology 96: 83-96.

Miles, B., Maji, R., Sudicky, E.A., Teutsch, G. and Peter, A. (2008b): A pragmatic approach for estimation of source-zone emissions at LNAPL contaminated sites. Journal of Contaminant Hydrology 96(1-4): 83-96.

Moeschlin, S. (1986): Klinik und Therapie der Vergiftungen. Georg Thieme Verlag. Stuttgart. 759 pp.

Moran, M.J., Zogorski, J.S. and Squillace, P.J. (2006): Chlorinated Solvents in Groundwater of the United States. Environmental Science & Technology 41(1): 74-81.

Mualem, Y. (1976): A New Model for Predicting the Hydraulic Conductivity of Unsaturated Porous Media. Water Resources Research 12(3): 513-522.

National Research Council (NRC) (1994): Alterantives to groundwater cleanup. National Academy Press. Washington, D.C.

Page, J.W.E., Soga, K. and Illangasekare, T. (2007): The significance of heterogeneity on mass flux from DNAPL source zones: An experimental investigation. Journal of Contaminant Hydrology 94(3-4): 215-234.

Pankow, J.F. and Cherry, J.A. (1996): Dense Chlorinated Solvents and Other DNAPLs in Groundwater. Waterloo Press. Waterloo. 522 pp.

Parker, J.C. and Lenhard, R.J. (1987): A Model for Hysteretic Constitutive Relations Governing Multiphase Flow in Porous Media. 1. Saturation-Pressure Relations. Water Resources Research 23(12): 2187-2196.

Parker, J.C., Lenhard, R.J. and Kuppusamy, T. (1987): A Parametric Model for Constitutive Properties Governing Multiphase Flow in Porous Media. Water Resources Research 23(4): 618-624.

Parker, J.C. and Park, E. (2004): Modeling field-scale dense nonaqueous phase liquid dissolution kinetics in heterogeneous aquifers. Water Resources Research 40: 12 PP.

Pedretti, D. and Masetti, M. (2009): Monitoring and modelling unsaturated and saturated flow to evaluate performance of slurry walls in Rho (Italy). Estudios en la Zono no Saturada del Suelo 9: 1-8.

Pedretti, D., Masetti, M., Marangoni, T. and Beretta, G. (2012): Slurry wall containment performance: monitoring and modeling of unsaturated and saturated flow. Environmental Monitoring and Assessment 184(2): 607-624.

Poling, B.E., Prausnitz, J.M. and O´Connell, J.P. (2007): The Properties of Gases and Liquids. The McGraw-Hi,, Companies, Inc. Singapore.

Poulsen, M. and Kueper, B.H. (1992): A field experiment to study the behavior of tetrachloroethylene in unsaturated porous media. Environ. Sci. Technol. 26: 889-895.

Powers, S.E., Abriola, L.M. and Weber, W.J., Jr. (1992): An experimental investigation of nonaqueous phase liquid dissolution in saturated subsurface systems: steady state mass transfer rates. Water Resources Research 28(2): 2691-2705.

Powers, S.E., Abriola, L.M., Dunkin, J.S. and Weber Jr., W.J. (1994a): Phenomenological models for transient NAPL-water mass-transfer processes. Journal of Contaminant Hydrology 16: 1-33.

Powers, S.E., Abriola, L.M. and Weber, W.J., Jr. (1994b): An experimental investigation of nonaqueous phase liquid dissolution in saturated subsurface systems: Transient mass transfer rates. Water Resources Research 30(2): 321-332.

Pozzani, U.C., Weil, C.S. and Carpenter, C.P. (1959): The Toxicological Basis of Threshold Limit Values: 5. The Experimental Inhalation of Vapor Mixtures by Rats, with Notes upon the Relationship between Single Dose Inhalation and Single Dose Oral Data. American Industrial Hygiene Association Journal 20(5): 364-369.

Pruess, K. and Battistelli, A. (2002): TMVOC, A Numerical Simulator for Three-Phase Non-isothermal Flows of Multicomponent Hydrocarbon Mixtures in Saturated-Unsaturated Heterogeneous Media. Report LBNL-49375. Berkeley.192 pp.

Pruess, K., Oldenburg, C. and Moridis, G. (2002): TOUGH2 User´s Guide, Version 2.0. LNNL-43134. Berkeley.210 pp.

Pruess, K. and Battistelli, A. (2003): TMVOC, a simulator for multiple volatile organic chemicals. TOUGH Symposium 2003. Proceedings of TOUGH Symposium 2003. Lawrence Berkeley National Laboratory, Berkely, California.

Putzlocher, R., Kueper, B.H. and Reynolds, D.A. (2006): Relative velocities of DNAPL and aqueous phase plume migration. Journal of Contaminant Hydrology 88(3-4): 321-336.

Rivett, M.O. and Feenstra, S. (2005): Dissolution of an Emplaced Source of DNAPL in a Natural Aquifer Setting. Environmental Science & Technology 39(2): 447-455.

Saba, T., Illangasekare, T.H. and Ewing, J. (2001): Investigation of surfactant-enhanced dissolution of entrapped nonaqueous phase liquid chemicals in a two-dimensional groundwater flow field. Journal of Contaminant Hydrology 51(1-2): 63-82.

Saenton, S., Illangasekare, T.H., Soga, K. and Saba, T.A. (2002): Effects of source zone heterogeneity on surfactant-enhanced NAPL dissolution and resulting remediation end-points. Journal of Contaminant Hydrology 59(1-2): 27-44.

Sale, T.C. and McWhorter, D.B. (2001): Steady State Mass Transfer from Single-Component Dense Nonaqueous Phase Liquids in Uniform Flow Fields. Water Resources Research 37: 393-404.

Schwille, F. (1988): Dense chlorinated solvents in porous and fractured media. Translation of: Leichtfüchtige Chlorkohlenwasserstoffe in porösen und klüftigen Medien. Lewis Publishers, Inc. Chelsea.

Soga, K., Page, J.W.E. and Illangasekare, T.H. (2004): A review of NAPL source zone remediation efficiency and the mass flux approach. Journal of Hazardous Materials 110(1-3): 13-27.

Stone, H.L. (1970): Probability Model for Estimating Three-Phase Relative Permeability. Trans. SPE of AIME 249: 214-218.

Stroo, H.F., Unger, M., Ward, C.H., Kavanaugh, M.C., Vogel, C., Leeson, A., Marqusee, J.A. and Smitz, B.P. (2003): Remediating Chlorinated Solvent Source Zones. Environ. Sci. Technol.: 224-235.

TeKrony, M.C. and Ahlert, R.C. (1998): Residual saturation of packed columns with chlorinated solvents. Journal of Hazardous Materials 60(2): 127-142.

Teutsch, G., Grathwohl, P. and Schiedik, T. (1997): Literaturstudie zum natürlichen Rückhalt / Abbau von Schadstoffen im Grundwasser. Landesanstalt für Umweltschutz Baden-Württemberg. Karlsruhe.55 pp.

Teutsch, G., Rügner, H., Grathwohl, P. and Kohler, W. (2001): Entwicklung von Bewertungskriterien natürlicher Schadstoffabbauprozesse in Grundwasserleitern als Grundlage für Sanierungsentscheidungen bei Altstandorten. LAG 00-05/0460.

Thunderhead Engineering (2011): PetraSim - Interactive Model Creation for Advanced Flow, Transport and Heat Transfer Models. In: T.E.C. Inc. (Editor). Manhattan, USA.

Thunderhead Engineering (2012): PetraSim Release Notes. http://www.thunderheadeng.com/category/petrasim-release-notes/ [2012,06.12.].

Umweltbundesamt (2011): Bundesweite Übersicht zur Altlastenstatistik (Stand 7/2011). http://www.umweltbundesamt.de/boden-und-altlasten/altlast/web1/deutsch/1_3.htm [2012,30.10.].

Unger, A.J.A., Forsyth, P.A. and Sudicky, E.A. (1998): Influence of alternative dissolution models and subsurface heterogeneity on DNAPL disappearance times. Journal of Contaminant Hydrology 30(3-4): 217-242.

Van Genuchten, M.T. (1980): A Closed-form Equation for Predicting the Hydraulic Conductivity of Unsaturated Soils. Soil Science Society of America 44(5): 892-898.

Von Gunten, H.R., Karametaxas, G., Krähenbühl, U., Kuslys, M., Giovanoli, R., Hoehn, E. and Keil, R. (1991): Seasonal biogeochemical cycles in riverborne groundwater. Geochimica et Cosmochimica Acta 55(12): 3597-3609.

Werban, U., Leven, C., Reboulet, E., Leccese, M., Viotti, P. and Dietrich, P. (2007): Technologies for a fast characterization of subsurface structures - an example from the Milano-Rho site. Italian Journal of Engineering Geology and Environment(Special Issue 2007): 8.

Wilson, J.L., Conrad, S.H., Mason, W.R., Peplinski, W. and Hagan, E. (1990): Laboratory investigation of residual liquid organics from spills, leaks and the disposal of hazardous wastes in groundwater. Washington, DC.

Yang, Z., Zandin, H., Niemi, A. and Fagerlund, F. (published online 2012): The role of geological heterogeneity and variability in water infiltration on non-aqueous phase liquid migration. Environmental Earth Sciences: 1-13.

Yoon, H., Oostrom, M., Wietsma, T.W., Werth, C.J. and Valocchi, A.J. (2009): Numerical and experimental investigation of DNAPL removal mechanisms in a layered porous

medium by means of soil vapor extraction. Journal of Contaminant Hydrology 109(1-4): 1-13.

Zhu, J. and Sykes, J.F. (2000): The influence of NAPL dissolution characteristics on field-scale contaminant transport in subsurface. Journal of Contaminant Hydrology 41(1-2): 133-154.

Curriculum vitae

Katharina Erning

Date of birth	20.09.1978
Place of birth	Bonn, Germany
Nationality	German
Address	Mühlenweg 112, 24116 Kiel

Scientific experience

06/2008 – current	Scientific assistant at Christian Albrechts-University of Kiel, Department of Applied Geology, Hydrogeology and Engineering Geology
04/2011	Further training in Basics in Professional University Teaching
01/2011	DAAD lecture and research exchange at La Sapienza, Rome / Italy
12/2007 – 05/2008	Scientific assistant at Brandenburg University of Technology, Cottbus Department of Brownfields
09/2005 – 02/2007	Scientific student assistant at Helmholtz-Zentrum für Umweltforschung – UFZ, Department Hydrogeology
07/2002 – 05/2003	DAAD-scholarship holder at Norges Tekniske of Naturvitenskapelige Universitet NTNU, Trondheim / Norway
04/2001 – 03/2002	Scientific student assistant at University of Leipzig, Department Geology
10/1999 – 04/2007	Study of Geology at University of Leipzig and University of Halle
10/1997 – 09/1998	Study of Geography at University of Leipzig
10/1997 – 09/1998	Study of Medicin at University of Leipzig
09/1988 – 06/1997	Kaiser-Heinrich Gymnasium Bamberg

Scientific publications and conferences

Peer-reviewed

2013 K. Erning, A. Dahmke, D. Schäfer:
Multiphase modeling of the impact of groundwater pore velocities on DNAPL migration in the multi-aquifer formation of Rho, Italy
(work in progress)

2012 K. Erning, S. Grandel, A. Dahmke, D. Schäfer:
Simulation of DNAPL infiltration and spreading behaviour in the saturated zone at varying flow velocities and alternating subsurface geometries.
Environmental Earth Sciences.65 (4). 1119-1131.
DOI: 10.1007/s12665-011-1361-9

2010 K. Erning, D. Schäfer, A. Dahmke, A. Luciano, P. Viotti, M. PetrangeliPapini:
Simulation of DNAPL distribution depending on groundwater flow velocities using TMVOC.
In: Schirmer M, Hoehn E, Vogt T (eds) IAHS Publication: Groundwater Quality Management in a Rapidly Changing World. Proceedings of the 7th International Groundwater Quality Conference held in Zurich, Switzerland, 13-18 June 2010, vol 342. Red Books. IAHS, Oxfordshire.

Reports

2011 K. Erning, D. Schäfer:
Multiphase model driven site assessment of the area of the former industrial facility Chimica di Bianchi in Rho / Italy.
In: M. Kästner et al. (eds.): ModelPROBE report second period (12/2009 - 05/2011): Workpackage 9.2: Field Demonstration and Cross Validation. pp. 187-197.

2009 K. Erning, D. Schäfer:
Box modeling of DNAPL-infiltration. In: M. Kästner et al. (ed.): ModelPROBE report first period (06/2008 - 11/2009): Workpackage 9.2: Field Demonstration and Cross Validation. pp. 136-137.

Conference Proceeding

2010 K. Erning, D. Schäfer, S. Grandel, A. Dahmke, A. Luciano, P. Viotti, M. Petrangeli Papini:
Model investigation of DNAPL distribution in the saturated zone for varying groundwater flow velocities and subsurface geometry.
ConSoil 2010. Salzburg. Österreich.

2010 K. Erning, D. Schäfer, A. Dahmke, A. Luciano, P. Viotti, M. Petrangel Papini:
Simulation of DNAPL distribution depending on groundwater flow velocities using TMVOC.
International Groundwater Quality Conference 2010. Zürich, Schweiz

2009 K. Erning, D. Schäfer, A. Dahmke, A. Luciano, P. Viotti, M. Petrangeli Papini:
Simulation of DNAPL infiltration into groundwater with differing flow velocities

using TMVOC combined with PetraSim.
TOUGH Symposium 2009. Berkeley, USA.

Oral Presentations

2011 K. Erning, D. Schäfer, A. Dahmke, A. Luciano, P. Viotti, M. Petrangeli Papini:
Computer-based field site investigation of Ex Chimica Bianchi / Rho: Multiphase Modeling of Spill History and Position of DNAPL Source Zone Depending on Groundwater Flow Velocities.
Guest Lecture at La Sapienza University, Rome. DAAD-Sholarship.

2010 K. Erning, D. Schäfer, A. Luciano, P. Viotti, M. Petrangeli Papini:
Computer-based field site investigation Rho/Italy & Multiphase Modeling of Contaminants
3rd ModelPROBE Meeting, Liberec, Czech Republic

2010 K. Erning, D. Schäfer, S. Grandel, A. Dahmke, A. Luciano, P. Viotti, M. Petrangeli Papini:
Model investigation of DNAPL distribution in the saturated zone for varying groundwater flow velocities and subsurface geometries.
ConSoil 2010. Salzburg, Austria.

2010 K. Erning, D. Schäfer, A. Dahmke, A. Luciano, P. Viotti, M. Petrangeli Papini:
Simulation of DNAPL distribution depending on groundwater flow velocities using TMVOC.
International Groundwater Quality Conference 2010. Zurich, Switzerland.

Poster Presentations

2009 K. Erning, D. Schäfer, A. Dahmke, A. Luciano, P. Viotti, M. Petrangeli Papini:
Simulation of DNAPL infiltration into groundwater with differing flow velocities using TMVOC combined with PetraSim.
TOUGH Symposium 2009. Berkeley, USA.